

Characterization of the rehydration behavior of food powders

**Dissertation zur Erlangung des Doktorgrades
der Naturwissenschaften (Dr. rer. nat.)**

**Fakultät Naturwissenschaften
Universität Hohenheim**

Institut für Lebensmittelwissenschaft und Biotechnologie
Fachgebiet Lebensmittelverfahrenstechnik und Pulvertechnologie (150c)

vorgelegt von
Julia Wangler

aus *Stuttgart*
2019

Dekan: Prof. Dr. Uwe Beifuß
1. berichtende Person: Prof. Dr.-Ing. Reinhard Kohlus
2. berichtende Person: Prof. Dr.-Ing. Jörg Hinrichs
Eingereicht am: 09.08.2019
Mündliche Prüfung am: 05.12.2019

Die vorliegende Arbeit wurde am 08.11.2019 von der Fakultät Naturwissenschaft der Universität Hohenheim als „Dissertation zur Erlangung des Doktorgrades der Naturwissenschaften“ angenommen

*“Everybody is a genius.
But if you judge a fish by its ability to climb a tree,
it will live its whole life believing
that it is stupid”*

*ALBERT EINSTEIN (*1879 - †1955)*

DANKSAGUNG

An erster Stelle gilt mein Dank Prof. Dr.-Ing. Reinhard Kohlus für die engagierte Betreuung. Das große Interesse an meiner Arbeit, die vielen hilfreichen Diskussionen und Ideen sowie die stets positive und motivierende Atmosphäre werde ich immer in Erinnerung behalten. Herzlichen Dank!

Prof. Dr.-Ing. Jörg Hinrichs danke ich für die freundliche Übernahme des Zweitgutachtens.

Bei Dr.-Ing. Peter Gschwind bedanke ich mich sehr für die vielen hilfreichen Ideen und die große Hilfsbereitschaft sowohl bei fachlichen Fragen als auch im Laboralltag.

Peter Lang und Peter Sonntag danke ich für Ihre Hilfe bei allen technischen Problemen und für die guten Ideen bei der Umsetzung zahlreicher Versuchsaufbauten.

Für Ihr Engagement und die große Motivation bei der Durchführung Ihrer Bachelor- und Masterarbeiten möchte ich mich bei allen Studenten, die ich in dieser Zeit betreuen durfte, bedanken: Elena Konstanz, Mareike Beck, Annika Buck, Tanita Bugbee, Christina Hübner, Pascale Schwis, Alexa Kanzleiter, Jana Rau, Kevin Sicko, Stephan Straub und Frederic Löpke.

Allen aktuellen und ehemaligen Doktoranden und Mitarbeitern des Fachgebiets Lebensmittelverfahrenstechnik und Pulvertechnologie danke ich sehr für die Unterstützung im Laboralltag und die nette Arbeitsatmosphäre: Julia Harnacke, Nora Ruprecht, Jakob Fröhlich, Andreas van Kampen, Martin Šrámek und Patrick Wilms sowie Theresa Anzmann, Erika Denzel, Silvia Meintzinger-Gaul, Hildegard Eismann und Steffi Pavlov.

Ganz besonders bedanken möchte ich mich hier bei Heike Teichmann, Annika Linke und Tobias Linke. Vielen Dank Heike für Deine Hilfe bei der Simulation und für das Korrekturlesen dieser Arbeit! Vielen Dank für die vielen hilfreichen Diskussionen und Eure Unterstützung bei fachlichen Fragen, aber vor allem für die vielen schönen Momente und Eure emotionale Unterstützung in allen Lebenslagen! Ich werde Euch sehr vermissen!

Co-AUTHORS

The scientific work was partially conducted in cooperation with other scientists working at the department of Process Engineering and Powder Technology, University of Hohenheim. Prof. Dr.-Ing. Reinhard Kohlus was supervising the whole Ph.D thesis.

CHAPTER 2: Julia Wangler planned the study and carried out the experimental work presented in this chapter. Prof. Dr.-Ing. Reinhard Kohlus supported this study by establishing the simulation model.

CHAPTER 3: Julia Wangler planned the study and was also responsible for the experimental work. Prof. Dr.-Ing. Reinhard Kohlus aided with the conception of the study and evaluation of experimental results.

CHAPTER 4: Julia Wangler planned the study and partially conducted the experimental work. Heike Teichmann built-up the simulation model and conducted the simulation study. Elena Konstanz supported this study by conducting the experimental work as part of her master thesis. Prof. Dr.-Ing. Reinhard Kohlus aided with the conception of the study and with helpful discussions regarding the set-up of the model and data interpretation.

LIST OF PUBLICATIONS

PEER-REVIEWED PUBLICATIONS

- Experimental investigation and simulation of rehydration dynamics of biopolymer powders
Julia Wangler, Heike Teichmann, Elena Konstanz and Reinhard Kohlus
Published 2019 in Powder Technology, Volume 355, p. 461-473
DOI: <https://doi.org/10.1016/j.powtec.2019.07.022>
- Development and validation of methods to characterize rehydration behavior of food hydrocolloids
Julia Wangler, Reinhard Kohlus
Published 2018 in Food Hydrocolloids, Volume 82, p. 500-509
DOI: <https://doi.org/10.1016/j.foodhyd.2018.04.018>
- Dynamics of Capillary Wetting of Biopolymer Powders
Julia Wangler, Reinhard Kohlus
Published 2017 in Chemical Engineering and Technology, Volume 40, No. 9, p. 1552-1560
Accessible under DOI: 10.1002/ceat.201600607
- Tagungsband Agglos 10 2013, Kobe (Japan)
High Shear Mixer Granulation of Xanthan Gum

ORAL PRESENTATIONS

- ParTec 2016, Nürnberg
Dynamics of capillary wetting of biopolymer powders
- World Congress of Particle Technology 2014 (Peking, China)
Dispersion of food powders dependent on rheology of wet particle aggregates
- ProcessNet Agglomeration und Schüttguttechnik 2014, Magdeburg
Modellbasierte Beschreibung des Dispergierverhaltens von Lebensmittelpulvern hinsichtlich einer optimierten Agglomeration
- ProcessNet Lebensmittelverfahrenstechnik und Phytoextrakte 2014, Freising
Beschreibung und Katalogisierung des Dispergierverhaltens von Lebensmittelpulvern
- Agglos 10 2013, Kobe (Japan)
High Shear Mixer Granulation of Xanthan Gum

POSTER PRESENTATIONS

- ProcessNet Lebensmittelverfahrenstechnik 2019, Lausanne
Experimental Investigation and Simulation of Food Powder Rehydration
- UK Particle Technology Forum 2016, Surrey (UK)
Influence of dynamic effects on biopolymer rehydration
- IFPRI 2012, Ludwigsburg
Dispersion of critical food powders under turbulent stirring conditions
- ProcessNet Lebensmittelverfahrenstechnik, Rheologie und Trocknungstechnik
2011, Stuttgart
Dispergierung von kritischen Lebensmittelpulvern unter turbulenten
Rührbedingungen

TABLE OF CONTENTS

CHAPTER 1	GENERAL INTRODUCTION AND THESIS OUTLINE	1
1.1	FOOD POWDERS	3
1.2	FOOD HYDROCOLLOIDS	5
1.2.1	Xanthan gum	7
1.2.2	Guar gum	11
1.2.3	Alginate	15
1.3	FOOD POWDER REHYDRATION	20
1.3.1	Wettability of powders	21
1.3.2	Sinkability of powders	26
1.3.3	Dispersion and disintegration of particles	28
1.4	DYNAMICS OF FOOD POWDER REHYDRATION	30
1.4.1	Swelling and viscosity development of hydrocolloids	33
1.5	THESIS OUTLINE	38
CHAPTER 2	DYNAMICS OF CAPILLARY WETTING OF BIOPOLYMER POWDERS	40
2.1	INTRODUCTION	42
2.2	MATERIAL & METHODS	45
2.2.1	Water uptake by capillary rise	45
2.2.2	Contact angle	47
2.2.3	Rheological characterization	47
2.2.4	Swelling behavior	48
2.3	SIMULATION	49
2.4	RESULTS & DISCUSSION	51
2.4.1	Wetting behavior	51
2.4.2	Rheological characterization	53
2.4.3	Swelling behavior	55
2.4.4	Simulation of the rehydration process	56
2.5	CONCLUSION	59
2.6	SYMBOLS USED	60

CHAPTER 3	DEVELOPMENT AND VALIDATION OF METHODS TO CHARACTERIZE REHYDRATION BEHAVIOR OF FOOD HYDROCOLLOIDS	62
3.1	INTRODUCTION	64
3.2	MATERIAL & METHODS	66
3.2.1	Materials	66
3.2.2	Preparation of model hydrocolloid granules	66
3.2.3	Methods	66
3.2.3.1	Wetting behavior	66
3.2.3.2	Rheological characterization	67
3.2.3.3	Swelling behavior	68
3.2.3.4	NMR-Measurements: Gel formation and water binding strength	69
3.2.3.5	Water uptake capacity	69
3.2.3.6	Aggregate disintegration	69
3.2.3.7	Dissolution experiments	70
3.3	RESULTS & DISCUSSION	71
3.3.1	Wetting behavior	71
3.3.2	Dynamics of hydrocolloid rehydration	74
3.3.3	Aggregate stability	76
3.3.4	Gel strength and water binding capacity	78
3.3.5	Water uptake capacity of hydrocolloids	79
3.3.6	Rehydration and disintegration of hydrocolloid powders	81
3.3.7	Dissolution of hydrocolloids	82
3.4	CONCLUSION	85
CHAPTER 4	EXPERIMENTAL INVESTIGATION AND SIMULATION OF REHYDRATION DYNAMICS OF BIOPOLYMER POWDERS	87
4.1	INTRODUCTION	89
4.2	MATERIALS & METHODS	90
4.2.1	Materials	90
4.2.2	Methods	90
4.2.2.1	Preparation of the biopolymer model system	90
4.2.2.2	Characterization of physical powder properties and dynamic rehydration behavior	92
4.3	SIMULATION OF BIOPOLYMER REHYDRATION	93

4.4	RESULTS & DISCUSSION	99
4.4.1	Coating process	99
4.4.1.1	Efficiency of the coating process	99
4.4.1.2	Coating quality	100
4.4.2	Contact angle	101
4.4.3	Capillary rise	101
4.4.3.1	Blank-correction of experimental data	101
4.4.3.2	Evaluation of capillary rise experiments	102
4.4.4	Gel formation and water binding strength	106
4.4.5	Simulation of biopolymer rehydration	109
4.5	REMARKS CONCERNING CAPILLARY LIQUID RISE IN FOOD POWDERS	112
4.6	CONCLUSION	114
4.7	SYMBOLS USED	116
CHAPTER 5	DISCUSSION AND CONCLUDING REMARKS	117
CHAPTER 6	SUMMARY	124
CHAPTER 7	ZUSAMMENFASSUNG	127
CHAPTER 8	REFERENCES	130
CHAPTER 9	APPENDIX	141
9.1	CHARACTERIZATION OF FOOD POWDER REHYDRATION: METHODS AND GENERAL ASPECTS	141

LIST OF FIGURES

Fig. 1.1: SEM-image of xanthan gum. (Magnification: 160 x).....	7
Fig. 1.2: Basic molecular structure element of a xanthan gum molecule. Adapted from [20].	8
Fig. 1.3: Shear rate dependency of the viscosity of xanthan gum in comparison to guar gum and alginate solutions. Adapted from [19].....	9
Fig. 1.4: SEM-image of guar gum. (Magnification: 160 x).....	11
Fig. 1.5: Molecular structure of guar gum. Adapted from [26].....	12
Fig. 1.6: SEM-image of Alginate. (Magnification:160x).....	15
Fig. 1.7: Molecular structure and chair conformation of an alginate chain (G: α -L-guluronic acid; M: β -D-mannuronic acid). Modified from [34].....	16
Fig. 1.8: Principle of Ca^{2+} binding and egg-box formation in alginate gels (G: α -L-guluronic acid). Adapted from [33,34,40].	17
Fig. 1.9: Schematic draw of contact angles analyzed by sessile drop measurements illustrating wetting (A), limiting case (B) and non-wetting behavior (C).....	22
Fig. 1.10: Shape of FBRM curves obtained from rehydration experiments. Adapted from [87]	29
Fig. 1.11: Schematic drawing of dynamic processes during food powder reconstitution	31
Fig. 1.12: Schematic drawing of a hydrocolloid aggregate, the mechanism of water uptake and the resulting concentration profile within the aggregate and the surrounding layer.....	35
Fig. 2.1: Experimental setup of the capillary-rise experiment	46
Fig. 2.2: Capillary rise experiment. A: Water uptake ($\text{H}_2\text{O}_{\text{dist.}}$, 20 °C) and water uptake rate of xanthan gum powder (200 mesh). B: Linear water uptake rate of xanthan gum, guar gum and alginate powder	52
Fig. 2.3: Concentration dependent viscosity of guar gum, alginate and xanthan gum. (Plate-plate geometry, gap: 1 mm, temperature 20 °C, shear rate: 0.1 s ⁻¹)	54

Fig. 2.4: Viscosity increase _{rel.} of guar gum, alginate and xanthan gum powder in contact with H ₂ O _{dist.} determined by rheological measurements. (c: 0.04 g mL ⁻¹ , shear rate 0.1 s ⁻¹ , 20 °C)	54
Fig. 2.5: Swelling behavior of xanthan gum, alginate and guar gum in contact with dist. water (20 °C, c=4.0 %(w/v), Normal Force: 0.2 N)	55
Fig. 2.6: Effect of parameter variation on dynamic capillary water uptake of powder rehydration. A: Influence of swelling rate (Viscosity development: 0 Pas g g ⁻¹ , d _{3,2} : 30.6 μm); B: Influence of viscosity development (Swelling rate: 0.5 μm s ⁻¹ , d _{3,2} : 30.6 μm); C: Influence of particle size (Swelling rate: 0.5 μm s ⁻¹ , Viscosity development: 10 Pas g g ⁻¹).	57
Fig. 2.7: Summary of parameter variation study. Wetted powder height after 5 s rehydration time. A: Variation of swelling rate (Viscosity development: 0 Pas g g ⁻¹ , d _{3,2} : 30.6 μm); B: Variation of viscosity development rate (Swelling rate: 0.5 μm s ⁻¹ , d _{3,2} : 30.6 μm); C: Variation of particle size (Swelling rate: 0.5 μm s ⁻¹ , Viscosity development: 10 Pas g g ⁻¹).....	59
Fig. 3.1: Contact angle between distilled water (20 °C) and alginate (A), xanthan gum (B) and guar gum (C).....	72
Fig. 3.2: Viscosity increase _{rel.} of guar gum, alginate and xanthan gum powder in contact with H ₂ O _{dist.} determined by rheological measurements (c = 0.04 g mL ⁻¹ , shear rate 0.1 s ⁻¹ , 20 °C).	75
Fig. 3.3: Swelling behavior of xanthan gum, alginate and guar gum powder in contact with dist. water (20 °C, c = 0.04 g mL ⁻¹ , Normal Force: 0.2 N).	76
Fig. 3.4: Concentration dependent yield point of guar gum, alginate and xanthan gum. (Amplitude sweeps, serrated plate-plate geometry, 20 °C).	77
Fig. 3.5: Change of relaxation time over time as indicator for gel strength and water binding strength of hydrocolloid granules (425-500 μm) measured by NMR analysis.	78
Fig. 3.6: Schematic draw of a hydrocolloid aggregate and the concentration profile within the aggregate and the surrounding layer.....	80
Fig. 3.7: Relative water uptake of hydrocolloid samples (A) and influence of different layer heights (B).	81

Fig. 3.8: Dissolution and disintegration of xanthan gum powder and aggregates dependent on applied shear stress. (Rheometer set-up: Bob-cup geometry, 20 °C, distilled water, c: 5 mg/mL 81

Fig. 3.9: Dissolution of hydrocolloid granules (425-500 µm) in distilled water (c = 0.1 %, pitched blade stirrer, 800 rpm)..... 83

Fig. 4.1: Schematic draw of sample preparation for NMR-measurements. 93

Fig. 4.2: Viscosity development during biopolymer rehydration in concentrated situations. **(A)** Effect 1: Dissolution state, **(B)** Effect 2: Non-dissolution state..... 96

Fig. 4.3: SEM-images of biopolymer coated glass beads (Coating layer thickness: 5 µm). **(A)** Xanthan gum, **(B)** Guar gum, **(C)** Alginate. (Magnification: Xanthan gum, alginate 180x, guar gum 160x). 100

Fig. 4.4: Water uptake of biopolymer coated glass beads (400 - 600 µm) dependent on coating layer thickness (0.5 µm - 5 µm) measured by capillary rise experiments. (A) Xanthan gum, (B) Guar gum, (C) Alginate, (D) Determination of capillary rise time. 103

Fig. 4.5: Transition point between capillary and diffusional liquid uptake dependent on the biopolymer and coating layer thickness..... 104

Fig. 4.6: Variation of capillary pressure dependent on biopolymer concentration... 105

Fig. 4.7: Percentage of fast relaxing protons over time obtained from bi-exponential regression of NMR results. 107

Fig. 4.8: Influence of swelling and dissolution on the capillary liquid uptake of food biopolymers obtained from simulation studies. (A) Xanthan gum, (B) Alginate, (C) Guar gum. Red dots represent simulated liquid heights corresponding to the physical characteristics of the respective biopolymer. Liquid heights represent the maximum heights before liquid velocity is 0. 109

Fig. 4.9: Influence of swelling **(A)** and dissolution **(B)** on capillary liquid rise obtained from simulated parameter variation study. Crossed diamonds represent the liquid height corresponding to the respective physical parameters of the biopolymer. Data are given relative to a situation without dissolution or swelling, corresponding to a liquid uptake height of 0.1 m. 110

Fig. 4.10: Time for complete dissolution of the biopolymer coating layer and liquid viscosity after 250 s dependent on the coating layer thickness. Calculation is based on the specific dissolution rate, biopolymer concentration and available particle surface. 112

Fig. 9.1: Schematic draw of the cone method to analyze wettability of powders. ... 142

Fig. 9.2: Cone method to analyze wettability of food powders..... 142

Fig. 9.3: Experiment to determine drop penetration time of water into loosely packed powder bed of xanthan gum 143

Fig. 9.4: Sinking behavior of powder particles determined by image analysis 147

Fig. 9.5: Change of size of xanthan gum aggregate over time (dissolver stirrer, $d/D = 0.345$, $P/V = 0.64 \text{ W/m}^3$) 149

LIST OF TABLES

Table 1.1: Sources of hydrocolloids. Selected examples, modified from [12].	5
Table 1.2: Application and functionality of xanthan gum in different industrial sectors (modified from [18,20]).	10
Table 1.3: Applications, concentrations and functionalities of guar gum in food products (modified from [26]).	14
Table 1.4: Application and functionalities of alginate in food products (modified from [18,38]).	19
Table 2.1: Powder characteristics: Bulk density, powder density, porosity and particle size	46
Table 2.2: Physical parameters of powder samples determined from sessile drop method and rheological measurements	51
Table 3.1: Powder characteristics: Bulk density, powder density, porosity and particle size	73
Table 3.2 Physical characteristics of hydrocolloid powders	73
Table 4.1: Powder characteristics: Bulk density, powder density, porosity and particle size.	98
Table 4.2: Physical parameters of powder samples determined from sessile drop method and rheological measurements [88,109].	98
Table 4.3: Target and experimentally determined coating layer thickness of xanthan gum-, guar gum- and alginate coated glass beads (400 - 600 μm).	99
Table 9.1: Contact angle between distilled water and biopolymer sample dependent on sample preparation method	144
Table 9.2: Surface roughness of compressed biopolymers (compaction pressure 550 bar) and dried powder layers.	145

Chapter 1 GENERAL INTRODUCTION AND THESIS OUTLINE

Rehydration of food powders is influenced by dynamic processes such as dissolution, viscosity development and swelling. The kinetics of these processes decisively affects the product performance. Especially for instant products, the ease of powder reconstitution determines handling and convenience of use and represents an important quality criterion for consumers. In the industrial application of powders, the rehydration process should be accomplished preferably without the formation of aggregates or floating layers, in order to reduce process times and costs. Therefore, powders with good reconstitution properties are highly demanded.

Beside powder characteristics, the rehydration process is influenced by environmental conditions such as pH, ionic strength or temperature as well as by process parameters and equipment. The influence of environmental conditions strongly depends on the material. Considering protein powders an acidic pH, a high ionic strength and high temperatures may lead to denaturation. For thickening agents as such xanthan gum, guar gum and alginate, an increase of temperature will accelerate processes triggered by powder-water interactions. Consequently, particle dispersion is worsened and lump formation more pronounced. In addition, rehydration in multi-component systems is influenced by the recipe and the order in which the ingredients are added. The competition for available water in such mixtures is especially relevant under sparse water condition, as e.g. during dough formation or for the dispersion of highly swellable hydrocolloids.

To improve dispersion several strategies are applied. To reduce the formation of particle aggregates, critical powders can be diluted and separated from each other by mixing with easily soluble materials as e.g. sugar. A further strategy is to modify the material properties as for example particle size, density, porosity or surface tension. Typically, this is achieved by agglomeration and instantization.

From a process-specific viewpoint, dispersion can be improved by the application of high-shear mixers or by using injector systems which cause elongational flow. Both results in an effective separation into individual particles. However, this strategy is not applicable for shear-sensitive materials, which in particular include food.

In this context, food powders represent a special case due to their solubility, their rheological behavior and their swelling ability. These processes result in highly dynamic changes of the physical powder characteristics throughout the rehydration process. In order to improve the rehydration behavior of food powders, a deeper knowledge of the dynamic changes of the physical powder properties taking place during the rehydration process is mandatory. To achieve this, this thesis focuses on the characterization of the powder properties affecting the different rehydration steps – wetting, sinking, dispersing and dissolution – with the objective to identify critical powder properties. This should provide a more purposeful approach for powder quality improvement.

The findings represented in this thesis are valid and suited to describe rehydration of powders in general. However, this work is restricted to the hydrocolloid powders xanthan gum, guar gum and alginate which were chosen as exemplary model systems for powdered products showing critical rehydration properties. As cold-soluble hydrocolloids, the immediate onset of viscosity increase and swelling processes after contact with aqueous rehydration liquids makes dispersion in particular a critical task. For other food hydrocolloids, as for example gelatin and starch- or protein-based powders, the dispersion process, respectively lump formation, is less critical. The reason for this is that these hydrocolloids react with water only at higher temperatures and that the change of the powder properties is less pronounced and slower. Due to that, rehydration is assumed to be less critical for such hydrocolloids. Especially for protein-based powders, as for example milk proteins, the focus is rather on the recovery of functionality. However, this issue was not further investigated within this thesis. The focus was placed on the investigation of the rehydration behavior of highly dynamic biopolymer powders.

1.1 FOOD POWDERS

Food powders are widely used as industrial intermediate products and as convenience products for consumers. Reasons for that high demand compared to raw materials or liquid preparations are their prolonged shelf-life due to a higher physical- and chemical stability, easier storage and handling as well as lower transport weight and costs. Industrially, powders are commonly used as intermediate products for further processing as for example dairy-, egg- or starch based products as well as food additives like spices, colorants, stabilizing or texturizing agents.

Beside their functional properties, powders can also be categorized in terms of composition (protein, fat, carbohydrates), microstructure, chemical and physical properties and particle size. According to the range of their particle size distribution powders are classified as “dust” (5-100 μm), “powders” (50-200 μm), “coarse granules” (200-4000 μm) and “flour” (100-5000 μm) [1]. These powder properties determine the behavior of the powder with regard to flowability, dust formation, dosing as well as rehydration behavior.

Considering these different requirements and functionalities, a wide range of different quality criterions exists. Especially in case of food products, safety aspects as well as the maintenance of the nutritional value and functionality of valuable components is of high importance throughout the whole production process. To be able to produce high quality powders a variety of processes and technologies has been developed, where the source material can either be solid or liquid. For food powder production the following technologies are most commonly used (modified from [1–4]).

- | | |
|-------------------------------------|--|
| (1) Comminution of solids: | Cereals, corn, coffee, cocoa, sugar |
| (2) Crystallization: | Sugar, salt, acids, fat powder |
| (3) Spray drying of liquids/pastes: | Dairy and egg products, instant coffee and tea, |
| (4) Freeze drying: | Instant coffee and tea, vegetables, fruits, flavor concentrates |
| (5) Drum drying: | Milk products, baby food ingredients, potato flakes, instant cereals, starch |

These processes differ in drying speed and temperature conditions which has an impact on the product quality with regard to denaturation of temperature sensitive components, flavor loss, color and structural changes [5]. Furthermore, physical properties like moisture, shape, surface characteristics, particle size and distribution

as well as internal molecular and micro-structure are, beside the choice of the raw material, mainly influenced by the drying process and the applied drying conditions. Especially the moisture content and the corresponding water activity (a_w -value) determine the shelf-life of the product in terms of microbiological and storage stability. To ensure sufficient stability the water activity of powders should be in the range of 0.2-0.4 [6].

Dehnad *et al.* [7] reviewed the influence of drying technologies on functional properties of biopolymers. The comparison of different drying methods indicated that the application of high temperatures decreased the swelling capacity of carbohydrates whereas the susceptibility for hydrothermal breakdown increased. Furthermore, the functionality of carbohydrate-based raw materials as e.g. flour was improved by low temperature fluidized bed drying, oven and freeze drying [7].

The final powder product is provided to the consumer either as raw material, e.g. flour or spices, or as higher processed “instant” preparation like tea and coffee, soups and sauces, desserts or dried ready meals [1]. In general, these products are not directly consumed as powders but need to be processed further. In this context, especially the rehydration behavior is an important quality criterion for consumer acceptance. To be able to produce dried food products with a good handling and rehydration behavior the main improvement strategies are size enlargement by agglomeration, increasing the particle porosity and modifying the surface composition for example by lecithination. The correlation between these powder properties and the rehydration behavior was previously investigated by several research groups [8–10]. Due to the wide range of possible powder applications, a more detailed investigation and understanding of the property-function-relationship is necessary in order to overcome the difficulties in powder processing and to be able to produce high quality food powders.

1.2 FOOD HYDROCOLLOIDS

Hydrocolloids are large macromolecular polymers which belong to the class of polysaccharides or proteins [11]. Hydrocolloids are obtained from different sources. Selected examples are summarized in Table 1.1.

Table 1.1: Sources of hydrocolloids. Selected examples, modified from [12].

Source	Hydrocolloid
Marine algae	Na-Alginate (E401)
	Agar-Agar (E406)
	Carrageenan (E407)
Plant material	Starch
	Cellulose (E460)
	Locust bean gum (E410)
	Guar gum (E412)
	Pectin (E440)
Microorganisms/Fermentation	Xanthan gum (E415)
Animal material	Gelatin

Beside the classification according to their origin, hydrocolloids can also be categorized according to their chemical composition, their structure, the mechanism of gel formation as well as according to their solubility.

With the exception of starch and cellulose derivatives, the polysaccharides are usually heteropolysaccharides with different sugars units. These can be arranged in linear, irregular unbranched, in regular or irregular branched or in block structures [13]. The molecular structure and the ratio of the different sugars have an influence on the hydrocolloid characteristics such as solubility, viscosity and gelling behavior [11,12,14]. Hydrocolloids have a high affinity for water which is attributed to the large number of polar hydroxyl groups [11]. Due to their functional properties such as thickening, gelling, emulsifying and stabilizing, hydrocolloids are used in many industries. In food products, they are mainly used because of their high water binding capacity and the associated influence on the rheological structure of the product [11].

Depending on their functional properties, hydrocolloids can be classified as gelling, thickening or stabilizing agents [15]. Gel-forming hydrocolloids are able to solidify fluids

and to cause structures that are resistant to flow [11,15]. For hydrocolloids, gelling takes place by crosslinking of the biopolymer molecules to form a three-dimensional network in which the liquid phase is immobilized. The network structure is stabilized by hydrogen bonding, hydrophobic association or cation mediated cross-linking [11,12]. For food applications, typical representatives for gelling agents are alginate, pectin, carrageenan, agar and gelatin. Depending on the hydrocolloid, different conditions are necessary for gel formation. For example, the addition of cations induces gelling of alginate and low-methoxylated pectin. High sugar concentrations (~ 50 %) and a pH < 3.5 are necessary for gel formation in high-methoxylated pectin [12].

In case of methyl- and hydroxypropylmethylcellulose, gel formation can take place after heating by temperature-induced hydrophobic interactions of the methyl groups, which stabilize the gel structure [12]. Additionally, gel formation can be induced by synergistic interaction between hydrocolloids, as e.g. xanthan gum in combination with galactomannans and glucomannans [11].

For food applications, the best-known representative for a protein-based hydrocolloid is gelatin. Gelatin is extracted by a hydrolysis process out of animal collagen. It consists of a sequence of repeating units of the amino acids [Glycine-X-Y]_n whereby the amino acids X and Y often represent proline and hydroxyproline [16]. The gel strength and the gelling power of gelatin gels is mainly influenced by the content and proportion of these amino acids. The viscosity of gelatin gels depends on temperature, concentration, ionic content, pH and the molecular weight distribution of the gelatin molecules [13,16]. High molecular weights induce higher viscous gels [16]. Gelatin is a fibrous protein and gelling occurs by a cold-set mechanism after a previous heating step. Heating to temperatures above the denaturing temperature causes the transition from helical- to coil conformation. On cooling, the gelatin molecules reassemble to a collagen-like triple-helix-structure which is stabilized by hydrogen bonds [12,13,17]. The popularity of gelatin for food applications is attributed to a range of advantageous properties. The thermo-sensitivity and the low melting point is responsible for a good mouth-feeling. Gelatin has a neutral taste, is easy-to-use and the gels do not exhibit syneresis. Due to its emulsifying and foaming properties gelatin can be used to stabilize aerated products as e.g. mousses or whipped creams or fat-containing emulsions [16].

Thickeners are substances that cause an increase in product viscosity [18]. In contrast to gel formation, thickening takes place by an unspecific molecule entanglement of

conformationally disordered chains [11]. Above a critical overlap concentration, which mainly depends on the hydrodynamic volume of the hydrocolloid, a sharp increase of the viscosity can be observed [11,12]. Typical representatives for thickening agents are xanthan gum, guar gum, konjac mannan, locust bean gum and cellulose derivatives [12].

In this study xanthan gum, guar gum and alginate were analyzed with respect to their rehydration behavior. In the following section the characteristics of these hydrocolloids are described in more detail.

1.2.1 XANTHAN GUM

Industrially, xanthan gum is obtained from aerobic, submerged fermentation with pure cultures of *Xanthomonas campestris* or *phaeaeolis*. As an extracellular polysaccharide, xanthan gum is secreted into the fermentation broth and subsequently recovered by precipitation with isopropanol or ethanol after pasteurization. The isolated xanthan gum is dried, milled and possibly further processed to adjust different qualities with respect to rehydration behavior and appearance [19,20].

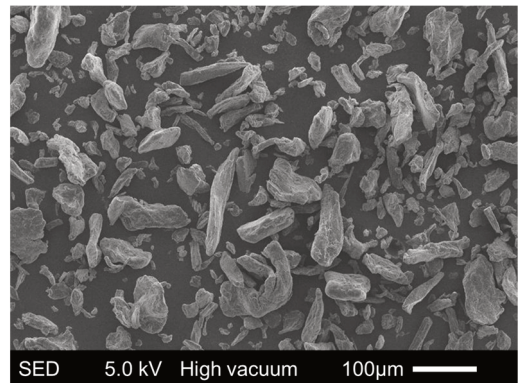


Fig. 1.1: SEM-image of xanthan gum. (Magnification: 160 x).

STRUCTURE

Xanthan gum is a white to yellowish-white powder. The xanthan gum molecule consists of D-glucose, D-mannose and D-glucuronic acid in a molar ratio of 2.8:2:2 [20]. The basic molecular structure unit is composed of a β -1,4-linked glucose chain with a trisaccharide composed of mannose-glucuronic acid-mannose on every second glucose molecule which is partly esterified with acetic- and pyruvic acid [19,20]. These side chains are negatively charged and are able to bind sodium, potassium or calcium ions. The molecular weight of xanthan gum is influenced by the fermentation conditions and varies from $2 \cdot 10^6$ - $20 \cdot 10^6$ Da [20]. Fig. 1.2 shows a schematic drawing of the basic structure of a xanthan gum molecule.

The tertiary structure of xanthan gum depends on the temperature and the ionic strength of the solution. With increasing temperature, the conformation changes from a helical rod to a disordered, more flexible structure which is a reversible process. The

rigid conformation of the xanthan gum molecules can be stabilized by low salt concentrations which leads to an increase of the transition temperature [19].

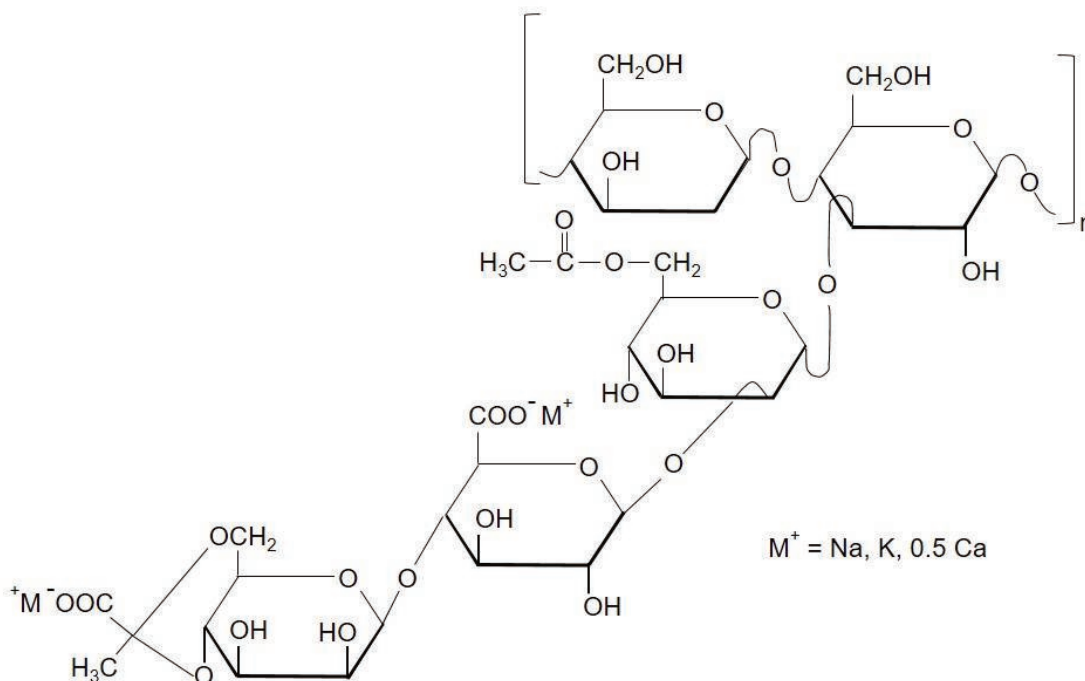


Fig. 1.2: Basic molecular structure element of a xanthan gum molecule. Adapted from [20].

RHEOLOGY AND PROPERTIES OF XANTHAN GUM SOLUTIONS

Xanthan gum is a thickening or stabilizing agent and aqueous solutions can be described as fluid gels [13]. In such weak gels the molecules start to overlap above a certain concentration which leads to the formation of aggregates and a network of entangled molecules. This network is stabilized by weak intermolecular interactions such as hydrogen bonds. Viscosity increase takes place due to the restriction of molecular flow of the hydrocolloid molecules [13].

Aqueous solutions of xanthan gum exhibit high viscosities even at low concentrations. Due to the relatively low intermolecular forces, these stabilizing structures are broken up under shear stress and the molecules are oriented in the shear flow. This leads to a decrease of the solution viscosity and explains the pseudoplastic behavior of xanthan gum solutions [13,19]. If the shear stress is removed, the initial viscosity is completely recovered. This shear thinning behavior is more pronounced with higher concentrations [19,21]. Compared to other hydrocolloids, xanthan gum solutions show a higher viscosity at low shear stress. The more pronounced shear thinning behavior of xanthan gum compared to other hydrocolloids (Fig. 1.3) is an advantageous characteristic with regard to pouring, filling or spraying operations [19].

Xanthan gum solutions exhibit a high stability against chemicals and enzymes, e.g. amylases, pectinases, peptidases or cellulases. This can be explained by the conformation of the side chains which envelop the cellulose framework and protect it against degradation [22,23].

Xanthan gum is used in a wide range of food systems due to its tolerance against high salt concentrations and its stability over a wide pH range (pH 2-12). With respect to temperature, the solution viscosity decreases with higher temperature which is reversible up to 80 °C [20]. Furthermore, the solution viscosity depends on the dissolution temperature; up to 40 °C the viscosity decreases, from 40-60 °C the viscosity was observed to increase and temperatures above 60 °C result in a decline of the solution viscosity which is attributed to conformational changes of the tertiary structure [20].

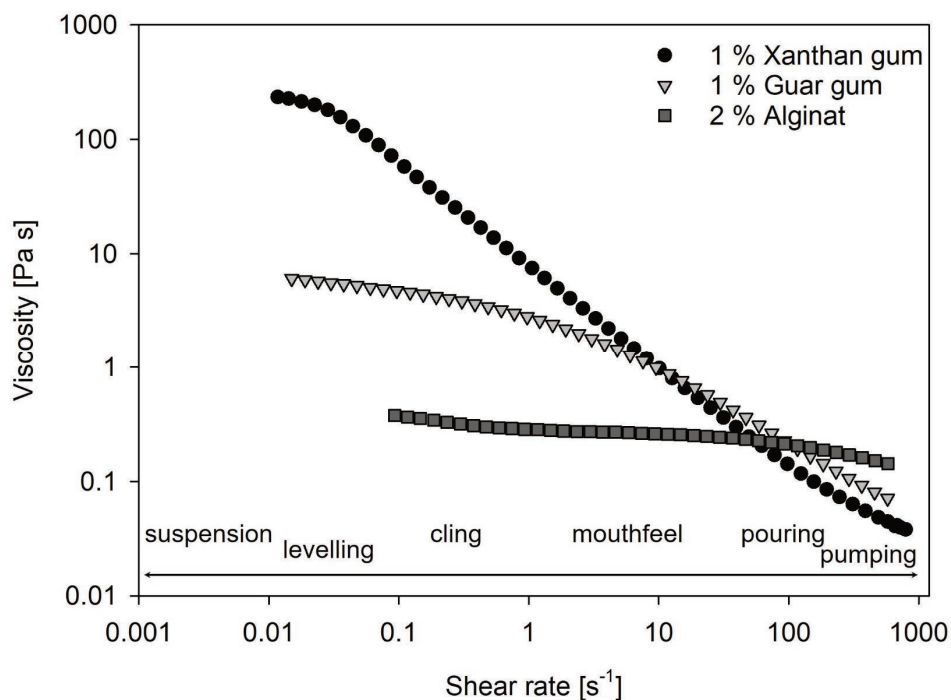


Fig. 1.3: Shear rate dependency of the viscosity of xanthan gum in comparison to guar gum and alginate solutions. Adapted from [19]

INDUSTRIAL APPLICATION

Xanthan gum is used in a wide range of industrial applications (Table 1.2). In food applications, xanthan gum is used as thickening agent and as stabilizer for suspensions and emulsions [20]. For xanthan gum no toxicological risks are known and it is allowed to use “quantum satis” [20,24]. Since the viscosity of xanthan gum is relatively independent of temperature, pH and ionic strength, it can be used in canned goods as well as in salted or pickled food preparations [19]. Furthermore, xanthan gum is used as a fat replacer in dietary products [12].

Under shear, the viscosity is reduced due to the pseudoplastic flow behavior of xanthan gum solutions. This provides a good mouthfeel and facilitates pouring, pumping and mixing processes [19,23]. An overview of applications, common concentrations and functionalities of xanthan gum is given in Table 1.2.

Table 1.2: Application and functionality of xanthan gum in different industrial sectors (modified from [18,20]).

Application	Concentration [% w/w]	Functionality
Salad dressings	0.1-0.5	Emulsion stabilizer, suspending agent, dispersant
Dry mixes	0.05-0.2	Eases dispersion in hot and cold water
Syrups, toppings, relishes, sauces	0.05-0.2	Thickener, heat stability, uniform viscosity
Beverages (fruit and non-fat dry milk)	0.05-0.2	Stabilizer
Dairy products	0.05-0.2	Stabilizer, viscosity control
Bakes goods	0.1-0.4	Stabilizer, facilitates pumping
Frozen foods	0.05-0.2	Improves freeze-thaw stability
Pharmaceuticals (crèmes, suspensions)	0.1-1	Emulsion stabilizer, uniformity in dosage formulation
Cosmetics	0.2-1	Thickener, stabilizer
Agriculture (animal feed and pesticides formulations)	0.03-0.4	Suspension stabilizer, improved sprayability, reduced drift, increased cling and permanence

Xanthan gum solutions show synergistic interactions with galactomannans such as guar gum and locust bean gum as well as with glucomannans as konjac gum. This

synergy results in an enhanced viscosity or gelation. The extent of interaction depends on the number of galactose side chains, where less galactose and more unsubstituted regions enhance the interaction [22]. Furthermore, the interaction is influenced by the xanthan gum/guar gum ratio, the pH, the ionic strength and the molecular weight of the guar gum molecules [22]. The optimum synergistic interaction is obtained with a guar gum to xanthan gum ratio of approximately 80:20 [22]. With higher total gum concentration, the synergism increases [23]. The addition of xanthan gum to a guar gum solution enhances the thermal stability and the salt tolerance, and compared to pure xanthan gum the mixtures are smoother and less expensive and thus often used in food applications [23]. Xanthan gum in combination with locust bean gum results in strong, cohesive, thermo-reversible gels with high elasticity and very low syneresis [23]. The optimal synergistic interaction is achieved between a ratio of 60:40 and 40:60 [19,23].

1.2.2 GUAR GUM

Guar gum is a plant-based hydrocolloid which is obtained from guar beans (*Cyamopsis tetragomoloba*). The endosperm of the seeds is mechanically isolated and milled. Antinutritive substances (enzyme inhibitors, phenols, saponine) which are present in the protein fraction are inactivated and removed by heating (“toasting”) or extraction. For further purification, guar gum is dissolved followed by

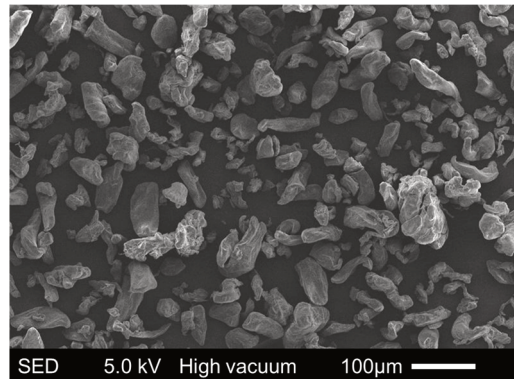


Fig. 1.4: SEM-image of guar gum. (Magnification: 160 x)

several filtration and ethanolic precipitation steps. Finally, the product is dried and milled [25,26]. Commercially, different grades are available which are classified according to color, mesh size, viscosity potential and rate of hydration [25].

STRUCTURE

Guar gum is an uncharged galactomannan, composed of 64-67 % D-mannose anhydride and 33-36.6 % D-galactose anhydride [18,25]. The linear chain of the guar molecule consists of 1,4-linked β -D-mannopyranosil units with one or several 1,6-linked α -D-galactopyranosil residues as side chains linked to approximately every second mannose molecule [25,26]. Several protein and mineral components are attached to the molecule. According to Chudzikowski [25] the molecular mass of a guar

gum molecule is ~ 200000 Da. However, for guar gum used as food additive a large variance of the molecular weight ranging from 50000-8.000.000 Dalton is reported [27]. The schematic structure of guar gum is shown in Fig. 1.5.

α -D-galactose

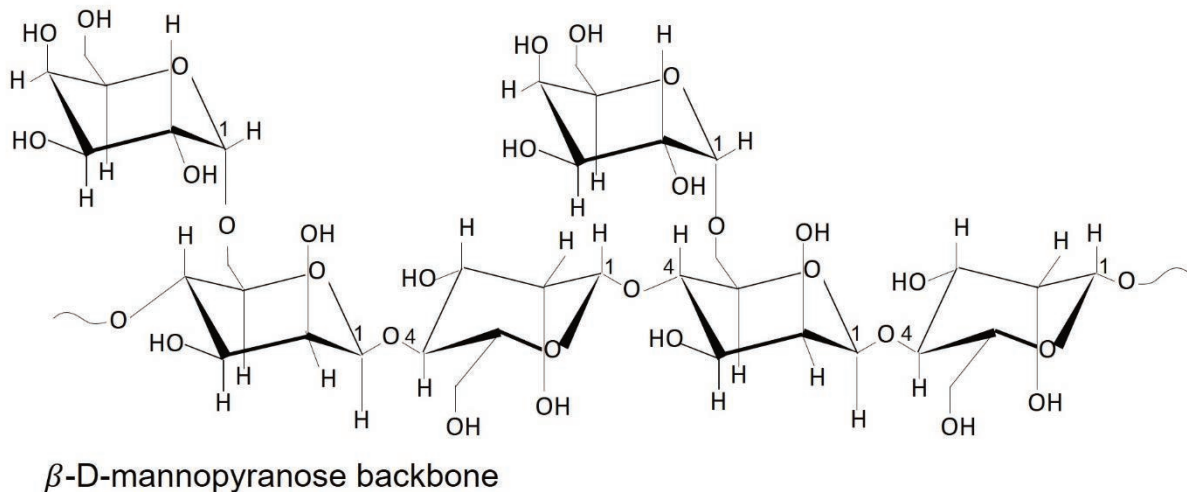


Fig. 1.5: Molecular structure of guar gum. Adapted from [26].

RHEOLOGY AND PROPERTIES OF GUAR GUM SOLUTIONS

Guar gum is known for its fast dissolution behavior, both in cold and hot water, and for its ability to form colloidal solutions. This fast solubility can be ascribed to the highly branched structure of the molecule and the galactose amount which is, with a galactose to mannose ratio of 1:2, higher compared to other galactomannans as for example locust bean gum (ratio: 1:4) [25,26,28]. The galactose units are assumed to act as “solubilizer” for the polymer due to steric effects whereas galactose-poor regions are less soluble but instead cause the intra- and intermolecular association to partially crystalline complexes [29,30]. Furthermore, the high galactose content improves the stability against acidic hydrolysis [25].

Aqueous solutions of guar gum show viscoelastic behavior and exhibit a high viscosity even at low concentrations [30,31]. In dissolved state, the mannan chains unfold to a disordered, flexible conformation [30]. With increasing concentration these chains interact with each other and an entanglement network is formed which leads to an exponential increase of the viscosity with increasing concentration [30]. Under shear the entangled guar gum molecules are oriented in the shear flow which explains the shear thinning behavior. This process is reversible and becomes more pronounced with higher polymer concentration and higher molecular weight [26,30].

Besides concentration and shear stress, the viscosity of guar gum solutions is influenced by temperature, ionic strength and pH [25]. As an uncharged molecule, guar gum is tolerant against large quantities of electrolytes and over a wide pH range [25,26]. Nevertheless, interactions between guar gum and certain ions have been observed which lead to a faster hydration rate (sodium chloride, calcium, chloride, sodium benzoate), an increase of solution viscosity (sodium benzoate) or an inhibition of hydration and a decrease of the solution viscosity (sodium sulfate) [25]. This behavior can be explained by the competition for freely available water between guar gum and the co-solutes. The higher the affinity of the salt for water the stronger the inhibition [25]. Gittings *et al.* [29] investigated the effect of salt addition on the network structure and rheological properties of guar gum solutions. Results showed that the rheological properties were only moderately affected by the addition of NaCl, Na₂CO₃, urea and NaSCN (1 M), except for a slight decrease of the complex viscosity. Scattering measurements showed an increase of the fractal dimension, indicating a more collapsed state of the polymer chains which could explain the decrease of the complex viscosity. Furthermore, it was found that the dissolution of guar gum in saline solution causes a disruption of the water molecule sheaths around the guar gum molecule. This leads to a local collapse and to the formation of a more connected network which could explain the reduced solubility of guar in the presence of salts [29].

The effect of temperature on guar gum viscosity was investigated by Casas *et al.* [31]. Within the analyzed temperature range of 25-80 °C, it could be demonstrated that the viscosity of guar gum solutions decreased with increasing temperature. This behavior was explained by a loss of hydration water around the polymer molecules which leads to a higher flexibility of the polymer chains. This process is completely reversible as the interaction between the molecules is re-established after cooling. Additionally, the effect of dissolution temperature was analyzed. It could be shown that the final viscosity increased with increasing dissolution temperature up to 60 °C. With increasing dissolution temperatures guar gum molecules with a higher mannose/galactose ratio can be dissolved. In consequence, the percentage of “smooth” mannose regions increases. This enables the formation of a higher number of intra- and intermolecular bonds and results in a higher viscosity. Dissolution temperatures higher than 60 °C resulted in a decline of the solution viscosity which was attributed to a thermal degradation, respectively to a weakening of intermolecular bonds [31].

Guar gum solutions are stable within a pH range of 1-10.5 and the viscosity is only slightly affected. The highest viscosity values are obtained at a pH between 7-9. The hydration rate, however, depends on the pH-value of the solvent; the fastest hydration is achieved between pH 6-9, whereas the slowest hydration was measured at a pH of 3.5 [25].

GUAR GUM IN FOOD INDUSTRY

Guar gum is used in a wide range of food products. Guar gum has no restriction on acceptable daily intake and is allowed to use “quantum satis” in food products up to a technologically necessary quantity [26,32]. Due to its high water binding capacity it is used as a stabilizer, emulsifier, thickening agent and to adjust rheological properties of the products [26,27,32]. Table 1.3 summarizes applications, functionalities and common concentrations of guar gum in food products.

Table 1.3: Applications, concentrations and functionalities of guar gum in food products (modified from [26]).

Application	Concentration [% w/w]	Functionality
Bread	0.5	Softness, leaf volume
Fried products	0.5-1.0	Oil uptake reduction
Yoghurt	2.0	Texture improver
Cake	0.15	Fat replacer, firmness
Sausage	0.13-0.32	Softness
Pasta	1.5	Texture improver
Ice cream	0.5	Smaller ice crystals
Baked goods	1.0	Dough improver
Tomato ketchup	0.5-1.0	Consistency improver Serum loss reduction

1.2.3 ALGINATE

Together with cellulose, alginate is a structural component of the cell wall of marine brown algae. In combination with sodium, calcium, magnesium, strontium and barium ions, insoluble gel structures are formed, which ensure strength and flexibility of the algae tissue [33]. Alginate can also be obtained from microorganisms, e.g. from some *Pseudomonas* and *Acetobacter ssp.*, where it

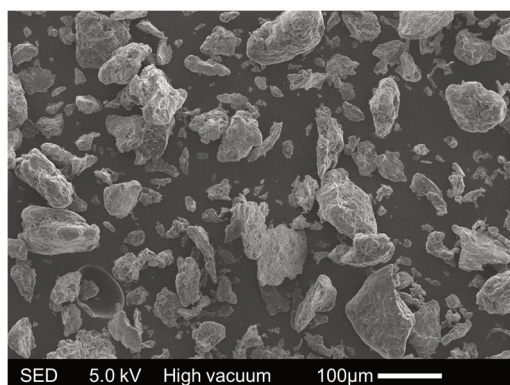


Fig. 1.6: SEM-image of alginate. (Magnification:160x).

serves as a capsule polysaccharide to protect against unfavorable environmental conditions [34]. For industrial production, alginate is extracted mainly from three different algae species, namely *Macrocystis* (west coast USA), *Laminaria* and *Ascophyllum* (Northern Europe) [34,35].

For extraction, the algae are treated with a mineral acid (0.1-0.2 M HCl) to obtain insoluble alginic acid. After washing and filtration the alginic acid is treated with alkali (Na_2CO_3 , NaOH) to convert the acid form into the soluble sodium salt. In the following purification steps, remaining algae cells are removed by filtration and centrifugation and finally, sodium alginate is precipitated by the addition of alcohol, CaCl_2 or mineral acid. In the last step the product is dried and milled [34].

STRUCTURE

Alginates are water soluble salts of alginic acid with a degree of polymerization ranging from 100-3000 which corresponds to a molecular weight of ~ 20000-600000 Da [36]. The high variability of the molecular weight can be explained by the enzymatically driven biosynthesis pathway and the depolymerization processes during extraction, e.g. by acid hydrolysis of glycosidic bonds [34]. The alginate molecule consists of unbranched 1,4-linked β -D-mannuronic acid (M) and α -L-guluronic acid (G) residues. The ratio between mannuronic- and guluronic acid varies between 1:0.4 and 1:1.9 depending on the source, the degree of maturity and the seasonal conditions. Consequently, the properties of the extracted alginate differ in terms of stiffness, elasticity and water binding capacity [33,37].

The monomeric M- and G-residues are arranged in sections consisting of homopolymeric M-blocks and G-blocks or heteropolymeric blocks of alternating M- and

G-residues [34,36,38,39]. The monomeric G-blocks are ordered in a 1C_4 , whereas the M-blocks are ordered in a 4C_1 -chair conformation [34]. Due to the different configurations, the alginate molecule consists of buckled and stiff regions in the G-blocks and flexible, ribbon-like polymer chains in the M-block regions. The heteropolymeric blocks show intermediate stiffness [36]. The molecular structure and chair conformation of alginate is shown in Fig. 1.7.

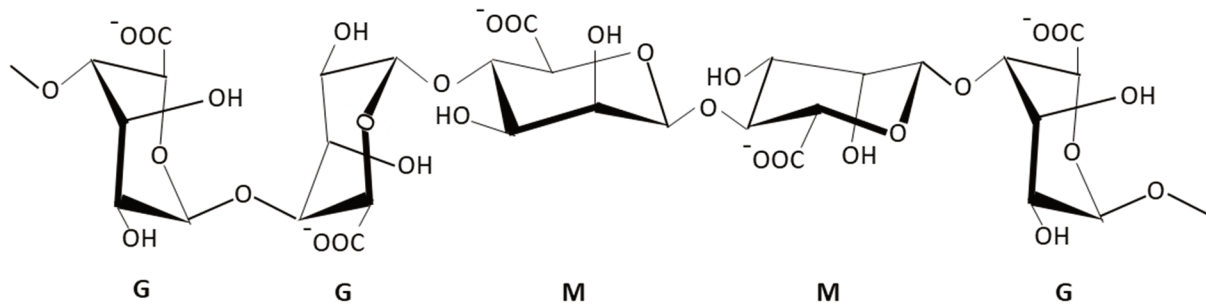


Fig. 1.7: Molecular structure and chair conformation of an alginate chain (G: α -L-guluronic acid; M: β -D-mannuronic acid). Modified from [34].

FORMATION AND PROPERTIES OF ALGINATE GELS AND SOLUTIONS

Alginates can be regarded as polyanions, which exhibit a hydrophilic character and good hydration properties. The hydration behavior is strongly influenced by the counter-ion which is associated with the alginate salt [33]. Alginate solutions are highly viscous which results from the large hydrodynamic volume that is occupied by the alginate molecules [34]. Viscosity development depends on the molecular conformation. It could be shown that an increase of the ionic strength results in a decrease of the viscosity as the alginate molecules will adopt a less extended conformation [34]. Alginate solutions show shear-thinning behavior, which can be explained by a parallel orientation of the molecules in the shear flow of the liquid [36]. Alginate gels are thermostable up to 100 °C [35]. Further temperature increase leads to a reversible decrease of the solution viscosity [34,35].

Gel formation in alginate solutions takes place due to the ion-binding ability of the alginate molecule. It could be shown that the polyguluronate molecules exhibit a selective affinity which increases in the order $Mg \ll Ca < Sr < Ba$. No selectivity was observed for polymannuronate. For this reason, it was concluded that the ions are bound not only electrostatically but also by the formation of chelate complexes [34]. These can be formed due to the structural conformation of the G-blocks within the alginate molecule. Polyguluronate blocks with a chain length of approximately 20

monomers are able to incorporate Ca^{2+} ions in the hollows which arise from their buckled conformation [28,40]. The resulting conformation, proposed by Grant *et al.* [40], resembles that of an egg-box as schematically shown in Fig. 1.8. Every Ca^{2+} ion is surrounded by and coordinated with ten oxygen atoms [34]. The interconnecting polymannuronate and heteropolymeric blocks can be considered as “solubilizing zones” [28].

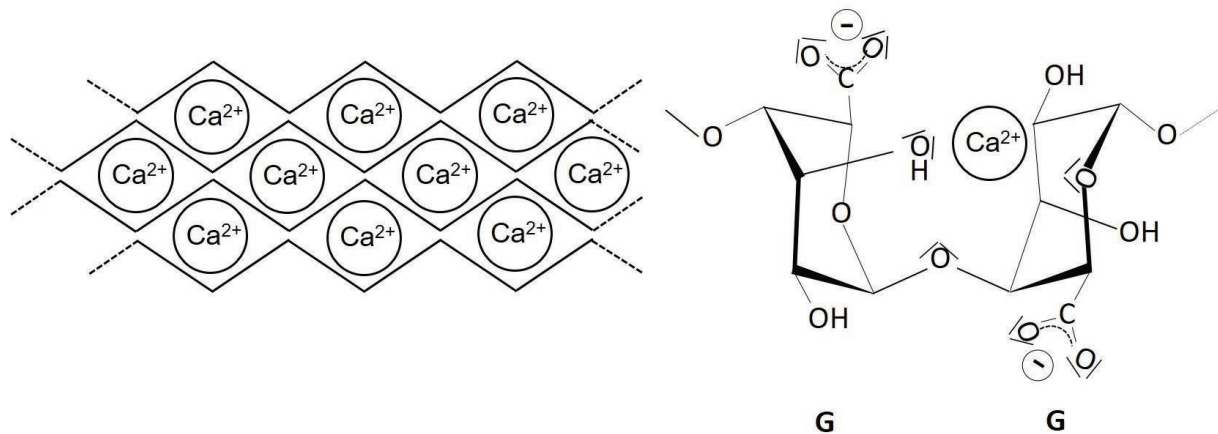


Fig. 1.8: Principle of Ca^{2+} binding and egg-box formation in alginate gels (G: α -L-guluronic acid). Adapted from [33,34,40].

The process of gel formation takes place immediately after the addition of Ca^{2+} ions to the alginate solution. This favors the formation of lumps and inhomogeneous structures. Different strategies have been developed to overcome this problem; e.g. the “dialysis method”, where Ca^{2+} ions slowly diffuse through a membrane or the “internal gelation method”, where Ca^{2+} ions are added as inactive phosphate-, citrate- or EDTA-complex, respectively as insoluble salt in combination with a slowly hydrolyzing acid (D-glucono- δ -lactone) [34].

The kinetic of gelling and the gel properties are also influenced by the type of the monovalent counter-ion and the content of guluronic acid. In general, gel formation of potassium-alginate is faster than that of sodium-alginate and increases with the content of guluronic acid due to its higher Ca^{2+} affinity compared to mannuronic acid [34].

Beside cation-induced gel formation, gelling can also be achieved by a slow addition of acids. In practice, this is done by adding slowly hydrolyzing lactones (D-glucono- δ -lactone) or by adding a mineral acid to a ionically cross-linked gel [34]. The addition of acids leads to a protonation of the negatively charged uronic acid residues which results in a reduced electrostatic repulsion. Subsequently, the homopolymeric

sequences interact and stabilize the gel network by hydrogen bonds (Smidsrød/Draget 1996, cited in [33]).

The solubility of alginate is influenced by the pH, the ionic strength and the amount of gelling ions in the solution [34]. A variation of the pH influences the electrostatic charge of the uronic acid residues. Analysis showed that alginates obtained from different sources exhibit different behavior with regard to acid solubility. These differences were attributed to variations in molecular weight, chemical composition and arrangement of the components [34,39]. A higher amount of homopolymeric blocks within the alginate molecule favors precipitation due to the formation of crystalline regions. The crystallization of heteropolymeric sequences is less pronounced, resulting in a higher acid compatibility [34,39]. Solubility is further affected by the ionic strength of the solvent. An increase, especially by the addition of inorganic salts, favors the precipitation of alginate fractions with a high amount of mannuronate residues [34]. Haug *et al.* [39] investigated the precipitation behavior of three alginate fractions which differed in their chemical composition - rich in guluronic acid (G), rich in mannuronic acid (M) or intermediate composition - by the addition of Ca^{2+} ions. The highest Ca^{2+} tolerance was found for M-rich fractions while the G-enriched fractions had the lowest tolerance. Based on these results the authors concluded that the precipitation with increasing ionic strength is influenced by the M:G ratio within the alginate molecule.

APPLICATION OF ALGINATE IN THE FOOD INDUSTRY

Alginates are generally recognized as safe and allowed to use *quantum satis* in food products [34,38]. The applied quantities typically range between 0.5-1.0 % for desserts, crèmes and fillings, 0.2-0.7 % for sauces, mayonnaise and ice-cream and 0.5-3 % for candies and snacks. In dietary products alginate is added up to 1 % [18]. Alginates are used as thickeners, stabilizers or, in combination with Ca^{2+} ions or acids, as gelling agents [33,35,38].

As thickener, alginate increases the viscosity of bakery products, especially of creams and fillings, and improves the heat stability, the freeze-thaw stability and the water-binding ability of the products [36]. In oil-water-emulsions alginate is used as a stabilizer to prevent phase separation. On the one hand this stabilizing effect is achieved by an increase of the solution viscosity, on the other hand, the alginate molecules are able to orient their more hydrophilic carboxyl group to the aqueous phase and the more nonpolar residues to the oil phase [33]. Subsequently, counter-

ions are bound by the negatively charged residues. This leads to the formation of electrical charged double layers which prevent the aggregation of the dispersed particles or droplets [33,36].

Further possible food applications of alginate are mayonnaise, whipped cream and margarine [34]. In ice-cream, alginate reduces the size of the ice-crystals to obtain a smooth mouth-feeling, prevents syneresis and improves the melting behavior [36]. To improve the emulsifying ability and stability of alginate under acidic conditions and higher Ca^{2+} contents, alginate is often used as a chemically modified propylene glycol ester, for example to stabilize salad dressings or fruit juices [36]. The gel-forming ability of alginate in combination with Ca^{2+} -ions is used to create gel structures in cake fillings, desserts and puddings. Furthermore, alginates are used to restructure food products, for example for the production of “artificial” fruits or vegetable analogs such as fried onion rings and pimiento fillings for olives [35,36]. Table 1.4 summarizes some common applications and functionalities of alginate in food products.

Table 1.4: Application and functionalities of alginate in food products (modified from [18,38])

Functionality	Application
Gel formation	<ul style="list-style-type: none"> - Restructuring of fruit, vegetables, fish and meat - Pudding, mousse and dessert - Fruit preparations, fruit fillings - Encapsulation, beads formation
Thickening /water binding	<ul style="list-style-type: none"> - Ketchup - Soups, sauces - Milk shakes - Thickened cream
Stabilizing	<ul style="list-style-type: none"> - Ice cream - Mayonnaise - Whipped cream - Baked goods
Film forming	<ul style="list-style-type: none"> - Glaze for frozen fish and meat - Coating for cakes and cookies - Coating for vegetables and fresh meats

1.3 POWDER REHYDRATION

Rehydration of food powders is usually the first step in further processing to the final product. This applies to both the industrial use of powders as intermediate products and to the use of dried convenience products by consumers. Consequently, the rehydration behavior represents an important quality parameter in terms of consumer acceptance [41–43].

In general, the rehydration process is divided into four steps. These are (1) wetting, (2) sinking, (3) dispersion and in case of soluble material (4) dissolution [44]. Depending on the applied powder mass, these steps run consecutively or overlap [44]. At the beginning the powder comes in contact with the rehydration liquid. The ability of the liquid to wet the powder surface is influenced by the contact angle between powder and liquid [45,46]. Spontaneous spreading of a liquid droplet occurs if the adhesive forces between powder and liquid are stronger than the inner liquid cohesion and the adhesive forces between powder and vapor [47,48]. Afterwards, the liquid is imbibed by the capillaries of the powder bulk. This step proceeds under the action of capillary forces and is a consequence of powder wetting [49,50]. Furthermore, wetting and liquid uptake into the powder bulk are associated with an increase of the bulk density. As soon as enough liquid has been absorbed by the powder bulk, the weight forces exceed the buoyancy, causing particles or parts of the powder bulk to sink into the rehydration liquid [51]. In the following dispersion step the particles and agglomerates are disintegrated into the primary particles and finally dissolved [44]. The velocity with which these steps proceed, and consequently how fast the rehydration process can be accomplished, is influenced by the physical powder characteristics. Under the assumption of constant conditions, the different steps of powder rehydration can be described by physical laws. However, the influence of the powder properties on the different rehydration steps is very complex. For example, contact angles and thus the wetting behavior of a powder are influenced by a variety of factors such as surface roughness, porosity or rheological properties of the liquid [45,47]. Within this study relevant aspects of powder rehydration and the influence of related physical powder properties were investigated. Their influence on the different rehydration steps is explained subsequently.

1.3.1 WETTABILITY OF POWDERS

The wettability of a powder is a decisive parameter for many processes such as drying, coating, granulation, dispersion and dissolution [45,47]. Powder wettability is often assumed to be rate-determining for the whole rehydration process. The wetting behavior is characterized by the contact angle that is formed between a liquid and a solid surface at the three phase contact line. According to Young [52], the contact angle θ is determined by the interfacial tension γ between solid-liquid (sl), solid-vapor (sv) and liquid-vapor (lv), respectively by the balance of forces between these three interfacial tensions, which is expressed by the Young's equation (Eq. 1.1).

$$\text{Young's equation} \quad \cos \theta = \frac{\gamma_{sv} - \gamma_{ls}}{\gamma_{lv}} \quad \text{Eq. 1.1}$$

Additionally, wetting can be characterized by the spreading power of a droplet on a solid surface. For ideal surfaces the equilibrium spreading coefficient (S_{eq}) depends on the equilibrium contact angle (θ_{eq}) and the interfacial tension between liquid and vapor (Eq. 1.2) [53].

$$\text{Spreading coefficient} \quad S_{eq} = \gamma_{lv}(\cos \theta_{eq} - 1) \quad \text{Eq. 1.2}$$

For $S_{eq} > 0$ the droplet is able to spread completely over the solid surface whereas for a spreading coefficient $S_{eq} < 0$ only partial wetting can be achieved

The contact angle and the spreading behavior is a characteristic property of a solid-liquid system, which under given conditions is only dependent on the three interfacial tensions of the system. This allows a quantitative characterization of the wettability of a powder by a certain liquid [47]. Depending on the contact angle the wettability is divided into different categories. The limiting value for wetting is a contact angle of 90° . Below 90° the liquid droplet spreads over the solid until a certain equilibrium contact angle is reached [47]. In general, the lower the contact angle, the better the wettability and consequently perfect wettability is achieved with a contact angle of 0° (Fig. 1.9) [54,55].

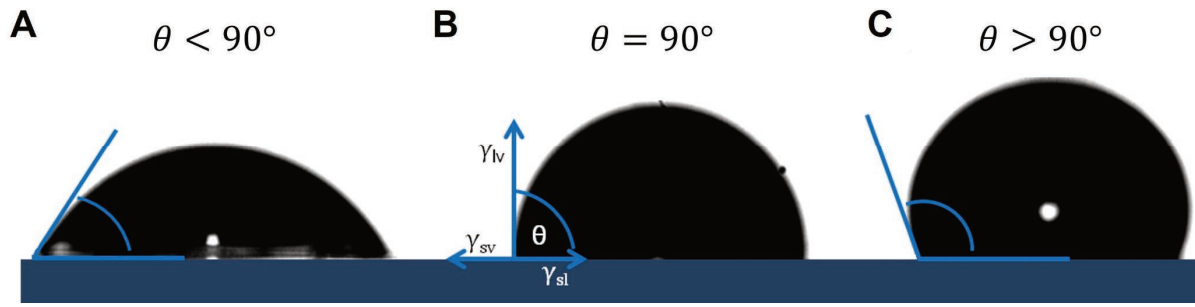


Fig. 1.9: Schematic draw of contact angles analyzed by sessile drop measurements illustrating wetting (A), limiting case (B) and non-wetting behavior (C)

For wetting the inter-molecular adhesion within the liquid phase has to be overcome and adsorbed vapor molecules on the solid surface have to be replaced by new solid-liquid bonds. Spontaneous wetting occurs if the preference for solid-liquid interactions and the strength of solid-liquid adhesion is higher than for liquid-liquid and liquid-gas interactions [47,53]. In wetting situations, the liquid is imbibed by the pores of the powder bulk. The driving force, which also influences the velocity and the height of the liquid rise, is the capillary pressure p_c [44,56].

$$p_c = \frac{4 \cdot \gamma_l \cdot \cos\theta}{d_h} \quad \text{Eq. 1.3}$$

γ_l : Surface tension of the liquid [Nm^{-1}], θ : Contact angle [$^\circ$],

d_h : Hydraulic pore diameter [m]

Assuming cylindrical capillaries and a laminar liquid flow, the liquid velocity in the capillaries can be calculated from Darcy's equation (Eq. 1.4). For fluid flow in tubes and porous layers, laminar flow is given for Reynold numbers ≤ 50 [57].

$$v = \frac{B p_k}{\eta_L h} \quad \text{Eq. 1.4}$$

v : Liquid velocity [m s^{-1}], η_L : Dynamic viscosity of the liquid,

h : Liquid height in the capillary [m]

The factor B was established by Carman and Kozeny to describe the permeability of a particle system.

$$B = \frac{\varepsilon^3 d_{3,2}^2}{180 (1 - \varepsilon)^2} \quad \text{for } 0.35 < \varepsilon < 0.7 \quad \text{Eq. 1.5}$$

ε : Porosity [-], $d_{3,2}$ = Sauter mean diameter of the particles [m]

Further requirements for the validity of Darcy's equation are a constant liquid viscosity (Newtonian fluid) and density (incompressibility), a fully developed flow profile, no-slip effects, e.g. at the capillary walls, and a negligible influence of the hydrodynamic pressure and of dynamic effects which implies a constant capillary pressure [45,58]. Combining Eq. 1.4 and Eq. 1.5, together with the Carman-Kozeny definition for the hydraulic pore diameter (Eq. 1.6), results in Eq. 1.7. This can be used to calculate the velocity v of the rising liquid based on the particle diameter d_p , the porosity ε and the constants $a_1 = 1/180$, $a_2 = 6-8$ found for spherical particles [44,59].

$$d_h = \frac{2}{3} \frac{\varepsilon d_p}{(1 - \varepsilon)} \quad \text{Eq. 1.6}$$

$$v = \varepsilon \frac{dh}{dt} = \frac{a_1 a_2 \varepsilon^2 d_p \gamma_l \cos \theta_{\text{eff.}}}{\eta_L (1 - \varepsilon) h} \quad \text{Eq. 1.7}$$

Integration of Eq. 1.7 enables the calculation of the necessary time to wet a certain height of a powder bulk, respectively to calculate the wetted height dependent on the wetting time.

$$t = \frac{15 \eta_L (1 - \varepsilon) h^2}{\varepsilon d_p \gamma_l \cos \theta_{\text{eff.}}} \quad h = \sqrt{\frac{\varepsilon d_p \gamma_l \cos \theta_{\text{eff.}} t}{15 \eta_L (1 - \varepsilon)}} \quad \text{Eq. 1.8}$$

The effective contact angle $\theta_{\text{eff.}}$ was introduced by Schubert [44]. Here, the real bulk structure was approximated by taking into account the irregular shape of the particles. The effective contact angle corresponds to the contact angle that would appear with the same liquid meniscus in a cylindrical pore with circular, constant cross section [44]. The relationship represented in Eq. 1.8 was used in a number of previous works to characterize and describe the water uptake by capillary rise. Assuming the conditions described above, it was proven to be valid and suited to describe the water uptake into powder bulks [60–63]. Additionally, the influence of different bulk porosities and particle sizes and the effect of the liquid viscosity on powder wettability was analyzed systematically using model powders and inert powder-liquid combinations [55,60,64,65].

Besides the method of capillary rise a variety of methods to analyze the wettability of powders are available which were reviewed by Alghunaim *et al.* [45]. The determination of the contact angle of a powder remains challenging as the measurement is influenced by many variables. In addition to the physical and chemical

characteristics of the liquid, the contact angle is also influenced by the surface roughness, porosity, chemical heterogeneity, sorption layers and molecular orientation of the powder sample. Furthermore, dynamic processes such as swelling and dissolution strongly influence contact angle analyses [45,47,66]. The influence of surface roughness was extensively studied in the past and several approaches to calculate the effect of roughness on the contact angle were established [45,53,67–69]. The measured “apparent” contact angle of rough surfaces deviates from the “true” contact angle that would be formed on ideal smooth surfaces. For calculation, two different cases can be distinguished. In homogeneous one-component systems the deviation from the “real” contact angle can be calculated by the Wenzel Equation (Eq. 1.9) [70], whereas for heterogeneous systems the Cassie-Baxter-Equation applies (Eq. 1.10) [68].

$$\cos \theta^* = r_r \cos \theta_{eq} \quad \text{with } r_r = \frac{\text{Surface}_{\text{real, rough}}}{\text{Surface}_{\text{projected}}} \quad \text{Eq. 1.9}$$

$$\cos \theta^* = f_1 \cos \theta_1 + f_2 \cos \theta_2 \quad \text{Eq. 1.10}$$

θ^* represents the apparent contact angle and r_r the average roughness ratio between the real and the projected area covered by the drop. In Eq. 1.10 f_1 and f_2 represent the area fractions of material 1 and 2 and θ_1 , θ_2 the corresponding contact angles of the pure materials.

Porous surface structures represent a special case of a heterogeneous system with air as second component. Entrapped air within the pores of the material always leads to a more hydrophobic character and consequently to higher apparent contact angles [67]. In this case, the Cassie-Baxter-Equation reduces to Eq. 1.11 as the contact angle between liquid and air (θ_2) is defined to be 180° .

$$\cos \theta^* = f_1 \cos \theta_1 - f_2 \quad \text{Eq. 1.11}$$

For both cases it applies that surface roughness enhances the present wetting situation; for wetting systems ($\theta < 90^\circ$) the wettability is further improved whereas for non-wetting systems ($\theta > 90^\circ$) apparent contact angles are increased [67]. Furthermore, contact angle measurements are influenced by hysteresis which describes the difference between advancing and receding contact angle. In a dynamic wetting situation, hysteresis is principally caused by surface roughness, porosity and by the heterogeneity of the solid surface [53,55]. Dynamic effects occur, for example, during capillary liquid uptake into porous material or as a result of droplet spreading

from initial to final equilibrium contact angle after the addition to a solid surface [55]. From a technological point of view contact angle hysteresis is of importance considering rehydration (wetting) and drying (de-wetting) processes [71]. To investigate the influence of the parameters surface roughness, porosity and wetting liquid in more detail, several studies have been conducted in the past. Results showed that contact angles strongly depend on the liquid velocity. With increasing liquid penetration speed the advancing contact angle progressively increased whereas the receding contact angle decreased [72]. Siebold *et al.* [72] studied the influence of different alkanes on the capillary liquid uptake. Although these liquids were assumed to be perfectly wetting liquids, measured contact angles were always higher than 0°. It could be demonstrated that the contact angles not only increased with higher liquid penetration velocities but also varied over measuring time. Based on these results they concluded that the determination of the geometrical structure constant K within the modified, mass-related Washburn equation (Eq. 1.12) and consequently the determination of the contact angle is not possible by dynamic liquid uptake measurements.

$$m = \frac{K \cdot \varepsilon \cdot d_{3,2} \cdot \gamma_l \cdot \cos \theta}{15 \cdot \eta \cdot (1 - \varepsilon)} \quad \text{with } K = \rho^2 \cdot n^2 \cdot r^4 \cdot \pi^2 \quad \text{Eq. 1.12}$$

Link and Schlünder [55] analyzed the influence of porosity on contact angle hysteresis on NaCl tablets and demonstrated that contact angles decreased with higher porosity. Kirdponpattara *et al.* [73] showed that larger voids slowed down liquid penetration speed which results in lower contact angles. Based on these results they recommended to use coarser particles for contact angle determination.

These manifold dependencies show that contact angle analyses on powdered materials are complex and difficult to interpret. The dynamic situation and the resulting hysteresis effects, which are apart from roughness and porosity also enhanced by swelling and dissolution processes, lead to a progressive deviation from the ideal surface postulated by Young [52,71]. For that reason, a reproducible contact angle determination is difficult and the measured contact angles on powders should be regarded as apparent contact angles [71,74].

1.3.2 SINKABILITY OF POWDERS

Once the wetting step is completed, particles or parts of the powder bulk start to sink into the rehydration liquid. This step is usually not rate-limiting for particles with a size $> 100 \mu\text{m}$ and a density of about 1500 kg/m^3 [44,49,50]. However, difficulties arise with fine particles or with particles with entrapped air. Such particles can be formed, for example, due to abrasion or during spray drying processes [49].

A necessary condition for sinking is that the weight forces of the powder bulk exceed the buoyancy. Here, the crucial parameter is the bulk density of the powder. For fine food powders the bulk density is typically in the range of $300 - 700 \text{ kg/m}^3$ with corresponding bulk porosities in the range of $0.5 - 0.6$. To achieve sinking conditions liquid uptake by capillary rise is necessary [51]. As consequence of the force balance, the powder bulk is drawn into the liquid if the sum of capillary and weight forces exceeds the buoyant forces.

A separate investigation of the sinking behavior of powders is difficult due to the strong dependence on the wetting behavior and further powder-water interactions such as swelling, viscosity development and dissolution.

It was found that sinking could be improved by agglomeration and size enlargement, by lecithination and by generating larger vortices in the rehydration liquid [49,50]. Recent research [75] showed that the sinking behavior is more influenced by the contact angle and the particle size than by the surface tension. In general, larger particles with higher density show faster sinking rates [2].

Mitchell *et al.* [76] studied the influence of the surface tension on the sinking behavior of maltodextrin and spray dried whole milk powder. Against their expectation it was found, that lowering the surface tension worsened the sinkability. This finding was explained by the Washburn equation. Here, the relationship between capillary liquid rise and surface tension showed that a reduced surface tension leads to a deceleration of the liquid rise. In accordance to the consideration described above, capillary forces cause counteracting drag forces which support powder sinking. Thus, if particle bulks instead of single particles are considered, the sinking behavior is not only determined by the ratio of buoyancy and weight forces but also by the velocity of the capillary liquid rise [76].

The influence of various process conditions on powder sinking was investigated in the past. Schober and Fitzpatrick [77] studied the influence of vortex formation, stirrer

position and effect of powder concentration on the sinking behavior of powders. They concluded that the creation and maintenance of a vortex is crucial for powder sinking. However, provided that enough power input can be generated by the stirrer, powder rehydration should not be limited by the sinking behavior. Vortex formation and thus sinking should be possible up to a critical powder concentration. This concentration is reached when the viscosity rises to a critical value above which the solution or dispersion behaves more like a solid than a liquid [77]. In contrast to their expectation, they observed faster sinking with higher powder concentration. This observation was explained by the higher suction effect generated by the higher power input which was required to maintain the vortex with increasing solution viscosity. Furthermore, a higher vortex depth and a stirrer position directly below the vortex was found to improve powder sinking rates. These findings confirmed previously published results of Fitzpatrick *et al.* [78,79] who additionally investigated the effect of temperature on powder sinking [79]. An increase of the temperature in the range of 20-70 °C was found to improve the sinkability and enabled the preparation of higher concentrated solutions. This correlation was explained by the reduction of the liquid viscosity with higher temperatures which raised the limiting viscosity before vortex collapse. Thring and Edwards [80] investigated the effect of different baffle configurations, impeller types, solid concentrations and stirrer positions on the minimum rotational speed for particle sinking. Results showed that sinking and maintaining the suspension state is only slightly influenced by the solid concentration or the stirrer position, while the stirrer type strongly influenced particle sinking. For optimum sinking conditions they recommended two possible set-ups: (1) One baffle in combination with a three-bladed propeller positioned at a height of 1/3 relative to the liquid height above the vessel bottom or (2) four baffles combined with a six-bladed turbine positioned at a height of 2/3 relative to the liquid height above the vessel bottom.

Besides these material- and process-based properties, sinking is further influenced by dynamic changes after powder-liquid contact [49]. Their influence is discussed in more detail in Sect. 1.4.

1.3.3 DISPERSION AND DISINTEGRATION OF PARTICLES

Dispersion describes the process of disintegrating aggregates or agglomerates into individual primary particles as well as their even distribution within the continuous phase. Dispersion represents an important task of mixing processes due to its influence on the final product quality with regard to dispersion stability and completeness of reconstitution.

The necessary shear forces for size reduction are usually generated by mechanical agitation (high shear mixers), by forcing the liquid to flow with high velocity through a narrow nozzle (high-pressure homogenizers), by the use of colloid mills or by ultrasonication [81]. A further option is the use of injector systems. For disintegration the applied shear forces have to overcome the inner-particle cohesive forces. For disintegration two possible mechanisms have to be considered. In the case that the applied shear forces exceed the cohesive forces a sudden rupture into several smaller fragments can be observed. Erosive processes, which are characterized by a slow and continuous detachment of smaller fragments from the surface, are mainly prevalent with lower shear forces [82,83].

Up to now, the disintegrating mechanisms of solid particles in agitated systems have not been completely clarified. Disintegrating forces arise from the relative movement between liquid and solid phase. They can be divided into hydrodynamic forces, which result from turbulent pressure variations, and forces which result from particle/particle-, particle/stirrer- as well as from particle/wall-collisions. The strength of the acting stress is influenced by the stirrer geometry, the rotational speed, the power input, the fluid viscosity, the particle density, the particle mass and shape as well as by the mechanical and structural properties of the solid particles [84,85].

According to Stieß [57], interactions and resulting stresses due to particle/particle-interactions can be neglected below a solid volume concentration of 0.5 %. Particle/agitator-collisions were shown to contribute most to particle disintegration as they cause highest impact stress.

Bouvier *et al.* [86] studied the influence of the rotational speed of the stirrer and of the process time on the attrition of viscoelastic pectin gel particles during dispersion in a viscous fluid. Results showed that particle damage is controlled by the mixing intensity and in particular by the number of particle/agitator-collisions. Based on these results, a power law dependency between process time and decrease of particle mass was

found. It could be shown that a minimum stress-time as well as a minimum stress-intensity is necessary for particle damage and that the extent of particle damage is influenced by the number of particle/agitator-collisions. Salas Cazón [85] investigated the damage of solid particles in an agitated vessel. The abrasion of limestone particles was analyzed as a function of stress load caused by hydrodynamic forces and particle/particle-, particle/stirrer- and particle/wall-collisions. It was concluded that hydrodynamic forces play only a minor role in particle damage. The influence of particle/particle-stress was found to be negligible below a particle volume concentration of 1 %. Particle abrasion by particle/agitator-collision was shown to be most effective. Furthermore, the influence of particle size and liquid viscosity on disintegration susceptibility was investigated. It was shown that larger particles were more easily deviated from the liquid flow path due to their mass inertia which resulted in a higher collision velocity and therefore to higher stress loads. Variation of the viscosity of the dispersion liquid showed that a higher viscosity reduced the stress load on particles resulting in a decreased disintegration efficiency [85].

An approach to model disintegration and dissolution of powders was developed by Mitchell *et al.* [87]. In this study, a focused beam reflectance measurement probe (FBRM) was used to study dispersion and dissolution of powdered solids separately. A typical shape of a FBRM curve obtained from these experiments is shown in Fig. 1.10.

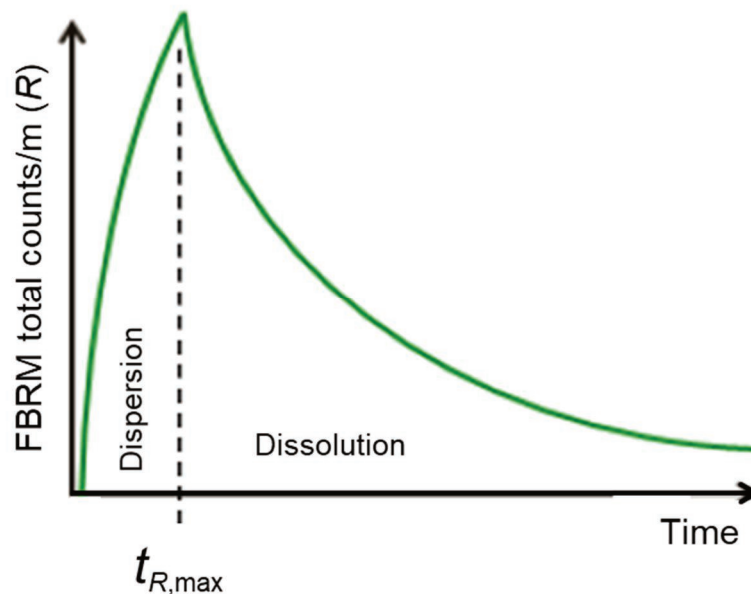


Fig. 1.10: Shape of FBRM curves obtained from rehydration experiments. Adapted from [87]

The initial increase in the number of counts was attributed to dispersion, while the gradual decrease after reaching the maximum was related to dissolution processes. For quantification of dispersion and dissolution a model was fitted to experimentally obtained FBRM curves. Dispersion was found to follow a first order reaction kinetic, dissolution could be described by a second order kinetic. By applying different agitation speeds during the rehydration experiments it has been shown that both dispersion and dissolution constants increase with higher agitation speed [87].

Similar results were obtained from own measurements [88] (Sect. 3.2.3.7). Dissolution of xanthan gum, guar gum and alginate was studied using an inline photometer. In accordance with Mitchell *et al.* [87] and Kravtchenko *et al.* [89] dissolution could be described by an exponential function.

1.4 DYNAMICS OF FOOD POWDER REHYDRATION

As described in Sect. 1.3 rehydration of powders proceeds by the steps wetting, sinking, dispersion and dissolution. Using the approach represented in Eq. 1.8, it is possible to predict the water uptake process into a powder bulk as function of the capillary pressure. The capillary pressure in turn depends on the contact angle, the particle size, the bulk porosity as well as on the viscosity and surface tension of the wetting liquid [58,90]. However, this approach is only valid under simplified assumptions, such as constant powder and liquid properties throughout the whole water uptake process (Sect. 1.3.1).

For food powders, dynamic processes especially dissolution, viscosity development and swelling lead to a continuously changing wetting situation. This in particular applies for hydrocolloids due to their gelling or thickening ability. Fig. 1.11 shows a schematic drawing of dynamic processes which take place during the reconstitution process of such powders.

After powder-liquid contact, in a wetting situation, the liquid spreads over the solid surface. Afterwards the liquid penetrates the interparticular pore system of the powder bulk. These processes depend on the spreading coefficient and thus on the interaction between the surface tension of the solid-liquid-gas phases as well as on the contact angle and the resulting capillary pressure which is responsible for capillary rise. The enlarged section in Fig. 1.11 schematically illustrates capillary liquid rise and contact angle formation in an ideal and a real capillary. Ideally, a capillary is assumed to be cylindrical with a smooth surface. In this case the contact angle is determined by the

meniscus of the rising liquid front and the capillary wall (Fig. 1.11 A). The height of the rising liquid front can then be calculated according to the Washburn-Equation (Eq. 1.8). In real powder systems, the capillaries deviate from this ideal model assumption, as indicated in Fig. 1.11 B. Due to the particle size distribution within the powder bulk and irregularly shaped particles, the capillaries commonly show alternating cross-sections, different diameters and rough surfaces. In contrast to a single ideal capillary, the pores of a powder bulk are mostly interconnected which leads to the formation of a complex capillary network. Additionally, the shape of the capillaries is often characterized by a high tortuosity which has influences on capillary liquid rise [91–93]. To be able to predict the water uptake in real powder systems, Schubert [44] introduced an effective contact angle (θ_{eff}) which takes the shape factor of the particles into account. In this way, a better approximation of the water uptake in real powder bulks could be achieved. Nevertheless, in wetting situations the determined contact angles are overestimated.

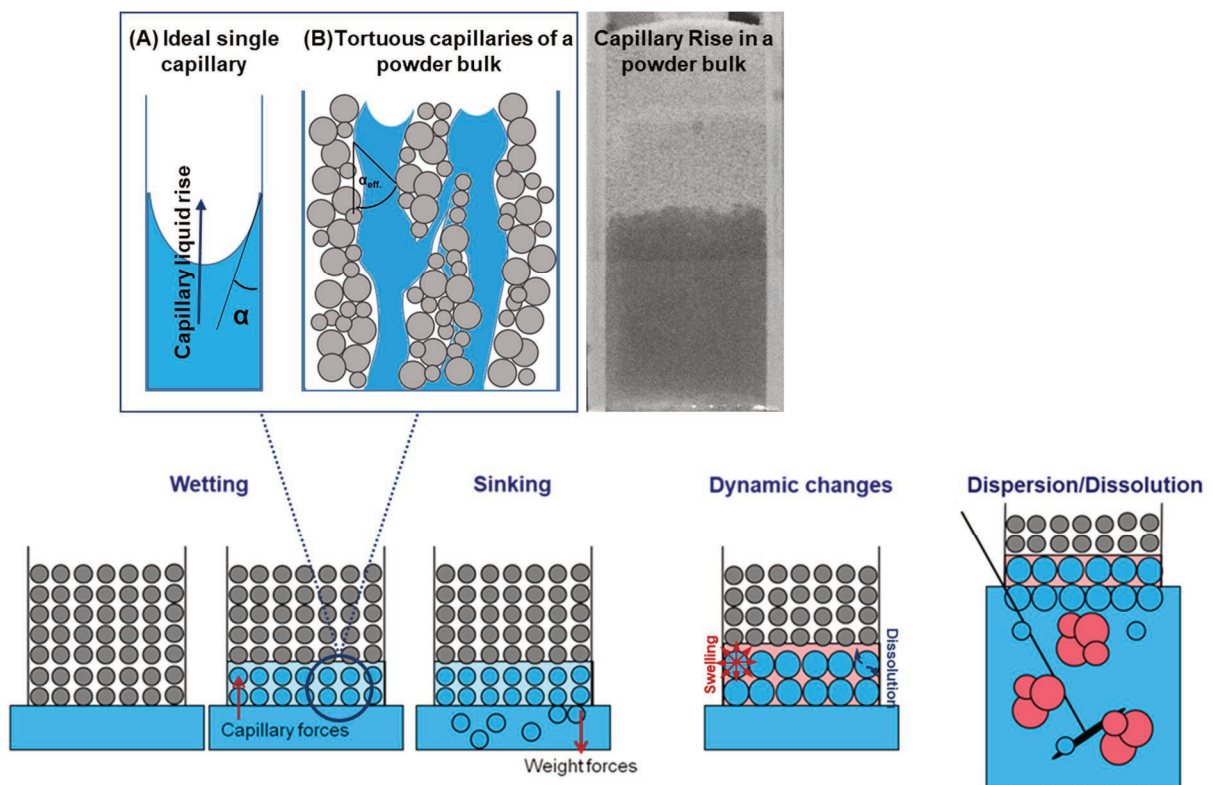


Fig. 1.11: Schematic drawing of dynamic processes during food powder reconstitution

Palzer [91] investigated moistening and wetting of several inert powder-liquid combinations. According to this study, water uptake into powder bulks can be calculated by the Washburn equation. Such porous systems can be regarded as an assembly of single capillaries. Therefore, capillary rise of a liquid into a powder bulk should follow the same principles as in single capillaries. Experimental water uptake curves were compared to theoretical calculations and a good consistency could be demonstrated. However, certain deviations between calculated and experimental data were found. In the beginning capillary rise was faster than calculated whereas in the final stage capillary rise was found to be slower than theoretically expected. This observation was assumed to arise from a dependency of the contact angle on the wetting velocity. Based on these results, it was proposed to determine a dynamic contact angle to calculate capillary rise [91].

For non-inert powder-liquid combinations, the interaction with water directly initiates swelling due to water uptake into the powder particles. Simultaneously, dissolution of hydrated molecules causes an increase of viscosity. If molecules detach from the surface of the swollen particles, the viscosity development concerns the characteristics of the rehydration liquid. However, if the cohesive forces are strong enough to inhibit a detachment, a highly viscous layer around the powder particles is formed. These dynamics and the related changes of the surface characteristics result in a change of powder wettability and in a slowdown of the liquid uptake.

Once the powder particles are wetted they should sink into the rehydration liquid. To achieve sinking conditions the powder (bulk) density has to exceed the liquid density [44]. This precondition is usually fulfilled if wetting is completed and if the pores of the bulk are filled with water. In general, this step is assumed to be noncritical and can be regarded as a consequence of wetting. However, as the different steps of rehydration take place simultaneously, powder sinking can be affected by the dynamic changes of the system. An increase of the liquid viscosity due to dissolution and a decrease of the capillary diameter due to swelling slows down or stops the capillary liquid transport. This leads to the formation of gel layers, which prevent a further penetration of water into the powder bulk and thus the sinking of powder particles into the rehydration liquid [44,94].

To avoid the formation of such floating layers, it is important to stay below the critical bulk height that can be wetted before dynamic processes cause a stop of further water

uptake [44]. Furthermore, the floating layers may also result from fast dissolving powder components which lead to a reduction of the density gradient, or from swelling processes, resulting in increased buoyancy.

Due to the viscous cohesion within the floating layer, the particles are usually no-longer dispersed into individual primary particles. Instead, the floating layer is drawn into the vortex of the stirrer which causes the formation of particle aggregates. For disintegration, the stabilizing intraparticle viscous forces have to be overcome by the applied shear forces [94].

1.4.1 SWELLING AND VISCOSITY DEVELOPMENT OF HYDROCOLLOIDS

Swelling and viscosity development are important characteristics of biopolymer powders in order to develop certain sensory properties or to improve the stability of food products. With regard to rehydration, swelling and viscosity development usually delay the process and are therefore critical in terms of process times and costs as well as the quality of convenience products.

Swelling of food biopolymers was extensively investigated by the example of starch. Starch and modified starch products are used as thickeners, gelling agents and emulsifiers and to improve mouthfeel in many industrial food applications [95]. Examples of common applications are bakery and pasta products, desserts and sauces as well as fruit fillings and jelly products [18,95].

Water transport in starch and processes during gelatinization were reviewed by Olkku & Rha [96] as well as by Ozturk & Takhar [97]. According to them, starch is able to swell below the gelatinization temperature although it is assumed to be insoluble in water. In this step the water molecules are reversibly complexed with the starch molecules by hydrogen bonds and a paste like structure is obtained [96,97]. With increasing temperature, the hydrogen bonds between the starch molecules are getting weaker until, when the initial gelatinization temperature is reached, the water can penetrate into the starch molecule. This leads to a tangential swelling of the starch granules proceeding from the hilum of the granule. Further heating leads to a progressive weakening of hydrogen bonds, further swelling and to an increase of starch solubility [96]. According to Mason [95], gelatinization describes the collapse of the molecular order within the starch molecule as a consequence of irreversible changes due to granular swelling, native crystallite melting, loss of birefringence and starch solubilization. With further heating, the starch granules continue to swell and

amylose starts to leach out of the granules into the surrounding liquid. Finally, the granular structure is completely disrupted, which is described as pasting process [95–97]. The associated changes of the starch structure lead to a change of water permeability and consequently to a change of rheological properties. According to Ollku & Rha [96], these rheological changes and increase of consistency are not attributed to swelling but primarily to the formation of a filamentous network built up by starch molecules which leaked from the granules.

Gelatinization and pasting of starch-based products is not comparable with the gel-formation process of hydrocolloid powders such as xanthan gum, guar gum or alginate. The process of swelling and, in particular, the mechanism of gel formation strongly depends on the structural characteristics of the hydrocolloid. As microbial-, plant- and algae-based hydrocolloids, xanthan gum, guar gum and alginate differ not only in their origin but especially in their molecular structure. Consequently, the way of gel-formation depends on the respective class of the hydrocolloid, the gelling conditions and the addition of additives (see Sect. 1.2).

Depending on the biopolymer and the present conditions such as ionic strength, pH-value and temperature, the viscosity can be increased either by thickening or by gel formation. Starting from an diluted situation, thickening starts above a certain concentration C^* which is connected to the intrinsic viscosity $[\eta]$ of the biopolymer by the relation $C^* = \frac{4}{[\eta]}$. The molecule chains of the biopolymer start to congregate and to form an entanglement network [11]. According to Belton [13], xanthan gum forms a weak entanglement network through the formation of hydrogen bonds. Within this network it is assumed that xanthan gum molecules aggregate and build-up double-helical structure elements. These microgel structures strongly influence the rheological behavior, e.g. shear-thinning, of the hydrocolloid solutions.

The gel-formation of alginate takes place by an ionotropic mechanism. In that case gelling proceeds only in the presence of bivalent cations, especially Ca^{2+} -Ions, which are complexed by the guluronic blocks of the alginate molecule [11,34].

The above described processes describe the gel formation due to an increasing interaction between dissolved biopolymer molecules starting from a diluted biopolymer solution. Contrary to that, for dry biopolymer particles, the starting point is a maximally concentrated, dry situation. In this case, swelling and viscosity development only take place if a liquid penetrates and consequently dilutes the particle. This water uptake

process, which is a precondition for dissolution and finally rehydration of the powder, depends on the rate of water diffusion into a particle and on the ability of the biopolymer molecules to disentangle [98]. The increasing mobility of the biopolymer molecules enables intermolecular interactions and the formation of a molecular network which is stabilized, for example, by hydrogen bonds. Within this network the liquid is incorporated and immobilized. The expansion and the increasing space requirement of the molecules, combined with the restricted mobility of the liquid and the interconnected biopolymer molecules, causes particle swelling and viscosity increase within the system. Fig. 1.12 schematically describes the process of water uptake into a biopolymer particle and the process of viscosity development in the surrounding layer.

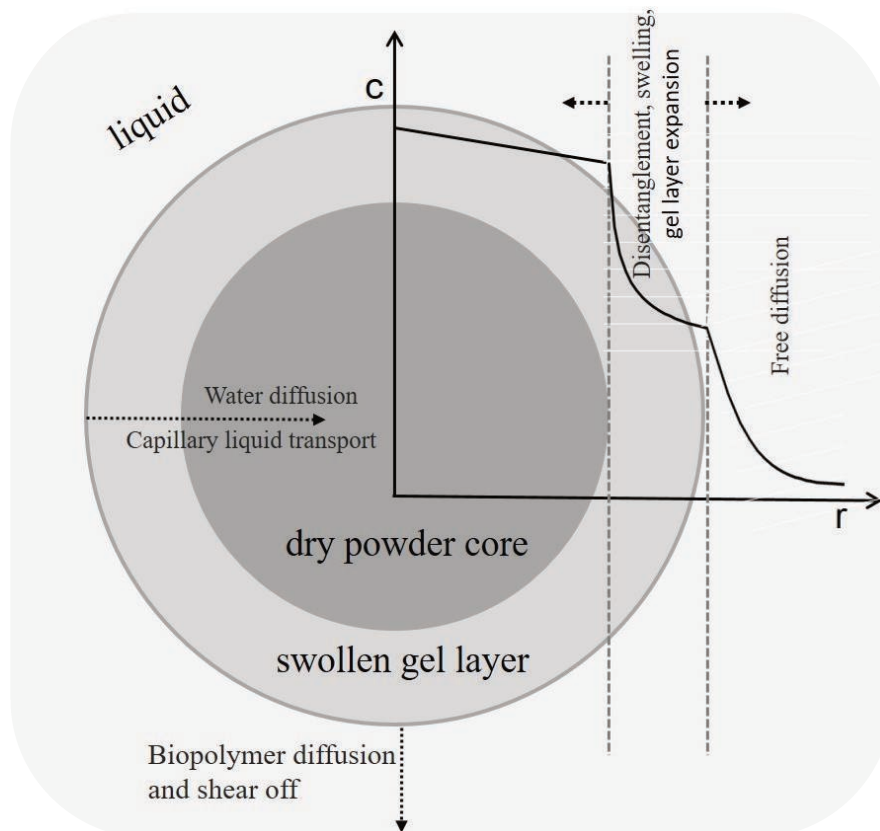


Fig. 1.12: Schematic drawing of a hydrocolloid aggregate, the mechanism of water uptake and the resulting concentration profile within the aggregate and the surrounding layer.

In case of porous biopolymer particles, water uptake is driven by capillary forces until swelling and viscosity development lead to a collapse of the porous structure. This gel layer formation has also been described by Parker *et al.* [99] and was used to explain the short water uptake times of polymer powders. In case of such a gel-layer formation process, further water uptake into the inner parts of the particle can only be accomplished by diffusion. As water uptake takes place from the out- to the inside of a particle, a concentration profile from a diluted outer region to a highly concentrated inner core develops.

Final dissolution of such hydrocolloid particles proceeds in three sequential steps: (1) diffusional supply of solvent to the dissolving surface, (2) transition from solid to solute state at the dissolution surface and (3) diffusional or convective transport of dissolved material from the particle surface into the liquid bulk [64,100]. According to Kravtchenko *et al.* [89] further steps have to be considered to describe polymer dissolution. These include, in particular, the transition from glassy to rubbery state, swelling of the rubbery polymer, disentanglement of the polymer chains from the swollen layer and finally transition of free polymer chains into the surrounding liquid. The first step of solvent penetration into the hydrocolloid particle is driven by capillary effects but mainly by diffusion as swelling leads to a rapid collapse of the pore network. Hellborg *et al.* [64] describe the dissolution of such hydrocolloid aggregates by a two-stage process: (1) Phase transition from solid to dissolved powder and (2) diffusion of dissolved material through the surrounding surface layer into the liquid.

The dissolution rate of a powder is influenced by liquid characteristics such as viscosity, density, surface tension and temperature as well as by specific material characteristics such as particle size, density, porosity and chemical composition [101]. Dissolution, solely driven by diffusional transport, is rather slow due to the usually high viscosity in the surrounding surface layer. Therefore, in industrial scale, the dissolution process is accelerated by adapting the process conditions, e.g. the stirrer speed. If attacking shear forces exceed the cohesion within the layer, they are assumed to cause an erosive detachment of hydrocolloid molecules out of the swollen layer.

Besides investigation of the contribution of diffusion on water transport processes during biopolymer rehydration, analysis of diffusion was done to obtain more insights about the structure of polymer networks and to describe and control drug release from polymer networks [98,102,103].

Diffusion is usually described by the 1. Fickian law, where the diffusion distance is proportional to the square root of time [104]. According to this approach the diffusion coefficient is constant and the diffusion rate is only a function of the concentration gradient. According to the model proposed in Fig. 1.12, the concentration, the degree of swelling as well as the properties of the gel network are changing over time. It is known that solvent diffusion in polymer gels depends on the physical properties of the polymer network and the interaction between the solvent and polymer molecules [103]. If diffusion in polymers followed the 1. Fickian law, the diffusion coefficient would be independent from the associated changes of the network structure and the involved changes of powder and liquid characteristics. For a more accurate description of diffusion processes in polymer gels further models have been proposed. These either suggest Case II diffusion where mass-uptake is linear with time [98,103] or models based on different physical principles as for example obstruction effects, hydrodynamic interactions or the free volume theory [103].

1.5 THESIS OUTLINE

The objective of this thesis was to provide a deeper understanding of the rehydration behavior of food powders. The findings should enable a more purposeful improvement and adaption of powder characteristics to consumer demands. Within this research the biopolymer powders xanthan gum, guar gum and alginate were chosen as model systems due to their difficult rehydration behavior. Powder rehydration is mainly influenced by physical characteristics. Especially their dynamic changes after contact with liquid have a significant impact on the rehydration process. Therefore, methods to analyze relevant powder characteristics were developed. Dynamic processes such as dissolution, viscosity development and swelling were investigated and correlated with the rehydration behavior.

Chapter 1 summarizes the basic fundamentals of hydrocolloids and powder rehydration. Special focus is given to the unique features of food powders.

In the first publication "*Dynamics of capillary wetting of biopolymer powders*" given in Chapter 2, the dynamic rehydration behavior of the biopolymer powders xanthan gum, guar gum and alginate was investigated. To predict the wetting behavior of dynamically changing powder systems, a model was established based on physical characteristics. The model allows a qualitative simulation and prediction of the influence of the changing parameters on capillary water uptake. It could be demonstrated that especially the interaction between the dynamic processes leads to a fast slowdown of the water uptake and to an incomplete water imbibition into the powder bulk.

Due to the importance of dynamic changing powder properties on the rehydration behavior of powders, the second publication "*Development and validation of methods to characterize rehydration of food hydrocolloids*" given in Chapter 3 focuses on methods to investigate the properties of hydrocolloids that are critical for rehydration, such as solubility, viscosity development, swellability and water uptake capacity. Furthermore, to draw conclusions about the disintegration behavior, the shear stability of hydrocolloid aggregates was assessed. The findings from powder characterization were used to explain dispersion experiments. Quantitative data are given for xanthan gum, guar gum and alginate.

In the manuscript "*Experimental investigation and simulation of rehydration dynamics of biopolymer powders*" in Chapter 4, powder rehydration was investigated based on a model system consisting of biopolymer coated glass beads. This model system

allows to systematically control and influence the extent of dynamic processes. Both experimental results and the results of the simulated parameter variation study provided deeper understanding of the dynamic processes involved in powder rehydration. Quantitative data about critical limits of the rehydration dynamics viscosity, swelling and dissolution are represented.

Chapter 5 discusses and interrelates the results presented in Chapter 2-4. The main findings obtained within this thesis are summarized in Chapter 6 and Chapter 7.

Chapter 9 contains supplementary material and unpublished data from experiments performed within this thesis. These additional data provide a more complete picture of the dynamic processes involved in the rehydration of food powders. Different methods to assess the rehydration behavior of food powders are described and evaluated with regard to their suitability for the characterization of swellable and viscosity-forming food powders.

Chapter 2 DYNAMICS OF CAPILLARY WETTING OF BIOPOLYMER POWDERS

By Julia Wangler¹, Reinhard Kohlus¹

¹ University of Hohenheim, Institute of Food Science and Biotechnology, Department of Process Engineering and Food Powders, Garbenstr. 25, 70599 Stuttgart, Germany

Published 2017 in Chemical engineering and Technology, Volume 40, No. 9, p. 1552-1560

Accessible under DOI: [10.1002/ceat.201600607](https://doi.org/10.1002/ceat.201600607)

ABSTRACT

The rehydration behavior of biopolymer powders was investigated. Problems that arise during powder rehydration, e.g. floating and formation of particle aggregates are mainly attributed to the dynamics of capillary water uptake. Common methods for analysis are too slow to assess the fast changes and do not allow conclusions about causal relationships. For a more detailed understanding, relevant powder properties were investigated. Results show that viscosity development in the rehydration liquid as well as swelling and in particular their dynamics are crucial for powder rehydration. The dynamic capillary rise was modeled based on the Washburn equation and results were linked to the physical powder characteristics. The approach allows the evaluation, whether viscosity or swelling effects lead to a critical rehydration behavior.

KEYWORDS: Capillary rise, Food powders, Hydrocolloids, Rehydration, Swelling

2.1 INTRODUCTION

Food powders are generally rehydrated before further industrial processing or consumption. This process is described by four consecutive but also overlapping steps (1) wetting, (2) sinking, (3) dispersing and in the case of soluble products (4) dissolution [8,44]. The velocity with which these four steps proceed and consequently, how fast and complete powder rehydration can be accomplished, depends on the process conditions and on the physical powder characteristics. For wetting, the liquid has to be imbibed into the pore system of the powder bulk. This step is influenced by the interfacial tension, i.e., the contact angle that is formed at the three-phase contact line. Once the wetting step is completed, particles or parts of the powder bulk start to sink. This requires the weight forces to be higher than the buoyant forces. In case of critical powders, such as biopolymers, swelling may lead to lower particle densities and higher buoyancy, which further impedes powder sinking. Therefore, water uptake by capillary forces plays an important role, not only for wetting, but also for powder sinking. The relevant physical parameters for characterization and quantification are the water uptake ability, viscosity, interfacial tension/contact angle as well as swelling behavior of the powder. After sinking, the powder particles have to be dispersed. In this step the adhesive forces between the powder particles are determining; these forces are mainly induced by viscous forces and structural effects. Finally, the dissolution behavior can be described by the diffusion coefficient and by the maximum solubility of the powder in the rehydration liquid. In general, the wetting step is assumed to be rate-determining in powder rehydration [44]. In the case of biopolymers there are further critical factors that have to be considered. In particular, swelling and viscosity development in the rehydration liquid due to dissolution lead to a continuously changing wetting situation and powder-water contact immediately induces the rapid formation of highly viscous surface layers. Further water uptake is slowed down or even stopped, which results in the formation of undispersed particle aggregates with undissolved powder inside. This leads not only to extended process times and costs but also to a quality loss of convenience products. This aggregate formation is supposed to correlate with the velocity and the maximal height of the liquid ingress in the capillaries.

The driving force for liquid uptake into porous powder systems is the capillary pressure p_c as shown in (Eq. 2.1):

$$p_c = \frac{4 \gamma_l \cos\theta}{d_h} \quad \text{Eq. 2.1}$$

in which γ_l is the surface tension of the liquid [N m^{-1}], θ is the contact angle [$^\circ$], and d_h is the hydraulic pore diameter [m].

Assuming a laminar liquid flow, the liquid velocity v in the powder capillaries can be calculated from Darcy's equation (Eq. 2.2).

$$v = \frac{B p_c}{\eta_l h} \quad \text{Eq. 2.2}$$

Here η_l is the dynamic viscosity of the liquid [Pas], h is the liquid height in the capillary [m] and B is a factor to describe the permeability of a spherical particle system established by Carman-Kozeny (Eq. 2.3):

$$B = \frac{\varepsilon^3 d_p^2}{180 (1 - \varepsilon)^2} \quad \text{for } 0.35 < \varepsilon < 0.7 \quad \text{Eq. 2.3}$$

in which ε is the porosity of the powder system [-] and d_p is the particle diameter [m].

Further requirements for the validity of the Darcy equation are a constant liquid density, a negligible influence of the hydrodynamic pressure and of dynamic effects, which implies a constant capillary pressure.

Combining Eq. 2.2 and Eq. 2.3, together with the Carman-Kozeny definition for the hydraulic pore diameter d_h ,

$$d_h = \frac{2}{3} \frac{\varepsilon d_p}{(1 - \varepsilon)} \quad \text{Eq. 2.4}$$

results in Eq. 2.5 that can be used to calculate the velocity v of the rising liquid based on the particle diameter d_p , the porosity ε and the constants $a_1 = 1/180$, $a_2 = 6-8$ found for spherical particles [44,59].

$$v = \varepsilon \frac{dh}{dt} = \frac{a_1 a_2 \varepsilon^2 d_p \gamma_l \cos\theta_{\text{eff.}}}{\eta_l (1 - \varepsilon) h} \quad \text{Eq. 2.5}$$

Integration of Eq. 2.5 enables the calculation of the time that is necessary to wet a certain height of a powder bulk, i.e., the wetted height dependent on the wetting time (Eq. 2.6):

$$t = \frac{15 \cdot \eta_l \cdot (1 - \varepsilon) \cdot h^2}{\varepsilon \cdot d_p \cdot \gamma_l \cdot \cos\theta_{\text{eff.}}} \quad h = \sqrt{\frac{\varepsilon \cdot d_p \cdot \gamma_l \cdot \cos\theta_{\text{eff.}} \cdot t}{15 \cdot \eta_l (1 - \varepsilon)}} \quad \text{Eq. 2.6}$$

The Washburn equation [90] has been used in many previous studies to analyze the water uptake by capillary rise. The influence of different bulk porosities, particles sizes and effect of liquid viscosity was systematically analyzed, mainly by using model powders and inert powder-liquid combinations [43,55,60,64,65]. Although more complex models have been developed to describe water penetration in powder bulks [105], the Washburn equation has been proved to be valid and suited to describe the basic wetting behavior of such systems. Only little research has been done to describe the capillary liquid uptake by dynamically changing powder systems such as food biopolymers [106]. In this work the rehydration behavior of food hydrocolloids was investigated with regard to relevant physical powder characteristics. The obtained data were used to simulate the dynamic situation. Results of parameter variation are shown, thereby explaining the underlying mechanism. The simulation model is based on a volume of fluid approach, which integrates results of physical powder characteristics.

2.2 MATERIAL & METHODS

The food powders xanthan gum (Satiaxane CX 801, 200mesh, Cargill, Germany; molecular weight: $> 1000000 \text{ g mol}^{-1}$), alginate (Algogel™, Cargill, Germany, molecular weight: $151200 \text{ g mol}^{-1}$, M/G ratio: 0.64) and guar gum (Lay Gewürze OHG, Grabfeld, Germany, molecular weight: $50000\text{--}8000000 \text{ g mol}^{-1}$) were analyzed with respect to their rehydration behavior. Owing to their characteristics as thickening agents they were expected to show a critical rehydration behavior. For further characterization the bulk density (ISO 60/DIN 53 466), the powder density (DIN EN ISO 1183-1 (2013-04)) and the particle size (Mastersizer 2000, Malvern Instruments Ltd., Herrenberg, Germany) were determined (Table 2.1).

2.2.1 WATER UPTAKE BY CAPILLARY RISE

Capillary rise experiments were performed to analyze the water uptake capability of the powders, which is important not only for powder wetting but also for sinking of particles into the rehydration liquid. The experimental set-up (Fig. 2.1) consisted of a container ($d = 40 \text{ mm}$, $h = 75 \text{ mm}$) into which the powder sample was added. To prevent powder sinking into the test liquid, a metal sieve (mesh size: $400 \mu\text{m}$, Haver&Boecker OHG, Oelde, Germany) and a filter paper (MN 85/70, Macherey-Nagel, Düren, Germany) were fixed at the bottom of the geometry. To achieve uniform bulk densities and bulk heights, the amount of powder was measured with a vessel ($d = 40 \text{ mm}$, $h = 10 \text{ mm}$) and then transferred into the sample holder. Following this, the geometry was placed onto a vibratory plate for 60 s (amplitude = 0.25 mm , AS 200 control, Retsch GmbH, Haan, Germany). The sample holder was fixed on a load cell (300 g , Soemer Messtechnik GmbH, Lennestadt, Germany) and moved down slowly with a linear positioner (x.act LT 100-2 ST, Qioptiq Photonics GmbH & CO.KG, Göttingen, Germany) until the geometry was exactly in contact with the liquid surface. Measurements were performed with distilled water at room temperature ($20 \text{ }^\circ\text{C}$). Increase of weight due to water uptake was recorded and used to characterize the water uptake ability of the powder sample.

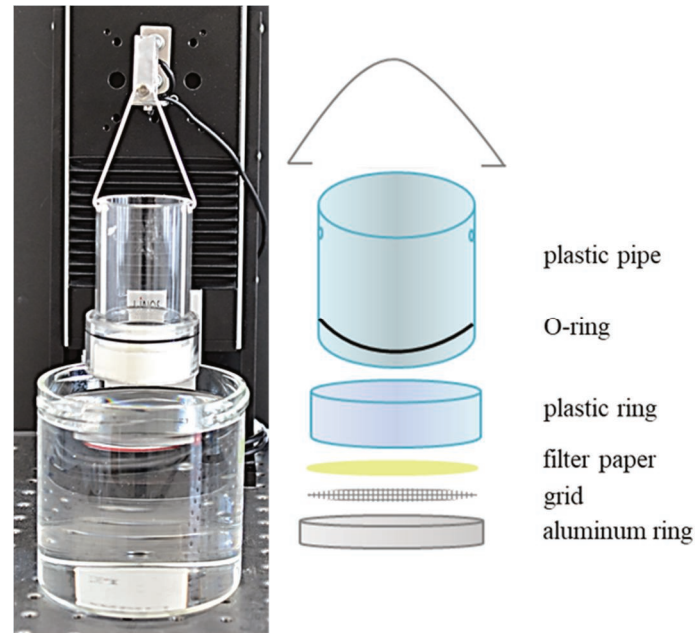


Fig. 2.1: Experimental setup of the capillary-rise experiment

Table 2.1: Powder characteristics: Bulk density, powder density, porosity and particle size

	Bulk density [kg m ⁻³]	Powder density [kg m ⁻³]	Porosity [-]	d_{10} [μm]	d_{50} [μm]	d_{90} [μm]	$d_{4,3}$ [μm]	$d_{3,2}$ [μm]
Alginate	721 \pm 0.2	1654 \pm 0.005	0.56	25.9 \pm 0.0	110.5 \pm 0.2	222.8 \pm 0.6	119.3 \pm 0.3	50.3 \pm 0.3
Alginate sieved < 80 μm				14.2 \pm 0.6	52.5 \pm 1.9	105.9 \pm 1.9	56.9 \pm 1.7	25.6 \pm 1.2
Xanthan gum	542 \pm 1.0	1511 \pm 0.002	0.64	17.3 \pm 0.3	54.1 \pm 0.6	115.2 \pm 0.9	61.0 \pm 0.5	30.6 \pm 0.6
Guar gum	594 \pm 4.0	1401 \pm 0.005	0.62	24.5 \pm 0.0	48.5 \pm 0.0	87.5 \pm 0.0	52.5 \pm 0.0	39.8 \pm 0.0

2.2.2 CONTACT ANGLE

The contact angle between the powder samples and distilled water (20 °C) was analyzed by the sessile drop method as described in the literature [47] with the following modifications. First, the biopolymer samples were dissolved in dist. water to a final concentration of 0.1 % (w/w). To obtain thin and smooth layers, 3 mL of these solutions were transferred to glass slides and dried at 40 °C in a convection oven (UF110, Memmert GmbH+Co.KG, Schwabach, Germany) for 12 h. A 10 μ L droplet (dist. water, 20 °C) was dropped from 2.5 mm height to the surface. For analysis, the initial contact angle formed between material and water droplet was recorded using a High Speed Camera (CR 600x2, Optronis GmbH, Kehl, Germany) equipped with an telecentric objective (OPTO ENGINEERING, Munich, Germany) and determined by image analysis (ImageJ, DropSnake plug-in; Version 2.1, 03.2006).

2.2.3 RHEOLOGICAL CHARACTERIZATION

Rheological characterization of the hydrocolloids was carried out to investigate the concentration-viscosity dependency and the influence of viscosity development on powder rehydration. Experiments were performed by a rheometer (Kinexus ultra, Malvern Instruments GmbH, Herrenberg, Germany) equipped with a plate-plate-geometry ($d = 25$ mm). Temperature was set to 20 °C. Viscosity-concentration-relationship was calibrated by using differently concentrated biopolymer solutions. Before measurement, these were allowed to hydrate for at least 24 h at 10 °C. The samples were transferred to the rheometer and allowed to rest for further 20 min. Shear thinning behavior was determined by shear rate ramps. Curves were fitted with an Ostwald-de-Waele equation to determine consistency value k and flow pattern index n .

The dynamic viscosifying process was investigated as described below. Double-sided adhesive tape was fixed on the upper plate and coated with a thin powder layer. Distilled water was dispensed on the lower plate to a final powder concentration of 0.04 g mL⁻¹. The shear rate was adjusted to 0.1 s⁻¹. The alginate powder was sieved to remove particles coarser than 80 μ m. The rate of viscosity development was determined from the viscosity increase over time. As the viscosity development results from dissolution processes, dissolution constants were calculated from these results by using the calibrated concentration-viscosity relationship as described above.

2.2.4 SWELLING BEHAVIOR

The swelling behavior of hydrocolloid samples was determined with a rheometer (Kinexus ultra, Malvern Instruments GmbH, Herrenberg, Germany). Sample preparation was as described above (Sect. 2.2.3). At the beginning of the measurement a defined normal force of 0.2 N was applied to the sample and the change of gap width due to swelling was recorded. Dist. water was added onto a filter paper that was fixed on the lower plate to ensure a continuous liquid availability and a uniform distribution. Measurements were performed at 20 °C. A swelling rate, defined as increase of the $d_{3,2}$ of a single particle, was determined from increasing gap width over time and calculated as described below. Powder data are summarized in Table 2.1.

1. Powder volume used for measurements

$$V_{\text{Powder sample}} = \frac{m_{\text{Powder sample}}}{\rho_{\text{Powder}}} \quad \text{Eq. 2.7}$$

2. Particle number per applied powder volume

$$\begin{aligned} N_{\text{Particle}}^* &= \frac{BD_{\text{Powder}}}{\rho_{\text{Powder}}} \cdot \frac{1}{V_{\text{Single particle}}} \cdot V_{\text{Powder sample}} \\ &= \frac{BD_{\text{Powder}}}{\rho_{\text{Powder}}} \cdot \frac{6}{\pi \cdot d_{3,2}^3} \cdot V_{\text{Powder sample}} \end{aligned} \quad \text{Eq. 2.8}$$

3. Swelling rate per single particle

During the measurements the increase of gap width over time was recorded and the volume increase of the particle collective ($SR_{\text{Particle collective}}$) was calculated from the linear section of the curve with the help of the geometric dimensions of the rheometer geometry. The volume increase of a single particle was calculated by Eq. 2.9:

$$SR_{\text{Particle, Volume}} = \frac{SR_{\text{Particle collective}}}{N_{\text{Particle}}^*} \quad \text{Eq. 2.9}$$

Based on Eq. 2.9, a $d_{3,2}$ -related swelling rate was calculated according to Eq. 2.10:

$$SR_{\text{Particle, } d_{3,2}} = \sqrt[3]{\frac{SR_{\text{Particle, Volume}} \cdot 6}{\pi}} \quad \text{Eq. 2.10}$$

2.3 SIMULATION

Simulation of dynamic capillary wetting was performed by using a one-dimensional Volume of Fluid (VoF) approach. The dynamic situation of the process mainly results from dissolution, viscosity development and swelling. This was considered by a stepwise adaption of the Washburn equation, which was used as basic equation, to the changing wetting situation. The fundamental idea of the simulation approach is the existence of a balance between the capillary forces, which were assumed to be constant, and the hydrodynamic flow resistance, which is subjected to dynamic changes. These are attributed to changing porosity, particle size and viscosity due to swelling and dissolution processes. These non-constant parameters and conditions were resolved both, temporally (t) and locally (x) (Eq. 2.11):

$$h = \sqrt{\frac{\varepsilon(t, x) \cdot d_{3,2}(t, x) \cdot \gamma_l \cdot \cos \theta_{\text{eff}} \cdot t}{15 \cdot \eta(t, x) \cdot (1 - \varepsilon(t, x))}} \quad \text{Eq. 2.11}$$

The change of porosity $\varepsilon(t, x)$ is correlated to the volume expansion of the individual particles due to swelling. For the calculation it was assumed that the volume of the powder bed remains constant, while the interparticle porosity continuously decreases. The time-dependent change of porosity was calculated by Eq. 2.12:

$$\varepsilon(t) = 1 - \frac{N \cdot \pi \cdot d_{3,2}^3(t)}{6 \cdot V_{\text{Powder}}} \quad \text{Eq. 2.12}$$

The change of the Sauter mean diameter $d_{3,2}$ and the corresponding swelling rate was calculated as described in Sect. 2.2.4.

For the simulation of the influence of viscosity on powder rehydration two parameters are regarded as significant. These are the speed of dissolution, i.e., the change of biopolymer concentration in the rising liquid and change of viscosity with hydrocolloid concentration. The former depends on the powder dissolution rate, which was calculated as described in Sect. 2.2.3. The concentration development was followed by a mass balance of dissolved hydrocolloid. The simulation model assumes that the viscosity of the rising liquid continuously increases as more powder is “absorbed” by the liquid.

For the concentration dependent viscosity rate the following correlations were found:

$$\text{Xanthan gum: } \eta = -2743 + 2749 \cdot e^{1.682 \cdot c}$$

$$\text{Alginate: } \eta = -65.55 + 27.05 \cdot e^{35.32 \cdot c}$$

$$\text{Guar gum: } \eta = -345.7 + 296.3 \cdot e^{39.37 \cdot c}$$

As dissolution is required for viscosity development, a dissolution rate was determined from viscosity development measurements and the dissolved biopolymer mass was calculated from calibration curves. The obtained dissolution constants are summarized in Table 2.2. The determination of these constants is not based on a diffusion model and only applies for this specific powder sample. In particular, particle size will have a non-trivial effect. Models describing polymer dissolution assume that this process consists of two steps. First, diffusion of the rehydration liquid into the dry polymer takes place, which leads to the formation of a swollen, viscous layer. Finally, the solid concentration within the swollen layer is progressively diluted and after a certain induction time until the critical swelling ratio is reached, the polymer molecules start to disentangle and dissolve into the rehydration liquid [107]. This critical swelling ratio was calculated from the swelling experiments by assuming that the time period of linear volume increase corresponds to water uptake/swelling of the particles (Fig. 2.5). In the further course of the experiment, a slowdown of the volume increase was observed and finally in the case of alginate a gradual decrease of the volume. The slowdown in the second phase could be attributed to a superposition of swelling and dissolution, whereas the decrease in the last step could be explained by dissolution of molecules from the swollen layer into the surrounding liquid. The end of the linear swelling section was achieved after ~100 s for alginate, ~ 90 s for xanthan and ~200 s for guar gum which corresponds to a critical water uptake of 1.6 g_{water}/g_{powder} for alginate, 5.6 g_{water}/g_{powder} for xanthan gum and 1.1 g_{water}/g_{powder} for guar gum. These values can be regarded as indicator for the critical water uptake of the biopolymers, however, these limits are strongly influenced by temperature and shear forces.

For simulation it was also assumed that the contact angle remains constant as the powder-liquid contact is always renewed due to liquid rise, as well as the effective capillary pressure and the liquid density.

Table 2.2: Physical parameters of powder samples determined from sessile drop method and rheological measurements

	Contact angle [°]	Swelling rate [$\mu\text{m s}^{-1}$]	Viscosity rate [Pa s^{-1}]	Dissolution rate [$\text{m}^{-2} \text{s}^{-1}$]
Alginate	49.3 ± 2.7	10.0 ± 0.4	1.68 ± 0.09	89.610 ± 9.875
Xanthan gum	69.8 ± 9.7	19.0 ± 0.8	0.20 ± 0.01	9.736 ± 0.501
Guar gum	56.3 ± 5.3	8.0 ± 0.7	4.69 ± 0.44	99.749 ± 13.682

2.4 RESULTS & DISCUSSION

2.4.1 WETTING BEHAVIOR

The water uptake capability of alginate, xanthan gum and guar gum was assayed by capillary rise experiments. A higher water uptake capability is assumed to correlate with a better sinking behavior and a reduced lump formation, thereby, improving the whole rehydration process. Results from capillary rise experiments are shown in Fig. 2.2. The course of the linear water uptake rate over time illustrates that the liquid is imbibed only during the first moments after contact with water. It cannot be avoided that the increase of the water uptake rate from the first contact to the maximum of the curve is influenced by the construction of the experimental set-up, especially by the water uptake of the filter paper. Subsequently, water is absorbed by the powder particles, which is expressed by a continuous decrease of the water uptake rate. This decrease can be explained by an increase of the liquid viscosity due to powder dissolution as well as swelling effects. According to Eq. 2.6 both effects cause a decrease of the velocity of the liquid rise and consequently longer rehydration times. Usually, results from capillary rise experiments are used to describe the wettability of powders with regard to wetting time, wetted height and contact angle. But within these experiments no linear correlation between time and squared mass of water uptake was observed, which elucidates the limitations of the classical Washburn approach to characterize such powder systems [58,108]. To be able to compare the wetting behavior of these samples a wetting time parameter was introduced. This time was defined as period between the beginning of the water uptake (maximum of the curve) and the point in time when it was slowed down below 0.3 mm s^{-1} which represents the lower resolution limit of the measurement. These wetting times were 1.0 s for xanthan gum and 0.8 s and 1.2 s for alginate and guar gum, respectively, with a total water uptake of 5.7, 6.5, and 7.6 g, respectively. From these results, it can be concluded that

the powders do not differentiate greatly with respect to water uptake ability. However, as results from further measurements showed, characteristic differences could be found in their dynamic rehydration behavior. These findings indicate that the capillary rise method is not exact enough to establish the differences in the dynamic behavior. For that reason, it is recommended to preferably analyze the dynamic capillary effects by investigating the swelling and viscosifying behavior instead of a direct capillary rise measurement. The short water uptake times and wetting heights further indicate that changes in the powder bulk may lead to a collapse of the pore network, so that further water uptake can only be accomplished by diffusive processes. Rehydration of polymer powders was also investigated by following procedures from the literature [99]. Here, the slow rehydration is explained by swelling and gel layer formation, which initiates “pore-blocking conditions” directly after powder-liquid contact. This observation would explain the short water uptake times of the analyzed biopolymer powders.

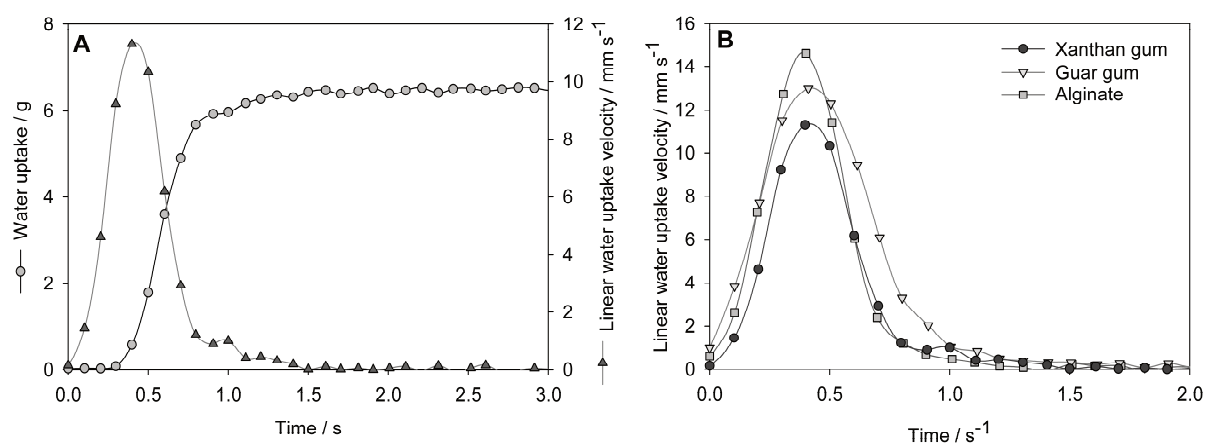


Fig. 2.2: Capillary rise experiment. A: Water uptake (H_2O_{dist} , 20 °C) and water uptake rate of xanthan gum powder (200 mesh). B: Linear water uptake rate of xanthan gum, guar gum and alginate powder

The contact angle between powder and rehydration liquid is an important parameter for powder wettability. A contact angle below 90° indicates wetting behavior, above 90° non-wetting behavior, and a contact angle of 0° means perfect wettability. Contact angles were determined on coated glass slides. As described in Sect. 2.2.2, sample preparation included dissolution and drying, which eventually could cause a change of the wetting behavior of the biopolymer sample. Compared to other sample preparation techniques, which were tested previously, e.g., contact angles on powder beds or thin powder layers (data not shown), this method proved to be the most representative and reproducible way for characterization, as surface roughness and sinking of the droplet into the sample could be minimized. Results are summarized in Table 2.2. All

biopolymers showed a contact angle below 90° , which means wetting conditions. This result was expected as these biopolymers show fast property changes after liquid contact, which requires wettability. Nevertheless, the determined contact angles, especially for xanthan gum with a contact angle of $69.8 \pm 9.7^\circ$, are quite high. A possible explanation could be the formation of a viscous layer immediately after contact with water which hinders the droplet from spreading further.

2.4.2 RHEOLOGICAL CHARACTERIZATION

Concentration dependent viscosity increase of biopolymer solutions is shown in Fig. 2.3. As curves show, viscosity and concentration are related by an exponential function in the analyzed concentration range. The rise in viscosity with increasing concentration can be explained by stronger interparticle interactions and molecule entanglement. The curves obtained from shear rate ramps were fitted with an Ostwald-de-Waele approximation. Especially for xanthan gum a strong shear thinning behavior was confirmed, which was further increased with higher concentration.

Time dependent viscosity development of the hydrocolloid samples was analyzed by rheological measurement as described in Sect. 2.2.3. The formation of difficult to dissolve particle aggregates during rehydration is favored by viscosity development. Viscous forces not only promote the aggregation of the particles, but viscous layers around these aggregates also slow down further water uptake. Both processes result in longer rehydration times, especially with regard to the dispersion process. Results from viscosity development analysis are summarized in Fig. 2.4 and Table 2.2. The viscosity development rate was determined from the initial linear section of the viscosity versus time curve. For a better comparison, the results are depicted as relative viscosity increase, based on the initial value. On comparing the viscosity development of the hydrocolloid samples, an approximately tenfold faster rate was found for guar gum compared to xanthan gum. Further differences were found in the time interval of linear viscosity increase (Fig. 2.4). For xanthan gum a linear viscosity increase was found over 500 s resulting in a final viscosity of approximately 104 Pa s, followed by guar gum (200 s) with a final viscosity of approximately 1150 Pa s and alginate with a final viscosity of approximately 109 Pa s after 120 s. The high viscosity values further illustrate the influence of viscosity on rehydration behavior of hydrocolloids.

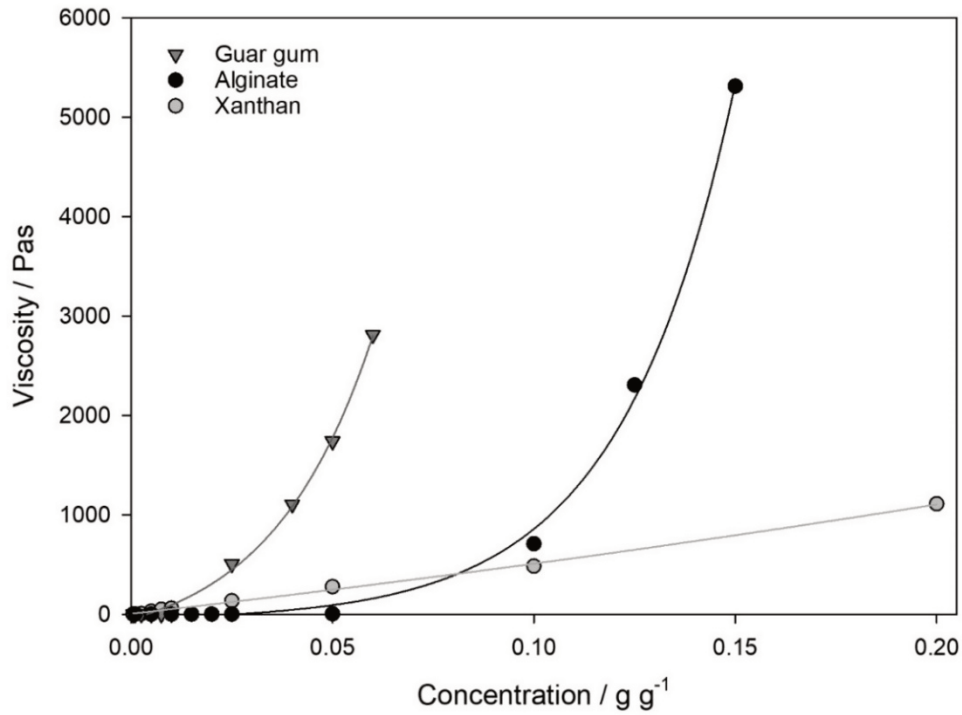


Fig. 2.3: Concentration dependent viscosity of guar gum, alginate and xanthan gum. (Plate-plate geometry, gap: 1 mm, temperature 20 °C, shear rate: 0.1 s⁻¹)

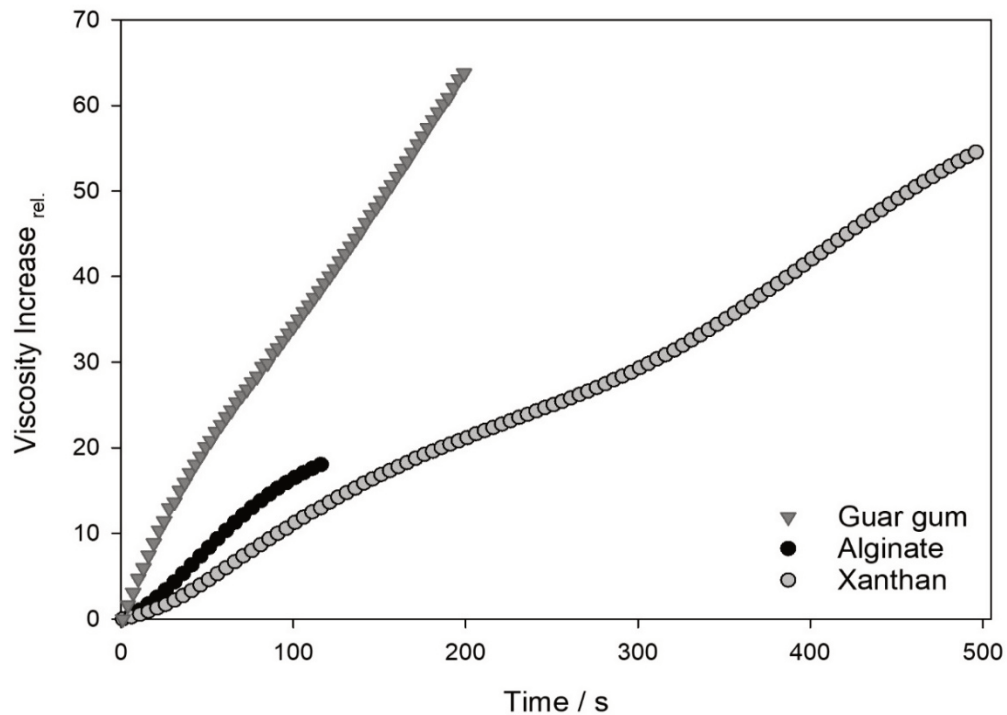


Fig. 2.4: Viscosity increase_{rel.} of guar gum, alginate and xanthan gum powder in contact with H₂O_{dist.} determined by rheological measurements. (c: 0.04 g mL⁻¹, shear rate 0.1 s⁻¹, 20 °C)

2.4.3 SWELLING BEHAVIOR

The swelling behavior of the hydrocolloid samples was analyzed by a rheological measurement set-up. Particle swelling was characterized by the increase of the gap width over time and an individual particle swelling rate was calculated from the slope of the linear section. Results are summarized in Table 2.2 and depicted in Fig. 2.5. The highest swelling rate of $19 \mu\text{m s}^{-1}$ was found for xanthan gum followed by alginate ($10 \mu\text{m s}^{-1}$) and guar gum ($8.0 \mu\text{m s}^{-1}$). Swelling causes an increase of the particle size and at the same time a decrease of the porosity. According to the Washburn equation (Eq. 2.6) this results in extended wetting times or even in cessation of further powder wetting.

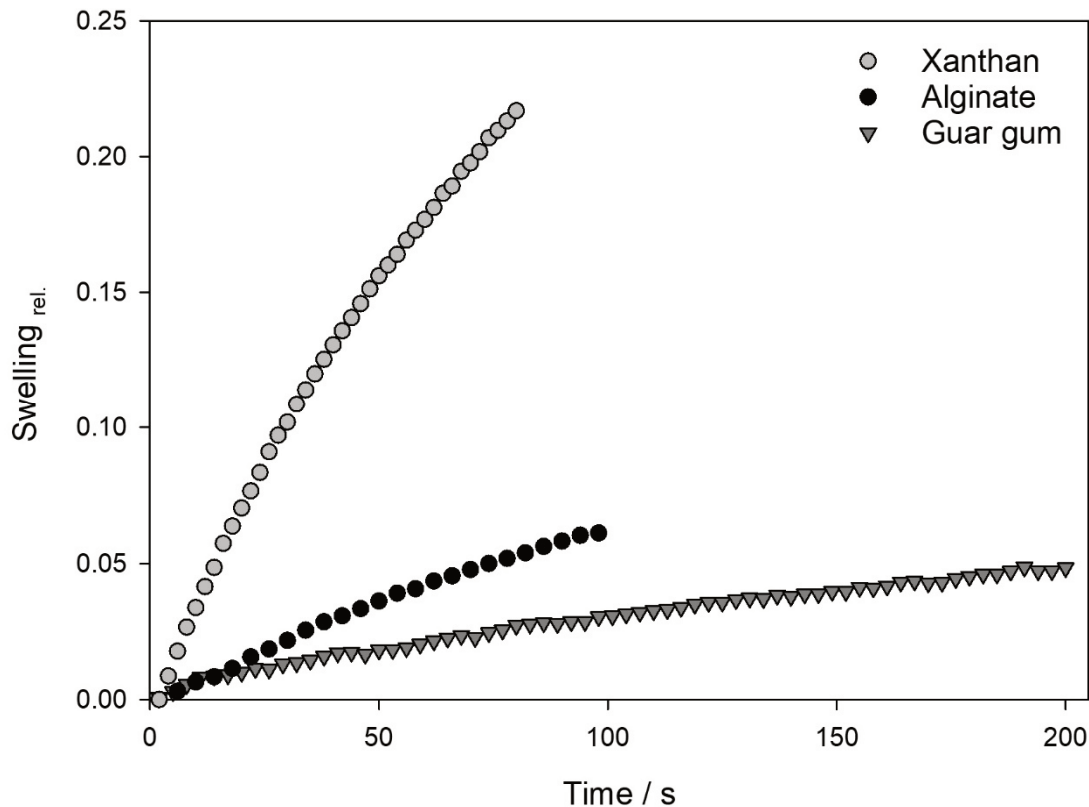
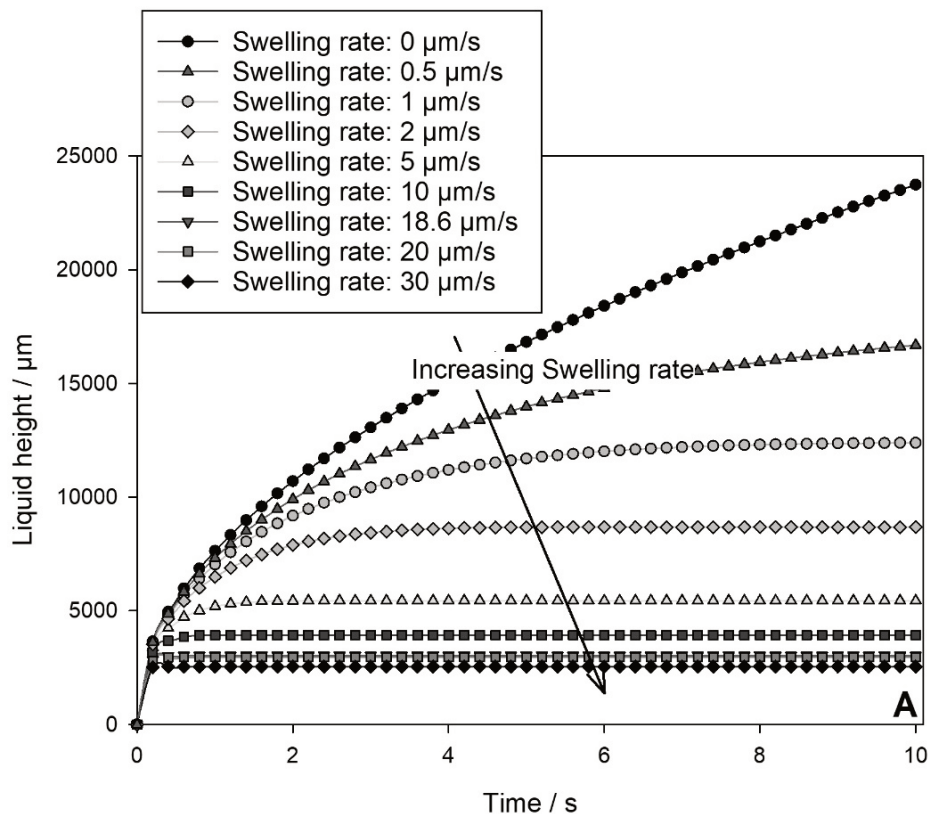


Fig. 2.5: Swelling behavior of xanthan gum, alginate and guar gum in contact with dist. water (20 °C, $c=4.0 \text{ \%}(w/v)$, Normal Force: 0.2 N)

2.4.4 SIMULATION OF THE REHYDRATION PROCESS

The dynamic water uptake of biopolymer powders by capillary rise was simulated as described in Sect. 2.3. The effect of parameter variation, specifically the influence of viscosity parameters, swellability and dissolution velocity, were studied. Results are shown in Fig. 2.6. Fig. 2.6 A shows the influence of the swelling rate. Here, the viscosity increase was neglected. As expected, swelling leads to a decrease of the water uptake rate and a decrease of the liquid rise. In Fig. 2.6 B a swelling rate of $0.5 \mu\text{m s}^{-1}$ was implemented in the model and the effect of viscosity increase was simulated. Results show that even a little viscosity increase delays water uptake and impedes liquid penetration into the powder bulk. The influence of different particle sizes is depicted in Fig. 2.6 C which illustrates the positive effect of bigger particles. In this simulation step a swelling rate of $0.5 \mu\text{m s}^{-1}$ as well as a viscosity development rate of 10 Pas g^{-1} was implemented. To conclude these simulation results, the wetted height after a rehydration time of 5 s was calculated and depicted over the respective simulation parameter. Fig. 2.7 shows that an exponential (swelling) or a power law relationship (viscosity, particle size) was found to fit the dependencies between the simulation parameters and the dynamic rehydration behavior.



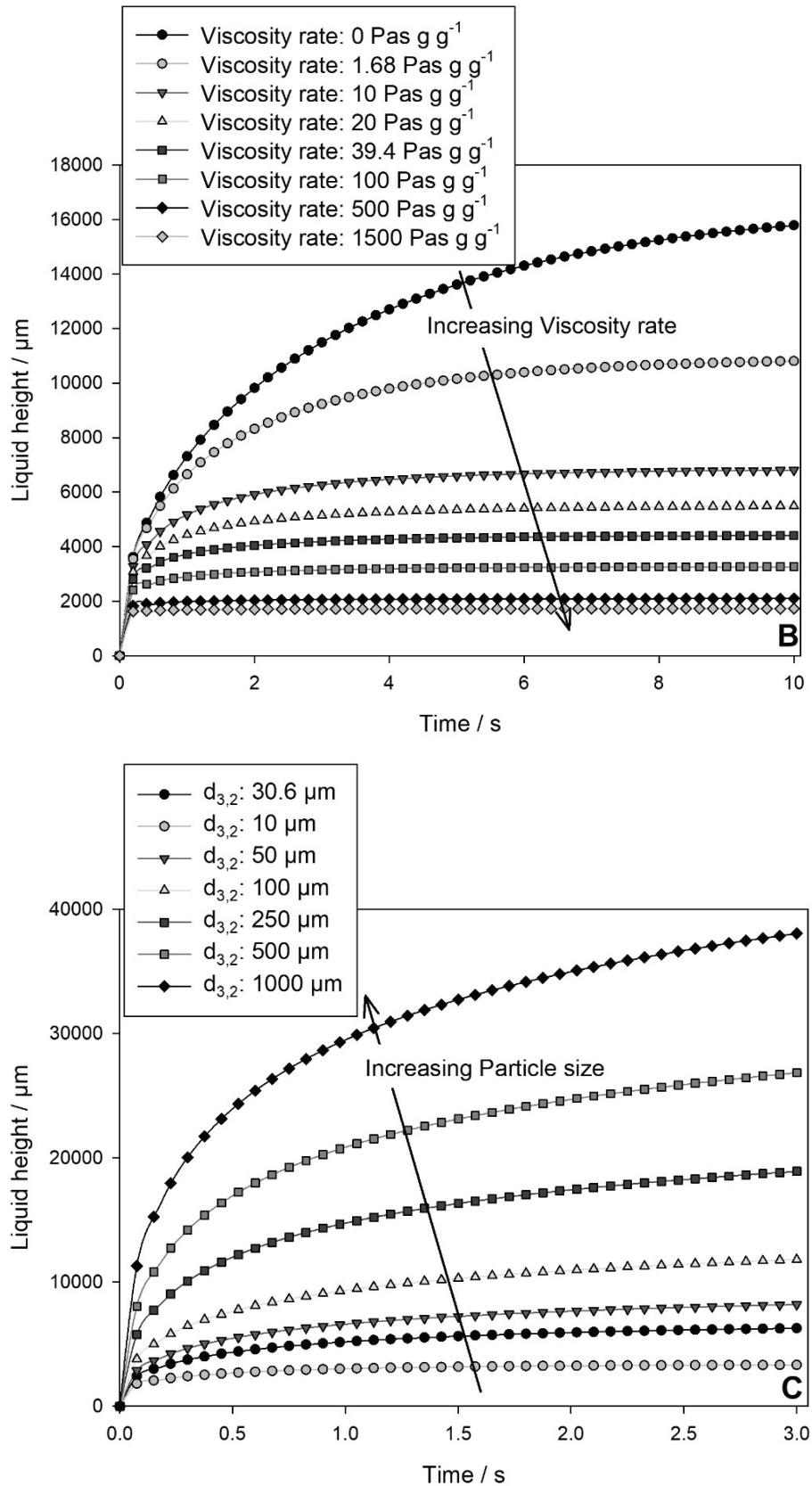
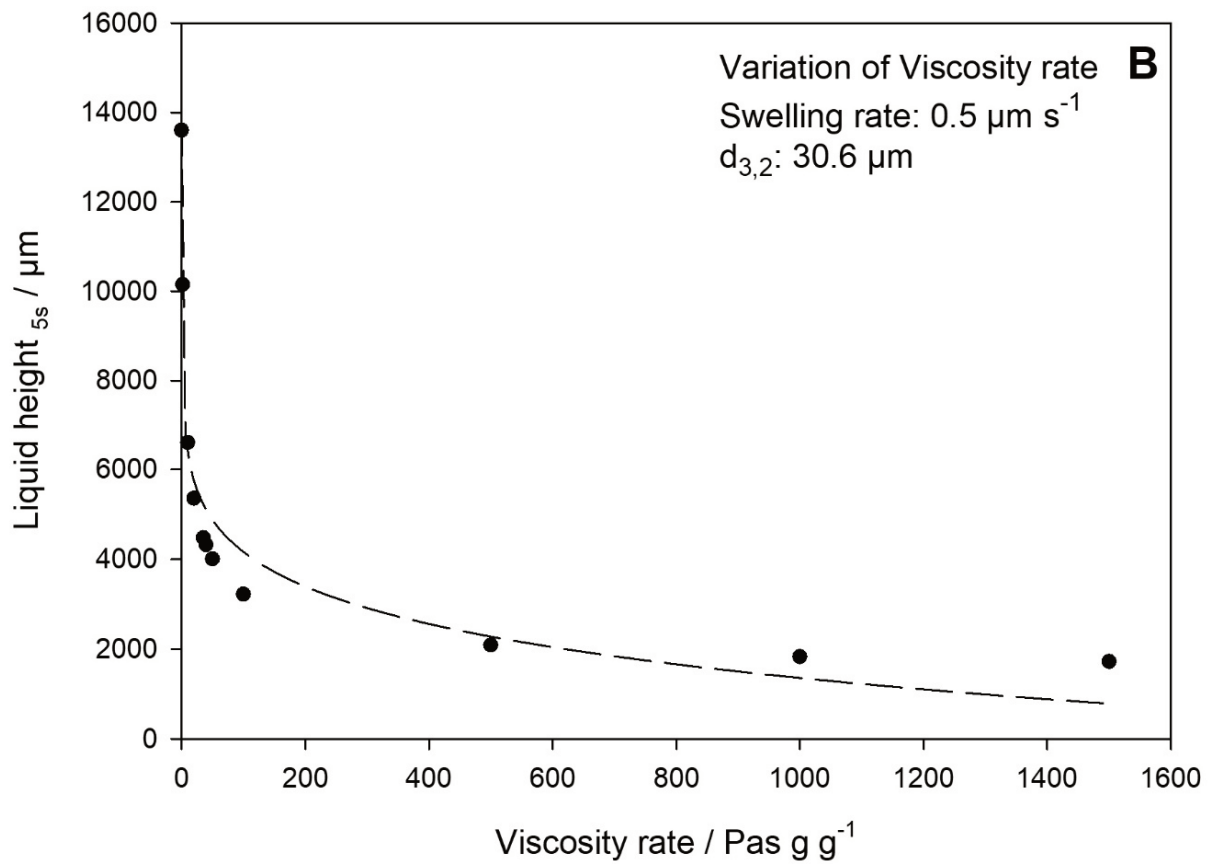
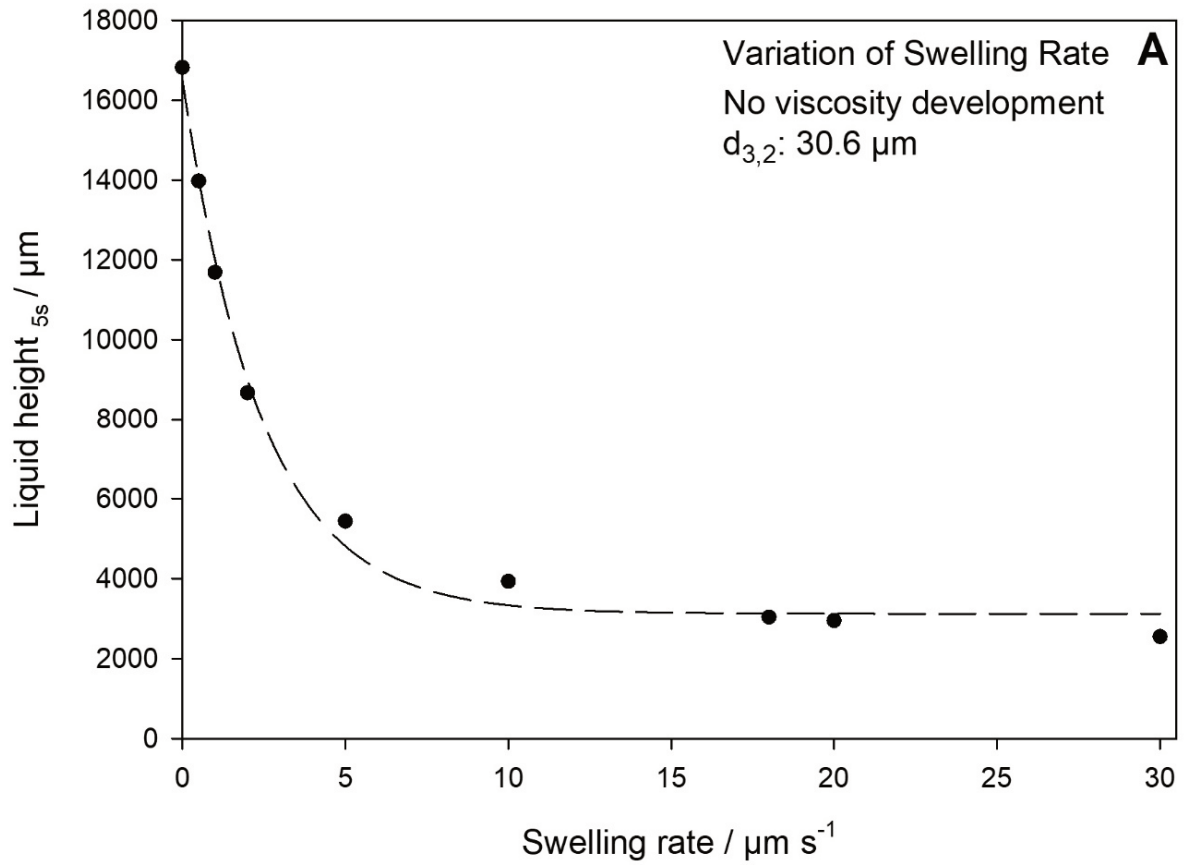


Fig. 2.6: Effect of parameter variation on dynamic capillary water uptake of powder rehydration. **A:** Influence of swelling rate (Viscosity development: 0 Pas g g^{-1} , $d_{3,2}$: $30.6 \mu\text{m}$); **B:** Influence of viscosity development (Swelling rate: $0.5 \mu\text{m s}^{-1}$, $d_{3,2}$: $30.6 \mu\text{m}$); **C:** Influence of particle size (Swelling rate: $0.5 \mu\text{m s}^{-1}$, Viscosity development: 10 Pas g g^{-1}).



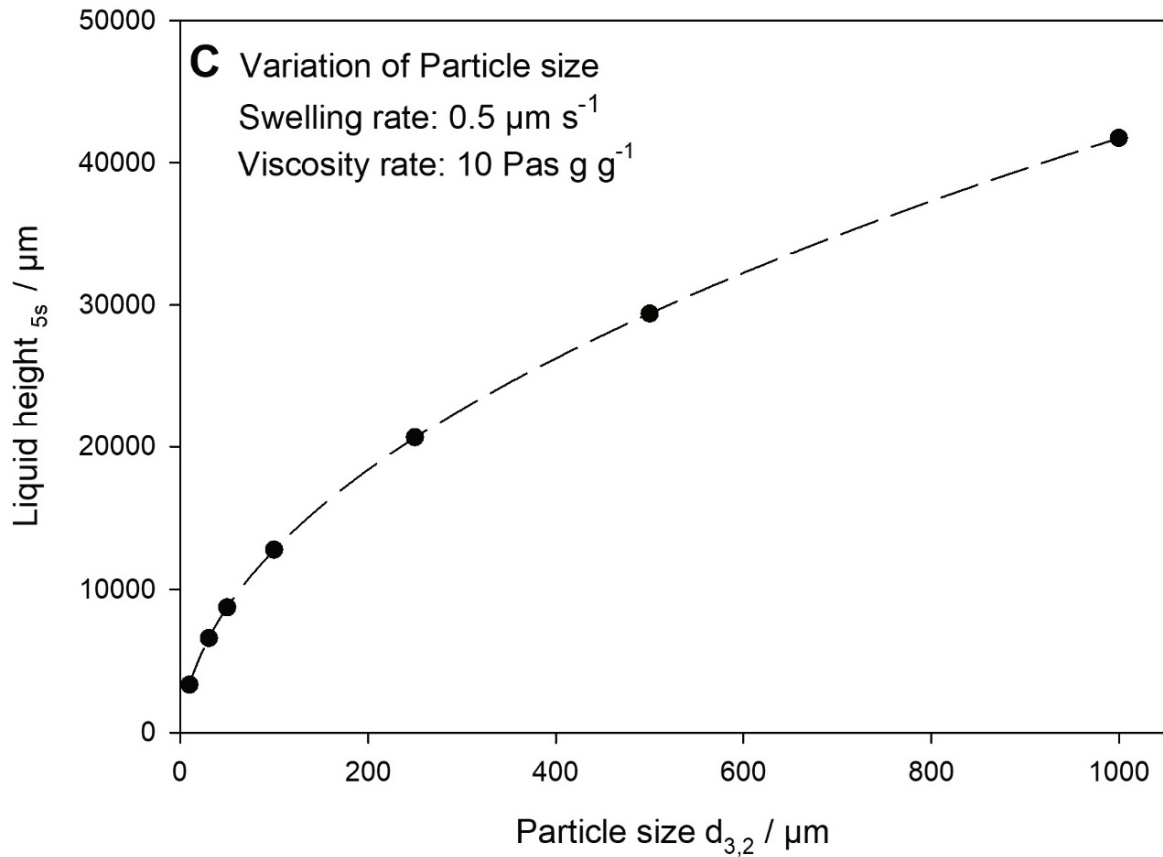


Fig. 2.7: Summary of parameter variation study. Wetted powder height after 5 s rehydration time. **A**: Variation of swelling rate (Viscosity development: 0 Pas g^{-1} , $d_{3,2}$: $30.6 \mu\text{m}$); **B**: Variation of viscosity development rate (Swelling rate: $0.5 \mu\text{m s}^{-1}$, $d_{3,2}$: $30.6 \mu\text{m}$); **C**: Variation of particle size (Swelling rate: $0.5 \mu\text{m s}^{-1}$, Viscosity development: 10 Pas g^{-1})

2.5 CONCLUSION

The rehydration behavior of the biopolymers xanthan gum, guar gum and alginate was studied. Results from physical characterization demonstrated the highly dynamic wetting situation especially with regard to viscosity development and swelling. It was found that, depending on the type of powder, specific characteristics are dominant, which is important with regard to the choice of the rehydration and dispersing strategy. For a fast rehydration, the formation of floating layers and particle aggregates with a core of undissolved powder should be prevented. Improved strategies for rehydration should focus on the separation of individual particles from each other after the initial liquid contact, e.g., by adapting the powder addition rate or the dispersing forces. Here the critical time periods depend on the specific powder characteristics. Dispersing experiments revealed that problems during xanthan gum rehydration primarily arise from swelling effects whereas guar gum rehydration is delayed by the highly viscous forces within the aggregates. To predict the wetting behavior of dynamically changing

powder systems, a model was established based on physical characteristics. The model allows a qualitative simulation and prediction of the influence of the changing parameters on capillary water uptake. It was demonstrated that the interaction between the dynamic processes leads to a fast decrease of the water uptake rate and to an incomplete water imbibition into the powder bulk, which favors the formation of particle aggregates and floating layers. In ongoing studies, the model will be further validated by parameter variation studies to allow a quantitative prediction of the dynamic rehydration behavior.

2.6 SYMBOLS USED

a_1, a_2	[-]	constants
B	[-]	permeability factor
BD	[kg m ⁻³]	bulk density
c	[g g ⁻¹]	concentration
d	[m]	diameter
$d_{3,2}$	[m]	Sauter mean diameter
h	[m]	height
k	[Pa s ⁿ]	consistency value
m	[kg]	mass
n	[-]	flow pattern index
N_{Particle}^*	[-]	theoretical particle number in powder sample
p	[N m ⁻²]	capillary pressure
SR	[μm ⁻³ s ⁻¹]	swelling rate
t	[s]	time
V	[m ³]	volume
x	[-]	local position

GREEK SYMBOLS

γ	[N m ⁻¹]	surface tension
ε	[-]	porosity
η	[Pas]	dynamic viscosity
θ	[°]	contact angle
ρ	[kg m ⁻³]	density
u	[m s ⁻¹]	velocity

SUB- AND SUPERSCRIPTS

c	capillary
h	hydraulic
l	liquid
p	particle
particle, $d_{3,2}$	single particle Sauter mean diameter
particle, volume	single particle volume
powder	powder sample

Chapter 3 DEVELOPMENT AND VALIDATION OF METHODS TO CHARACTERIZE REHYDRATION BEHAVIOR OF FOOD HYDROCOLLOIDS

By Julia Wangler¹, Reinhard Kohlus¹

¹ University of Hohenheim, Institute of Food Science and Biotechnology, Department of Process Engineering and Food Powders, Garbenstr. 25, 70599 Stuttgart, Germany

Published 2018 in Food Hydrocolloids, Volume 82, p. 500-509

Accessible under DOI: <https://doi.org/10.1016/j.foodhyd.2018.04.018>

ABSTRACT

A complete rehydration is essential for the functionality of hydrocolloids. Knowledge of powder-water-interactions at high concentration, i.e. sparse water conditions, allows an understanding of the competition for water under these conditions. This topic is of practical relevance for dispersing of swelling biopolymer particles and dough formation processes.

This study focuses on methods to investigate properties of hydrocolloids critical to rehydration, such as viscosity development, swellability and dissolution. These characteristics determine the rehydration behavior of dry products. Special consideration was given to the dynamics of these processes. Disintegration behavior of hydrocolloid aggregates was assessed and a special rheometer set-up was constructed to demonstrate the influence of shear stress. The findings from powder characterization were used to explain dispersion experiments. Quantitative data are given for xanthan gum, guar gum and alginate.

KEYWORDS: Hydrocolloids, Method development, Wetting, Rehydration, Physical characteristics, Rheology

3.1 INTRODUCTION

Hydrocolloid powders such as xanthan gum, guar gum and alginate are widely used in industrial applications to influence the structure and the rheological behavior of foods, cosmetics and pharmaceutical products. Their application affects the viscosity in order to achieve certain sensory characteristics or to increase the product stability. Usually, the use of small concentrations (0.05-1 %) is sufficient to achieve the desired product characteristics [20]. However, to develop these special structures, a preferably complete rehydration of these powders is necessary. In general, powder rehydration is divided into the four steps (1) wetting, (2) sinking, (3) dispersing and in case of soluble products (4) dissolution [8,44]. Wetting, which is often considered to be rate-limiting, is determined by the force balance on the three-phase contact line, respectively the resultant contact angle between powder and liquid. Further liquid imbibition into the powder bulk is achieved by the action of capillary forces. This liquid transport additionally enhances powder sinking and dissolution [64]. The capillary liquid transport is described by the Washburn-Equation [90] (Eq. 3.1), which balances the capillary pressure and the hydrodynamic flow resistance.

$$h = \left(\frac{\varepsilon \cdot d_p \cdot \gamma_l \cdot \cos\theta_{\text{eff}} \cdot t}{15 \cdot \eta_l (1 - \varepsilon)} \right)^{1/2} \quad \text{Eq. 3.1}$$

Here, the liquid height in the capillaries (h) is described as a function of the physical characteristics: porosity (ε), particle diameter (d_p), surface tension of the liquid (γ_l), contact angle (θ) and liquid viscosity (η_l). In the case of hydrocolloid rehydration, dissolution, viscosity development and swelling lead to a continuously changing wetting situation and the tendency to form aggregates is assumed to correlate with the velocity and extent of these dynamic changes. The stability of these aggregates as well as the necessary shear forces and time for disintegration, is correlated with these powder characteristics. After powder-liquid contact the powder is wetted and liquid imbibition into the powder bulk takes place. Simultaneously, dynamic changes of the powder properties are taking place. Dissolution causes an increase of the liquid viscosity and swelling causes a decrease of the bulk porosity. According to the Washburn-Equation (Eq. 3.1) both processes lead to a slowdown of further water uptake. The high swellability of hydrocolloid powders often ends in a breakdown of the pore system of the powder bulk [43]. As a result, further water penetration is stopped and the formation of particle aggregates with undissolved powder particles inside and

a highly viscous surface layer can be observed. These viscous forces determine the cohesion within the aggregate.

A better understanding of the critical powder characteristics and their dynamic behavior would facilitate the control of product properties, respectively to adapt the process parameters to increase the process efficiency. Methods to investigate the critical characteristics of such dynamically changing powder systems need to be further investigated. The aim of this study is to present methods to investigate relevant powder characteristics with special focus on their dynamics. The hydrocolloid powders xanthan gum, guar gum and alginate were used as model systems. Methods to investigate the water uptake, the viscosity development and swelling behavior were established. An NMR-method was used to investigate water binding strength and to draw conclusions on the stability of the hydrocolloid aggregates. A rheological measurement set-up was developed to illustrate the different rehydration steps. Finally, dissolution experiments were performed to transfer theoretical findings to real mixing processes.

3.2 MATERIAL & METHODS

3.2.1 MATERIALS

The food powders xanthan gum (Satiaxane CX 801, 200 mesh, Cargill, Germany), alginate (Algogel™, Cargill, Germany) and guar gum (Lay Gewürze OHG, Grabfeld, Germany) were analyzed regarding their rehydration behavior. Due to their characteristics as thickening agents, they were expected to show a critical rehydration behavior. For further characterization the bulk density (ISO 60/DIN 53 466), the powder density (DIN EN ISO 1183-1 (2013-04)) and the particle size (Mastersizer 2000, Malvern Instruments Ltd., Herrenberg, Germany) were determined (Table 3.1).

3.2.2 PREPARATION OF MODEL HYDROCOLLOID GRANULES

Hydrocolloid powders were high-shear granulated and sieve-fractionated to eliminate the influence of different particle sizes and to improve the mixing behavior during NMR measurements. Granulation was performed in a high-shear mixer (EL1, Maschinenfabrik Gustav Eirich GmbH & Co KG, Hardheim, Germany) and binding agent (26 % (w/w), distilled water) was added to 300 g powder by spraying ($d_{\text{Nozzle}} = 0.4$ mm, Düsen Schlick GmbH, Untersiemau/Coburg, Germany) with a flow rate of 62.94 mL/min. Granulation was performed with a pin agitator with a rotor tip speed of 20 m/s and vessel speed was set to 0.7 m/s in counter-rotation. After granulation the product was dried at 60 °C in a convection oven (UF110, Memmert GmbH+Co.KG, Schwabach, Germany) for 12 h.

3.2.3 METHODS

3.2.3.1 WETTING BEHAVIOR

CAPILLARY RISE EXPERIMENT

Capillary rise experiments were performed to analyze the water uptake of the powders, which is not only important for powder wetting but also for sinking of particles into the rehydration liquid. The experimental set-up consisted of a container ($d = 40$ mm, $h = 75$ mm) into which the powder sample was filled. To prevent powder sinking into the test liquid, a metal sieve (mesh size: 400 μm , Haver&Boeker OHG, Oelde, Germany) and a filter paper (MN 85/70, Macherey-Nagel, Düren, Germany) were fixed at the bottom of the geometry. To achieve uniform bulk densities and bulk heights, the powder amount was measured with a vessel ($d = 40$ mm, $h = 10$ mm) and transferred

into the sample holder. Then the geometry was placed onto a vibratory plate for 60 s (amplitude = 0.25 mm, AS 200 control, Retsch GmbH, Haan, Germany). The sample holder was fixed on a load cell (300 g, Soemer Messtechnik GmbH, Lennestadt, Germany) and moved down slowly with a linear positioner (x.act LT 100-2 ST, Qioptiq Photonics GmbH & CO.KG, Göttingen, Germany) until the geometry was exactly in contact with the liquid surface. Measurements were performed with distilled water at room temperature (20 °C). Increase of weight due to water uptake was recorded and used to characterize water uptake ability of the powder sample.

CONTACT ANGLE

The contact angle between the powder samples and distilled water (20 °C) was analyzed by the sessile drop method as described by Lazghab *et al.* [47] with the following modifications. Contact angles were measured on tablets, compacted with a pressure of 550 bar. A 10 µL droplet (distilled water, 20 °C) was directly added to the surface using a Hamilton syringe (Trajan Scientific and Medical, Victoria, Australia). For analysis, the initial contact angle formed between material and water droplet was recorded using a high speed camera (CR 600x2, Optronis GmbH, Kehl, Germany) equipped with a telecentric objective (OPTO ENGINEERING, Munich, Germany) and determined by image analysis (ImageJ, DropSnake plug-in; Version 2.1, 03.2006).

3.2.3.2 RHEOLOGICAL CHARACTERIZATION

VISCOSITY-CONCENTRATION-RELATIONSHIP

Rheological characterization of the hydrocolloids was employed to investigate the viscosity-concentration-dependency and the influence of viscosity development on powder rehydration. Experiments were performed with a rheometer (Kinexus ultra, Malvern Instruments GmbH, Herrenberg, Germany) equipped with a plate-plate geometry ($d = 25$ mm). Temperature and shear rate were set to 20 °C and 0.1 s^{-1} . The relationship between viscosity and concentration was calibrated using hydrocolloid solutions with different concentrations. Before measurement, the solutions were hydrated for at least 24 h at 10 °C. The samples were transferred to the rheometer and let rest for further 20 min before measurement was started.

DYNAMIC VISCOSIFYING PROCESS

To investigate the dynamic viscosifying process, double-sided adhesive tape was fixed on the upper plate and coated with a thin powder layer. Alginate powder was sieved to remove particles coarser than 80 μm . Distilled water was added onto the lower plate in order to give a final powder concentration of 0.04 g mL⁻¹. The shear rate was adjusted to 0.1 s⁻¹ and gap width was set to 1 mm. The rate of viscosity development was determined from viscosity increase over time. As the viscosity development results from dissolution processes, dissolution constants were calculated from these experiments, using the calibrated viscosity-concentration-relationship.

AGGREGATE STABILITY

For aggregate disintegration the cohesive forces within the aggregate have to be overcome by external forces. Most hydrocolloid solutions show a viscoelastic behavior and exhibit a yield point. If the applied external forces exceed this yield strength, the sample starts to flow and disintegration of the aggregates can proceed. In order to draw conclusions concerning the aggregate stability, concentrated hydrocolloid solutions were prepared and allowed to swell for at least 48 h. Samples were transferred to the rheometer and let relax for further 30 min. Amplitude sweep experiments were performed at 20 °C, using a serrated plate-plate-geometry to prevent wall-slip-effects. Yield points were defined as point of maximum decrease of loss-, respectively tensile modulus.

3.2.3.3 SWELLING BEHAVIOR

Swellability of hydrocolloid samples was determined with a rheometer (Kinexus ultra, Malvern Instruments GmbH, Herrenberg, Germany). Sample preparation was as described in Sect. 3.2.3.2. for dynamic viscosifying measurements. At the beginning of the measurement a defined normal force of 0.2 N was applied to the sample and the change of gap width due to swelling was recorded. Distilled water was added to a filter paper which was fixed on the lower plate to ensure a continuous liquid availability and a uniform distribution. Measurements were performed at 20 °C. A swelling rate, defined as increase of the $d_{3,2}$ of a single particle, was determined from increasing gap width over time. A detailed explanation about the calculation is given in Wangler & Kohlus [109].

3.2.3.4 NMR-MEASUREMENTS: GEL FORMATION AND WATER BINDING STRENGTH

The gel formation ability and the water binding strength of the powder granules in contact with distilled water was analyzed using NMR measurements (TD-NMR, Minispec 20 Hz, Bruker BioSpin GmbH, Karlsruhe, Germany). Transverse relaxation times were recorded using the software application "t2_cp_mb" a Carr-Purcell-Meiboom-Gill (CPMG) pulse sequence provided by Bruker. For each measurement 4000 data points were collected. Pulse separation between the 90° and the 180° pulse was 1 ms and the recycle delay was set to 5 s. Data were accumulated with 4 scans. T2 relaxation times were determined by a bi-exponential fit. For each measurement 0.01 g sample was placed in a NMR-glass tube (outside diameter 10 mm) and directly before measurement 500 µL distilled water (20 °C) were added. Measurements were run for 20 min and change of relaxation time T2 was measured every minute. Results are depicted relative to the relaxation time of dist. water at 20 °C which was 2260.5 ms. Measurements were performed with the granule size fraction of 425-500 µm obtained from high-shear granulation as described in Sect. 3.2.2.

3.2.3.5 WATER UPTAKE CAPACITY

To analyze the water uptake capacity of the hydrocolloids, glass slides were coated with 3 mL of a 1 % (w/w) solution of the respective powder, followed by drying in a convection oven (UF110, Memmert GmbH+Co.KG, Schwabach, Germany) at 40 °C for 4 h. The mass of the coating layer was measured ($m_{\text{dry layer}}$). The glass slides were immersed in distilled water (20 °C) for defined time periods. Excess water was carefully removed and weight after water uptake was measured (m_{wet}). Afterwards, samples were dried again (convection oven, 40 °C) to determine the dissolved hydrocolloid mass ($m_{\text{dissolved}}$). Water uptake capacity was calculated according to Eq. 3.2.

$$\text{Water uptake capacity} = \frac{m_{\text{wet}} - m_{\text{dry}}}{m_{\text{dry layer}} - m_{\text{dissolved}}} \quad \text{Eq. 3.2}$$

3.2.3.6 AGGREGATE DISINTEGRATION

To disintegrate highly viscous particle aggregates, the cohesive forces within the aggregates have to be exceeded by external (shear) forces. The following experiment was carried out, both to analyze the dynamics of the hydrocolloid rehydration process and to draw conclusions about the necessary shear forces for disintegration. The experiment consisted of a rheometer set-up with a coaxial bob-cup geometry. A

double-sided adhesive tape was fixed on the lateral surface of the cylinder and coated with a thin powder layer. Distilled water was poured into the cup to a final powder concentration of 5 mg/mL. Measurements were performed at 20 °C and mechanism and shear stress dependency of powder rehydration was analyzed.

3.2.3.7 DISSOLUTION EXPERIMENTS

Dissolution experiments were performed to relate results from physical characterization to powder rehydration behavior. Experiments were carried out in a 2 L beaker (diameter: 130 mm, height: 185 mm) filled with a total liquid mass of 1500 g (20 °C). Hydrocolloid granules (425-500 µm), which were obtained from high-shear granulation were added within ~ 2 s by a vibratory feeder to a final concentration of 0.1 % (w/w). For dispersion, a pitched blade stirrer (4 blades, 45° inclination, 50 mm diameter) was placed 40 mm above the bottom of the beaker. Rotation speed was adjusted to 800 rpm, which corresponds to a Reynold number of $3.3 \cdot 10^4$ and a volume specific energy input of 1.23 W/L. Dissolution over time was investigated with an inline-photometer (AvaSpec-ULS2048, Avantes BV, The Netherlands) equipped with a transmission dip probe. The optical path length was adjusted to 20 mm. Absorbance was measured at 400 nm (xanthan gum, guar gum) respectively 600 nm (alginate). Alginate was dyed with Ponceau 4R (Lay Gewürze OHG, Grabfeld, Germany) to intensify absorbance. Dissolved hydrocolloid mass was calculated by previously recorded calibration curves.

3.3 RESULTS & DISCUSSION

In the following section, results from physical characterization are shown and their influence on dissolution and disintegration of particle aggregates will be discussed with special focus on their dynamic behavior.

3.3.1 WETTING BEHAVIOR

Powder wettability was analyzed by capillary rise and sessile drop measurements as described in Sect. 3.2.3.1. For inert powder-liquid systems, water height and water uptake velocity can be calculated by the Washburn equation (Eq. 3.1). For powder systems like hydrocolloids, which undergo dynamic changes during rehydration, e.g. dissolution, viscosity development and swelling, it was shown that this approach is unsuitable to predict the rehydration process. As explained in detail in our previous study [109], a wetting time parameter was determined to describe the time interval, which is available for water uptake before viscosity development and swelling impede further rise. Results of water uptake times are summarized in Table 3.2. It was shown that, for hydrocolloids, this time frame is typically in the range of 1 s, which is usually too short to achieve complete rehydration of the powder bulk. Considering a rehydration process, it is recommended either to apply shear forces that are high enough to achieve dispersion before particles stick together, or the powder should be added slow enough so that the bulk height stays beyond the critical wettable height before aggregate formation occurs.

Contact angles between powder and distilled water were analyzed by the sessile drop method as described in Sect. 3.2.3.1. The contact angle influences the capillary forces and the wettability of the powder sample. Contact angles above 90° mean non-wetting conditions, whereas a contact angle of 0° means perfect wettability. Within this study, the highest wettability with a contact angle of $\sim 52^\circ$ was found for alginate, followed by xanthan gum ($\sim 58^\circ$). Accordingly, guar gum, with a contact angle of $\sim 70^\circ$, exhibits the lowest wettability (Fig. 3.1).



Fig. 3.1: Contact angle between distilled water (20 °C) and alginate (A), xanthan gum (B) and guar gum (C).

Together with the Wilhelmy plate method and methods using liquid penetration/capillary rise, the sessile drop method is a very common and often used method for contact angle determination. Sessile drop measurements can be performed using compressed powder tablets, loosely packed powder beds or thin powder layers, which are fixed onto an adhesive tape. Alternatively, dried powder solution can be used to analyze contact angles by the sessile drop method. Independently of the method used, sample preparation affects contact angle analysis due to the influence of surface roughness, compaction pressure for tablet preparation and change of bulk structure after powder-liquid contact. For that reason, contact angles should be regarded as apparent contact angles [47,72]. Indirect methods for contact angle determination, driven by liquid uptake due to capillary rise, require special focus on identical powder packing procedure [61,73]. Furthermore, the correct choice of the reference liquid, which is necessary for these kind of measurement, was shown to have an impact on determined material constant and thus analyzed contact angle. Additionally, it was shown that contact angles determined by dynamic capillary rise measurements are in general higher than static contact angles due to the advancing liquid front and also vary with the velocity of the liquid rise [72,73]. In literature, further methods for contact angle measurement are described. A detailed review is given by Alghunaim *et al.* [45]. Despite the difficulties of contact angle measurement and interpretation, we decided to use the sessile drop method to investigate differences in the wettability of the hydrocolloid powders. Several sample preparation methods (loosely packed powder beds, thin powder layers, dried powder solutions) were tested previously and in comparison, measurements on tablets were the most reproducible and precise. Although we are aware of the fact that contact angles may differ from contact angles formed on original powder particles, other methods were not expected to be more suitable. Results of contact angle analysis are summarized in Table 3.2.

3 DEVELOPMENT AND VALIDATION OF METHODS TO CHARACTERIZE REHYDRATION BEHAVIOR OF FOOD HYDROCOLLOIDS

Table 3.1: Powder characteristics: Bulk density, powder density, porosity and particle size

	Bulk density [kg m ⁻³]	Powder density [kg m ⁻³]	Porosity [-]	d ₁₀ [μm]	d ₅₀ [μm]	d ₉₀ [μm]	d _{4,3} [μm]	d _{3,2} [μm]
Alginate	721 ± 0.2	1654 ± 0.005	0.56	25.9 ± 0.0	110.5 ± 0.2	222.8 ± 0.6	119.3 ± 0.3	50.3 ± 0.3
Alginate sieved <80 μm				14.2 ± 0.6	52.5 ± 1.9	105.9 ± 1.9	56.9 ± 1.7	25.6 ± 1.2
Xanthan gum	542 ± 1.0	1511 ± 0.002	0.64	17.3 ± 0.3	54.1 ± 0.6	115.2 ± 0.9	61.0 ± 0.5	30.6 ± 0.6
Guar gum	594 ± 4.0	1401 ± 0.005	0.58	24.5 ± 0.0	48.5 ± 0.0	87.5 ± 0.0	52.5 ± 0.0	39.8 ± 0.0

Table 3.2 Physical characteristics of hydrocolloid powders

	Wetting behavior		Wetting dynamics			Aggregate disintegration		Dissolution	
	Capillary rise [s]	Contact angle [°]	Swelling rate [μm s ⁻¹]	Viscosity rate [Pas s ⁻¹]	Water uptake capacity [g g ⁻¹]	Gel strength [ms]	Shear stress Yield point, c=5% [Pa]	Diss. rate Rheometer [m ⁻² s ⁻¹]	Diss. coeff. Beaker [s ⁻¹]
Alginate	0.8	52.0 ± 3.2	10.0 ± 0.4	1.7 ± 0.1	63.4 ± 6.9	1982 ± 13	34.4 ± 2.3	89.6 ± 9.9	0.51 · 10 ⁻³
Xanthan gum	1.0	58.1 ± 0.9	19.0 ± 0.8	0.2 ± 0.0	133.5 ± 4.8	468 ± 2	61.1 ± 1.3	9.7 ± 0.5	0.08 · 10 ⁻³
Guar gum	1.2	70.0 ± 3.0	8.0 ± 0.3	4.7 ± 0.4	29.4 ± 1.4	1256 ± 17	581.0 ± 33.8	99.8 ± 3.7	0.96 · 10 ⁻³

3.3.2 DYNAMICS OF HYDROCOLLOID REHYDRATION

Rehydration of hydrocolloid powders includes dissolution, viscosity development as well as swelling and leads to changes in the bulk structure, which affect the liquid rise in the bulk capillaries. According to the Washburn equation (Eq. 3.1), the rise of the liquid is slowed down by viscosity increase, which is a result of dissolution processes, and by a decrease of the bulk porosity as a consequence of swelling. As shown previously [109], the velocity of the dynamic changes of the physical characteristics is a crucial factor influencing whether the powder tends to form aggregates or not.

VISCOSITY DEVELOPMENT

Results from dynamic viscosity development are shown in Fig. 3.2. Viscosity development rates were determined from the linear section of the viscosity versus time curves. For better comparison, results are depicted standardized by setting the initial viscosity value equal to zero and the following data as relative increase. Comparing the behavior of the hydrocolloid samples, a ~20-fold faster rate was found for guar gum compared to xanthan gum. Further differences were found in the time interval of linear viscosity increase. For xanthan gum, a linear viscosity increase was found over 500 s resulting in a final viscosity of ~104 Pas, followed by guar gum (200 s) with a final viscosity of ~1150 Pas and alginate with a final viscosity ~109 Pas after 120 s. The high viscosity values further illustrate the influence of viscosity on powder rehydration. Higher viscosities are assumed to correlate with a stronger cohesion within the particle aggregates and therefore with higher shear forces for disintegration. Viscosity development results from dissolution processes. Consequently, results from viscosity increase were used to determine dissolution rates, which are summarized in Table 3.2. For calculation, concentration-dependent viscosity was calibrated. Viscosity development rates were converted in dissolution rates, which were found to correlate with a linear regression approach. The fastest dissolution with a dissolution rate of $(99.8 \pm 13.7 \text{ m}^{-2} \text{ s}^{-1})$ was found for guar gum, which was in the same order as the dissolution velocity of alginate $(89.6 \pm 9.8 \text{ m}^{-2} \text{ s}^{-1})$. Xanthan gum, with a dissolution rate of $9.7 \pm 0.5 \text{ m}^{-2} \text{ s}^{-1}$, was found to dissolve ten times slower compared to guar gum.

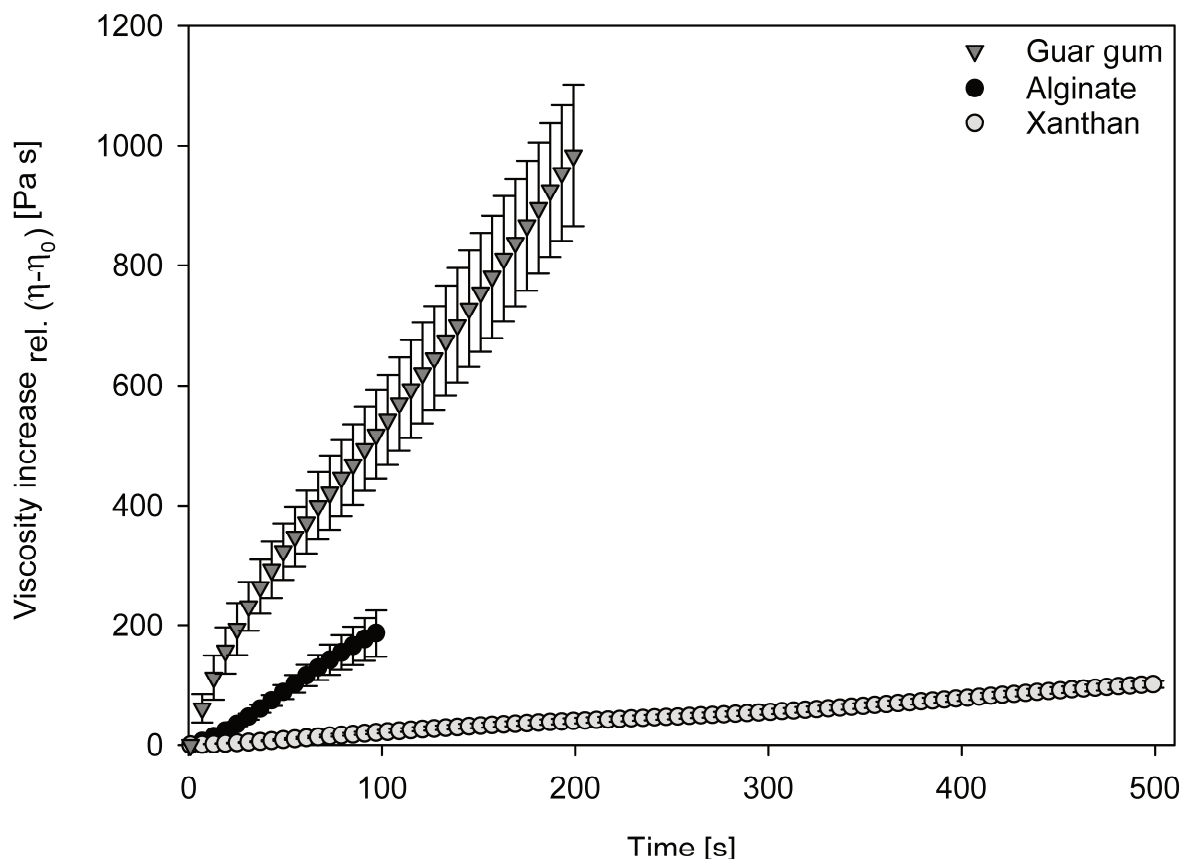


Fig. 3.2: Viscosity increase_{rel.} of guar gum, alginate and xanthan gum powder in contact with H₂O_{dist.} determined by rheological measurements ($c = 0.04 \text{ g mL}^{-1}$, shear rate 0.1 s^{-1} , $20 \text{ }^\circ\text{C}$).

SWELLING BEHAVIOR

According to Schubert [44], swelling, in contrast to viscosity development and dissolution, always results in a reduced water uptake velocity or even causes a stop of liquid rise, if swelling is high enough to achieve complete pore-blocking. Results are shown in Fig. 3.3 and Table 3.2. For better comparison, results are depicted standardized by setting the initial particle volume equal to zero and the following data as relative increase. Different swellability was found for the hydrocolloid samples. The highest swelling rate of $19 \mu\text{m s}^{-1}$ was found for xanthan gum followed by alginate ($10 \mu\text{m s}^{-1}$) and guar gum ($8 \mu\text{m s}^{-1}$). In comparison with the results from viscosifying experiments (Fig. 3.2), the time interval of linear particle size increase was found to be in reverse order. The longest linear particle size increase was found for guar gum, the shortest for xanthan gum. However, time intervals considered to analyze particle swelling are considerably longer than relevant for the rehydration processes. As discussed above, capillary rise stopped within $\sim 1 \text{ s}$, which is mainly attributed to pore blocking due to particle swelling. It is assumed that hydrocolloid swelling is not influenced by particle size, but only by the surface available for water uptake. This

3 DEVELOPMENT AND VALIDATION OF METHODS TO CHARACTERIZE REHYDRATION BEHAVIOR OF FOOD HYDROCOLLOIDS

assumption could be affirmed by the results of the water uptake capacity measurement described in Sect. 3.3.5. For that reason, it is assumed to be valid to specify a linear swelling rate of the particle diameter.

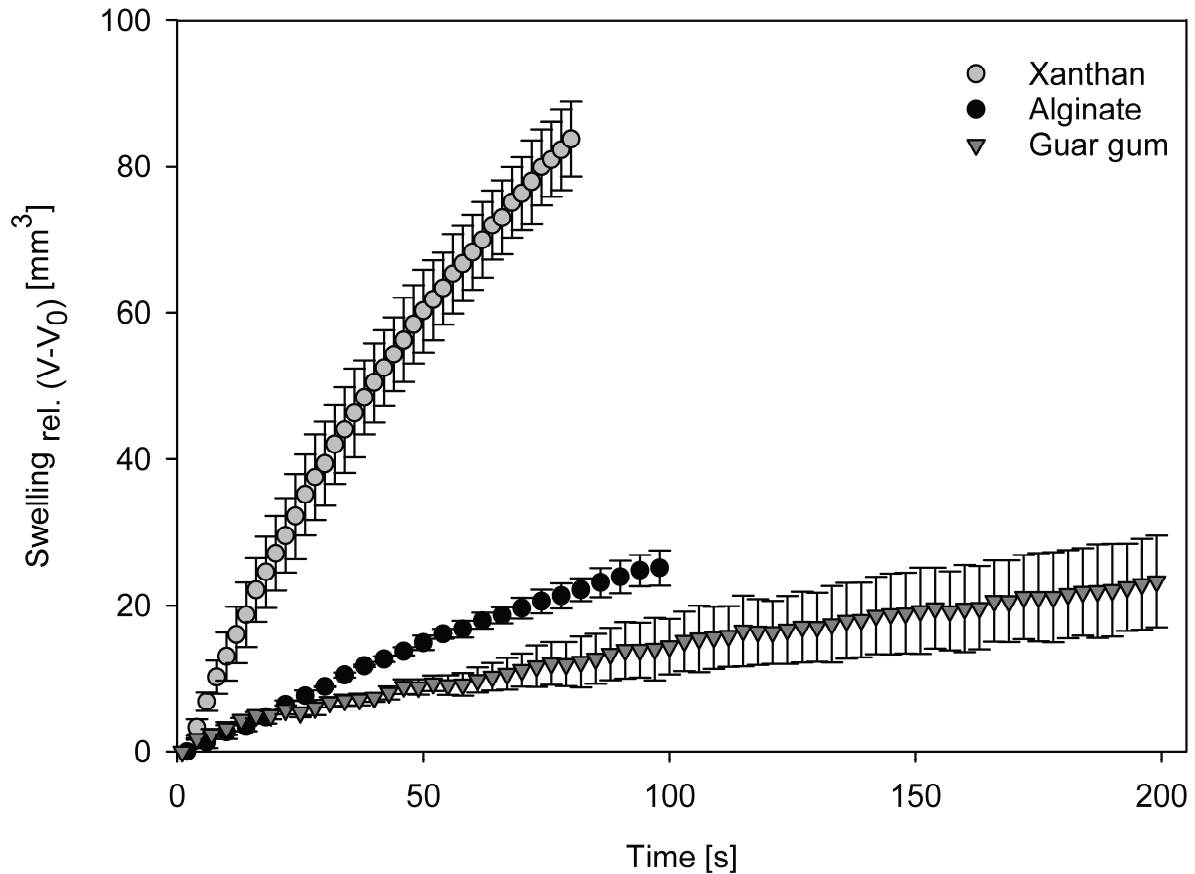


Fig. 3.3: Swelling behavior of xanthan gum, alginate and guar gum powder in contact with dist. water (20 °C, $c = 0.04 \text{ g mL}^{-1}$, Normal Force: 0.2 N).

3.3.3 AGGREGATE STABILITY

Beside aggregate formation, the stability of the aggregates is an important parameter with respect to process conditions to achieve disintegration. Yield points of differently concentrated hydrocolloid solutions were analyzed by amplitude sweeps to investigate the stability of hydrocolloid aggregates (Table 3.2). In Fig. 3.4, shear stresses σ^* acting at the respective yield point are depicted dependent on hydrocolloid concentration. For guar gum and alginate, results correlate with an exponential function, whereas data of xanthan gum showed a linear increase of the aggregate stability in the analyzed concentration range. The concentration of the hydrocolloid solutions was adjusted based on the behavior of the sample. It could be observed that guar gum concentrations higher than 5 % lead to brittle, inhomogeneous structures, while for alginate solutions below 5 % no yield point could be determined as no gel-like

structures were developed. In general, it was found that guar gum and xanthan gum showed a gel-like behavior ($G' > G''$), whereas viscous behavior was dominant for alginate concentrations below 12.5 %. In aggregates, xanthan gum concentration is typically in the range of ~10 %. Based on these results necessary shear stresses to disintegrate these aggregates should be higher than 144 Pa.

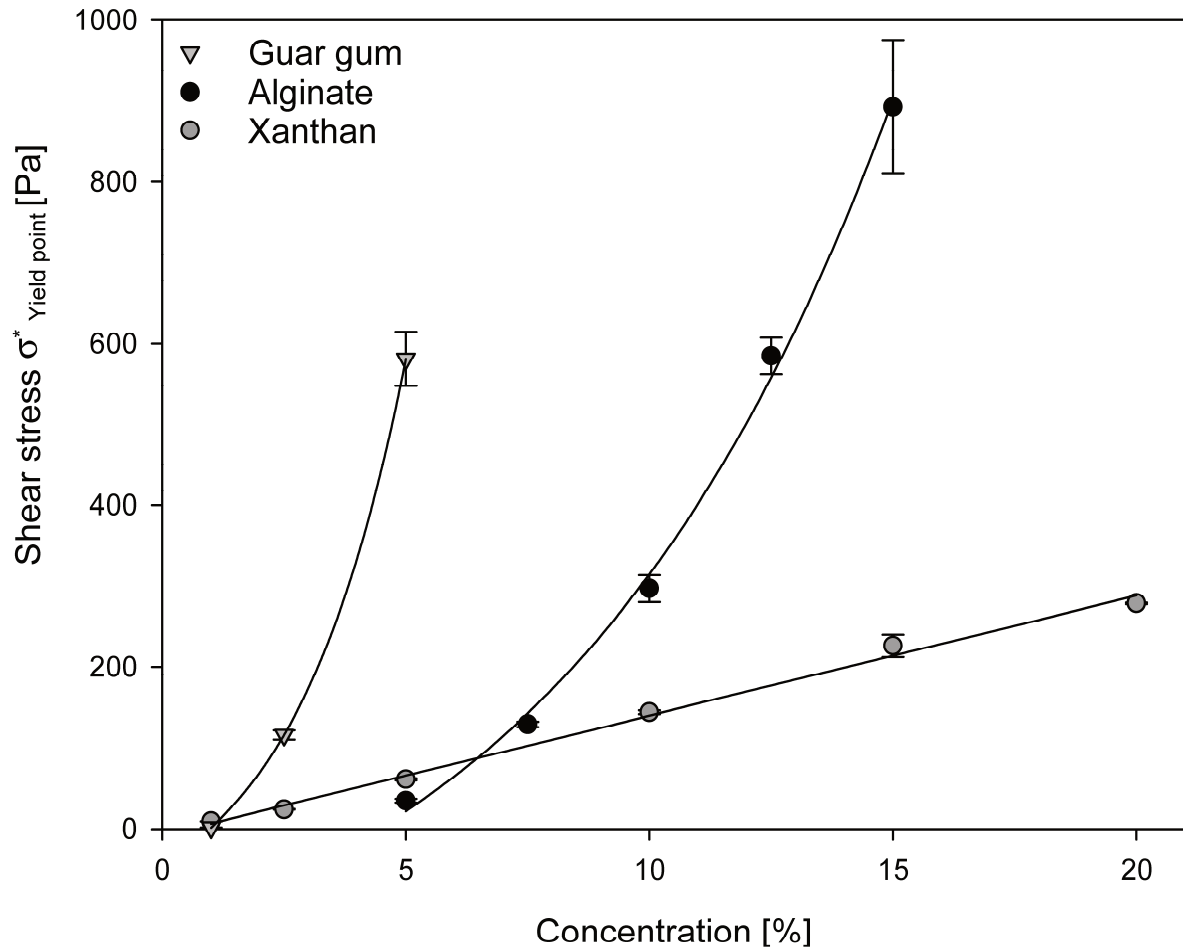


Fig. 3.4: Concentration dependent yield point of guar gum, alginate and xanthan gum. (Amplitude sweeps, serrated plate-plate geometry, 20 °C).

3.3.4 GEL STRENGTH AND WATER BINDING CAPACITY

The gel- and water binding strength of the hydrocolloid samples was investigated by NMR-analysis. The principle of the method was to measure the change of the relaxation time over time. To improve powder-water miscibility, measurements were performed with granules of the size fraction in-between 425-500 μm . Results of NMR analysis are summarized in Fig. 3.5 and Table 3.2. The value of the relaxation time at the end of the measurement was used as indicator for water binding capacity and gel strength. As a further parameter, the intersection between a power law fit of the first and second part of the curve was interpreted as water uptake time, as shown in Fig. 3.5.

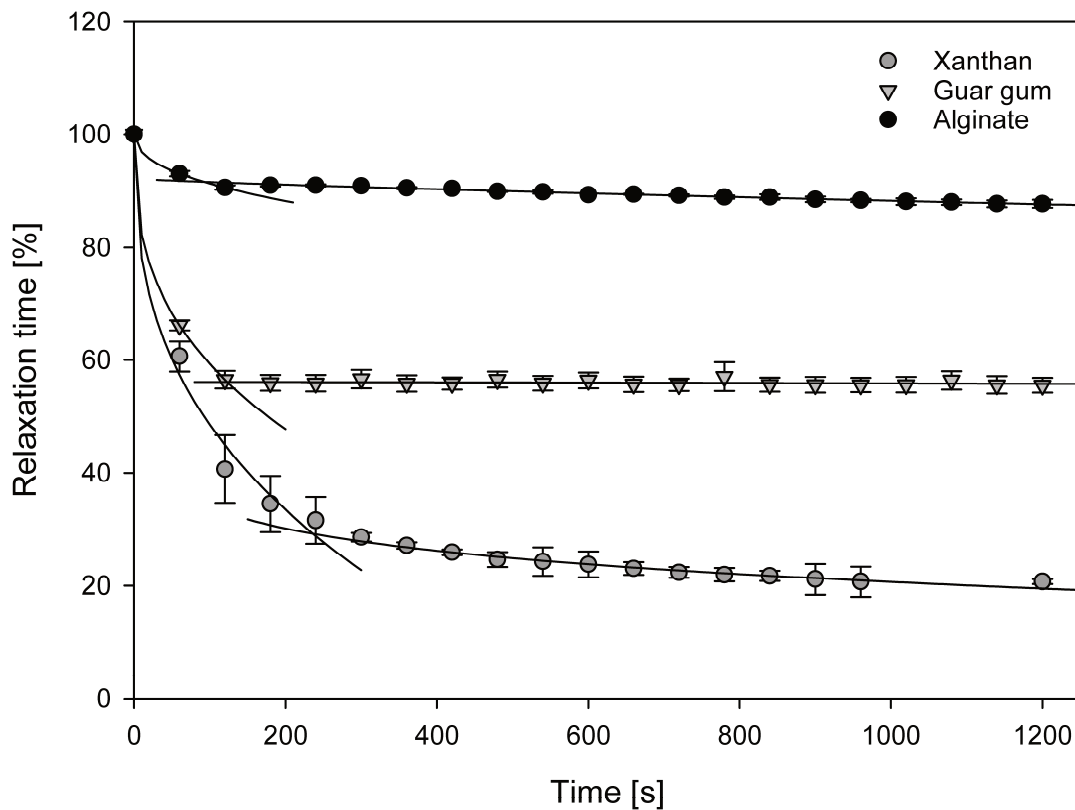


Fig. 3.5: Change of relaxation time over time as indicator for gel strength and water binding strength of hydrocolloid granules (425-500 μm) measured by NMR analysis.

As data were fitted by a bi-exponential function, two relaxation times were obtained. $T2(1)$ was supposed to be the relaxation time of the less mobile protons of the powder phase, whereas $T2(2)$ was correlated to the relaxation time of protons with higher mobility (liquid phase). Analysis showed that relaxation times $T2(1)$ only slightly increased (data not shown). Dissolution of biopolymers into the liquid phase associated with gel formation and water binding seemed to be the dominating process which is

shown by a decrease of T2(2). Gel formation ability can be described by the decrease of the T2(2) relaxation time in the first part of the curve. As qualitatively shown in Fig. 3.5, alginate showed a slower gel formation rate compared to xanthan gum and guar gum. Water uptake times were 235 s for xanthan gum, 122 s for guar gum and 99 s for alginate. Together with the T2(2) value at the end of the measurement (Table 3.2) these results further confirmed the stronger interaction between xanthan gum and water compared to guar gum and alginate. The relatively low gel strength and water binding capacity of alginate could be explained by the lack of bivalent ions, which are necessary for the formation of alginate gels.

3.3.5 WATER UPTAKE CAPACITY OF HYDROCOLLOIDS

Analyses of the water uptake capacity of the hydrocolloid samples were performed to simulate the situation during aggregate hydration. As described above, it is assumed that hydrocolloid aggregates consist of a highly viscous gel layer, which surrounds non-hydrated powder particles. Water transfer in the inner parts of these aggregates is driven by diffusion, respectively by capillary forces. According to the schematic draw in Fig. 3.6 the highest hydrocolloid concentration is in the inner core of the aggregate; the closer to the outer region the higher the dilution as water transfer takes place from the out- to the inside. According to Hellborg *et al.* [64], dissolution of the aggregates can be described by a two-step process: (1) Phase transition from solid to dissolved powder and (2) diffusion of dissolved material through the surrounding surface layer into the liquid. On the one side, the velocity of these steps depends on specific material characteristics as aggregate viscosity, liquid density and particle size, but on the other side it can be influenced by process parameters as e.g. stirrer speed. Due to the high viscosity of the hydrocolloids, it is assumed that aggregate disintegration follows an erosive mechanism. Molecule detachment takes place in the diffusive layer in case that attacking forces exceed the cohesive forces within the layer. Water uptake by the dried layers is expected to follow the same mechanism and should give more insight in the velocity of the water transfer in a particle aggregate as well as in the water uptake capacity of hydrocolloids. Results from water uptake over time are shown in Fig. 3.7 A. Measurements were run for a total of 5 min. After the first 60 s alginate and xanthan gum layers exhibit approximately the same water content. In comparison, guar gum could only bind half of the mass. In the further course of the curves (data not shown) xanthan gum showed a continuously increasing amount of bound water with a final

3 DEVELOPMENT AND VALIDATION OF METHODS TO CHARACTERIZE REHYDRATION BEHAVIOR OF FOOD HYDROCOLLOIDS

mass of ~133 g/g, which is twice as much as alginate (~63 g/g) and 4.5 times more than guar gum (~29 g/g). These results are in accordance to the data obtained from swelling experiments, which showed the same trend. The higher water uptake velocity of alginate compared to xanthan gum at the beginning can probably be explained by the lower viscosity of the layer and consequently a lower hydrodynamic flow resistance for liquid rise. For further analysis, experiments were performed with dried layers which differed in height. Results are shown in Fig. 3.7 B. Data are depicted standardized, relative to the present mass of the coating layer. An inversely proportional correlation was found between relative water uptake capacity and applied layer height. It could be confirmed that water transfer within the gel layer is the reason for the increasing water content and that higher water uptake capacities correlate with the available surface area and not with the applied powder mass.

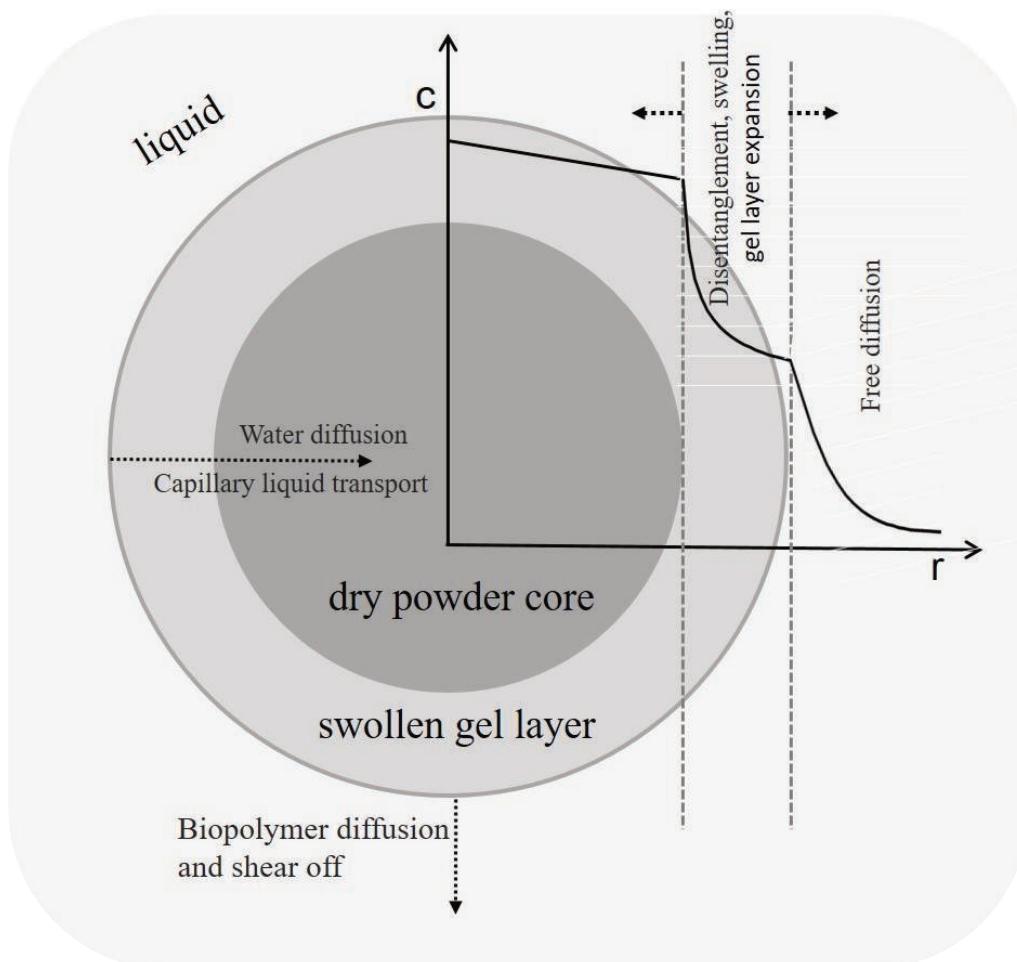


Fig. 3.6: Schematic draw of a hydrocolloid aggregate and the concentration profile within the aggregate and the surrounding layer.

3 DEVELOPMENT AND VALIDATION OF METHODS TO CHARACTERIZE REHYDRATION BEHAVIOR OF FOOD HYDROCOLLOIDS

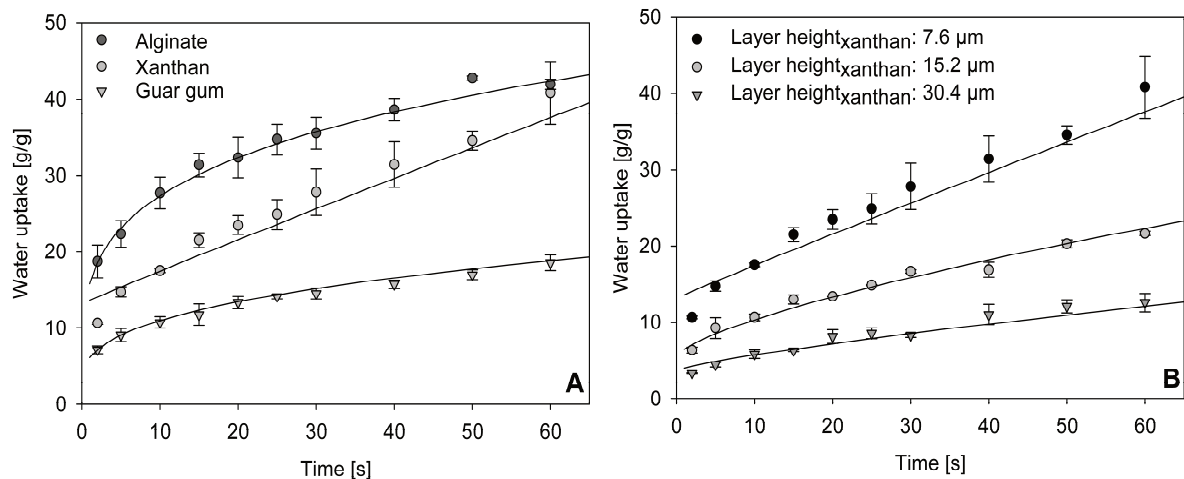


Fig. 3.7: Relative water uptake of hydrocolloid samples (A) and influence of different layer heights (B).

3.3.6 REHYDRATION AND DISINTEGRATION OF HYDROCOLLOID POWDERS

The aim of this experiment was to investigate powder rehydration in terms of wetting phase, dynamic changes of powder characteristics and disintegration of aggregates, simultaneously. Experiments were performed with xanthan gum powder as described in Sect. 3.2.3.6. Results are shown in Fig. 3.8. The change of viscosity over time is depicted as an indicator for the different rehydration steps.

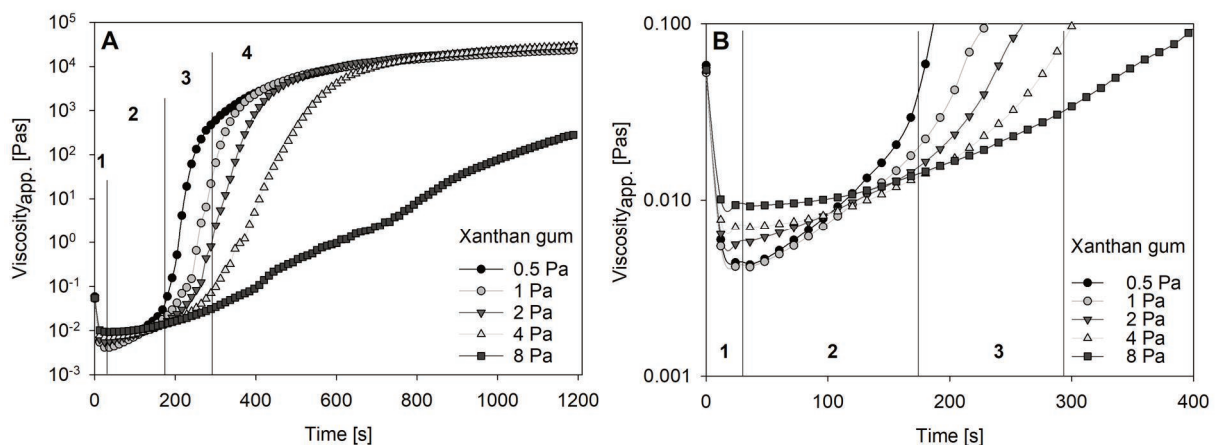


Fig. 3.8: Dissolution and disintegration of xanthan gum powder and aggregates dependent on applied shear stress. (Rheometer set-up: Bob-cup geometry, 20 °C, distilled water, c: 5 mg/mL

These are schematically shown in Fig. 3.8 A for the 0.5 Pa curves. The numbers 1-4 denote the different rehydration steps. In step one, xanthan gum powder comes in contact with the rehydration liquid. The viscosity decrease in this first phase can be explained by water uptake and swelling of the powder particles. This leads to a reduction of the gap size and consequently to a decrease of the apparent viscosity. In

the second phase a slight viscosity increase was detected due to initiation of molecule detachment out of the swollen gel layer. As shown in Fig. 3.8 B viscosity values in phase 2 are higher with increased shear stress. With higher shear stress molecule shear off out of the swollen layer is initiated earlier. Thus gel layer expansion and gap size reduction is less pronounced and hence apparent viscosity higher. The following third phase is characterized by a sharp increase of the apparent viscosity which is attributed to ongoing molecular diffusion. Driving force of the diffusion process is the concentration difference between the swollen gel layer and the surrounding liquid. As the shear stress is controlled, an increase in viscosity results in lower shear rate, which in turn results in an even higher viscosity. The strong shear thinning behavior of xanthan gum explains the steep increase of viscosity. It was shown that the concentration dependent viscosity increase of xanthan is more pronounced at lower than at higher shear rates [20]. This explains the order of the curves in phase 3. Finally, the viscosity gradually approaches its final value in phase 4. The gel layer concentration in this phase is close to the equilibrium concentration corresponding to the applied shear stress. Results in Fig. 3.8 A show that the variation of the shear stress influences the time period and apparent viscosity development of the different phases. To conclude these results, according to the phases observed from viscosity courses, rehydration steps of hydrocolloid particles can be classified as “wetting/swelling” (phase 1), “dissolution” and “diffusion” in phase 2 and 3 and finally balancing gel layer concentration and shear stress (phase 4).

3.3.7 DISSOLUTION OF HYDROCOLLOIDS

Rehydration of hydrocolloid powders is often time consuming as, depending on the hydrocolloid characteristics, both wetting and dispersion are critical process steps. Viscosity development and swelling cause the formation of sticky aggregates which are difficult to disperse. It is assumed that the tendency for aggregate formation and the necessary time for hydrocolloid rehydration correlate with the velocity of the dynamic changes. Dissolution curves of hydrocolloid granules are shown in Fig. 3.9. An exponential regression model was used to describe the dissolution behavior of the hydrocolloid model system. For all fits regression coefficients were higher than 0.8960.

Guar gum: $c = 0.103 \cdot (1 - \exp(-0.0956 \cdot t \cdot s^{-1}))$ Eq. 3.3

Alginate: $c = 0.1014 \cdot (1 - \exp(-0.0512 \cdot t \cdot s^{-1}))$ Eq. 3.4

Xanthan gum $c = 0.1216 \cdot (1 - \exp(-0.00768 \cdot t \cdot s^{-1}))$ Eq. 3.5

The necessary time to dissolve 95 % of the applied xanthan gum granules took the longest (~ 198 s) followed by alginate (~ 54 s) and guar gum which showed the fastest rehydration (~ 27 s). Comparing these results with their physical properties, it indicates that swelling is the most significant property to draw conclusion about the rehydration behavior of a powder. As granules were used for dissolution experiments, aggregate formation is less pronounced. This explains the fast dissolution of guar gum despite the high aggregate stability determined from amplitude sweeps.

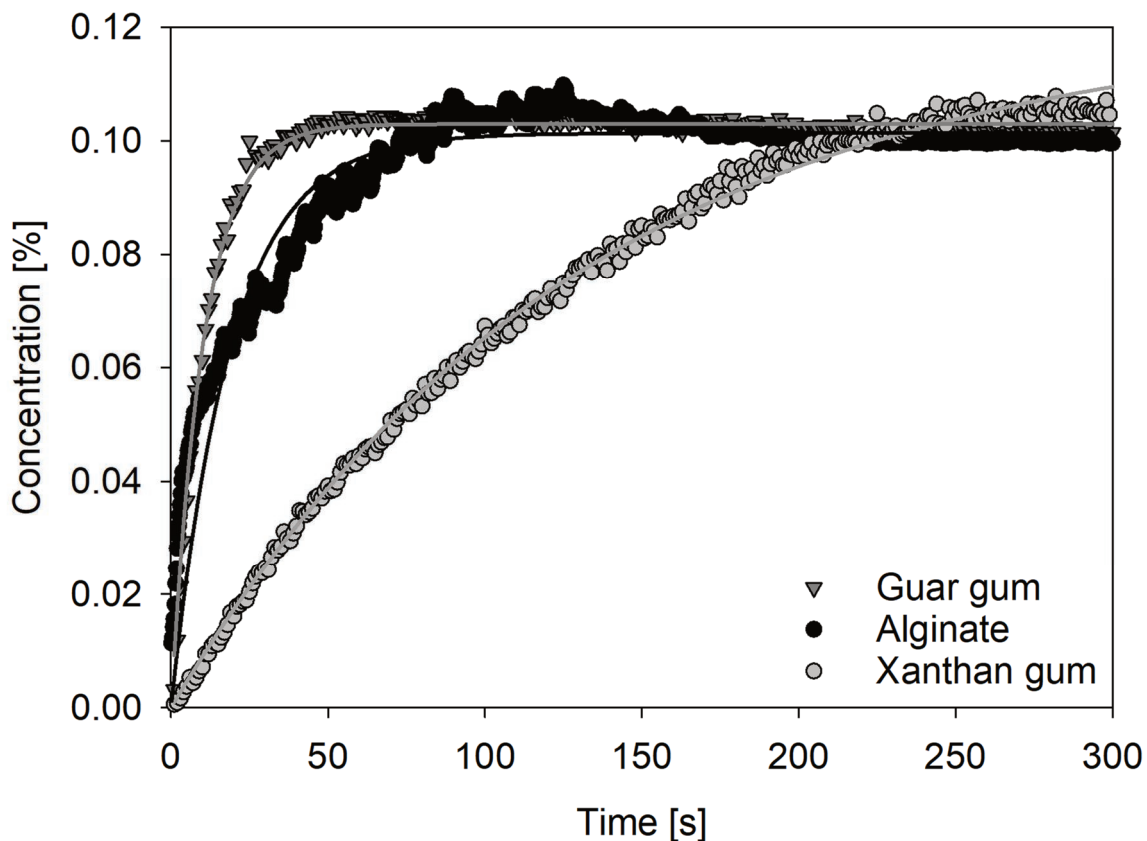


Fig. 3.9: Dissolution of hydrocolloid granules (425-500 μm) in distilled water (c = 0.1 %, pitched blade stirrer, 800 rpm).

Dissolution of hydrocolloid powders was also studied by Kravtchenko *et al.* [89]. Pectin powder dissolution was analyzed and in agreement to our results, dissolution curves were found to follow an exponential approach. According to the model proposed in Fig. 3.6, a hydrocolloid particle in contact with water simplified consists of an inner dry powder core and an outer swollen gel layer. Water transport into the particle takes

place from the out- to the inside and is driven either by capillary forces or by diffusion towards the concentration profile. With increasing hydration, the hydrocolloid molecules in the swollen layer disentangle more and more, and the gel layer expands. With a certain hydration state, molecules start to diffuse from the gel boundary into the rehydration liquid by free diffusion or are sheared off due to the applied shear forces. This model assumption is supported by a study conducted by Parker *et al.* [99]. According to the authors, dissolution of hydrocolloid particles consists of a three step process involving (1) water uptake through the grain surface and gel layer formation, (2) release of hydrocolloids from the gel layer and (3) transfer of released hydrocolloid molecules into the surrounding rehydration liquid. In their experimental set-up, step 2 was demonstrated to be rate-determining.

Comparing results from dissolution experiments and rheological measurements, it appears that they differ from each other (Table 3.2). In the set-up of the rheological measurement hydrocolloid concentration was higher (0.04 g/mL) compared to the dissolution experiment (0.001 g/g). For that reason, water was limited in rheological measurement set-up and determined dissolution rates correspond to “dissolution” and viscosity development in the swollen gel layer. In contrast to that, dissolution coefficients determined from dissolution experiments correspond to the dissolution of the hydrocolloid into the surrounding liquid. As available particle surface for dissolution remains constant in the rheometer set-up, particle dissolution is quantified by a dissolution constant dependent on the surface of the particles (Table 3.2).

Previous analyses have shown that water uptake of alginate was the fastest of the three hydrocolloids (Fig. 3.7). In addition, it generates gel strength at relatively low- but yet higher concentrations than guar gum. Both facts would favor alginate over guar gum in relation to dissolution speed (Fig. 3.8). Nevertheless, the faster dissolution of guar gum can be explained by a faster molecular diffusion of guar molecules in comparison to xanthan, which was shown by the dissolution experiments under low shear rates (Sect. 3.3.2, Table 3.2). The slow dissolution of xanthan gum supports the importance of this material characteristic. This interpretation is based on the qualitative model shown in Fig. 3.6. The dissolution speed is given by molecular diffusion out of the swollen layer. Only if swelling is slower than diffusion, swelling would be the rate limiting step. As explained in Sect. 3.3.6, shear stress determines the concentration at the diffusion boundary and will promote the dissolution speed.

In a series of consecutive studies [9,110,111] the dissolution behavior of guar gum was investigated. Contrary to our study, an empiric logarithmic hydration model was found to fit guar gum best. Similar to our results, they stated that hydration rates increase with the available effective specific surface area and that hydration is supported by particle-particle collision as well as by shear stress leading to deformation and abrasion of the swollen gel layer.

In conclusion, it is hypothesized that guar gum rehydration can be improved, if viscosity development is retarded. Accordingly, swelling which leads to a decrease or blocking of capillaries should be hindered to improve xanthan gum rehydration.

3.4 CONCLUSION

Rehydration of powders covers several aspects like wetting, sinking, dispersion and dissolution. Specific techniques were developed to investigate the rehydration behavior of xanthan gum, guar gum and alginate quantitatively. In earlier studies it was found to be strongly dependent on dynamic processes such as viscosity development and swelling, which were shown to be critical processes for powder rehydration. Capillary rise experiments showed that capillary liquid transport was stopped within ~1 s independently of the analyzed hydrocolloid. This suggests that capillary rise experiments are not suited to assess differences in the dynamic rehydration behavior of critical food powders. Differences in the wetting behavior could be demonstrated by the sessile drop method.

Rehydration dynamics were investigated in detail, considering viscosity development and swelling behavior of the hydrocolloid powders. Experiments showed that the dynamic physical characteristics correlate with the dissolution behavior of the hydrocolloids. Comparing xanthan gum and guar gum, it appears that the critical rehydration behavior of guar gum is attributed to viscosity development, whereas swelling dominates xanthan gum rehydration. These findings were additionally confirmed by NMR and water uptake measurements.

Qualitative observation of guar gum dispersion indicated that guar gum is less susceptible to aggregate formation, but once formed, disintegration was observed to be more time consuming than for xanthan gum aggregates. This could be confirmed by the results from yield point determination. Previous analysis showed that xanthan gum concentration in aggregates is typically in the range of 10 %, which would

3 DEVELOPMENT AND VALIDATION OF METHODS TO CHARACTERIZE REHYDRATION BEHAVIOR OF FOOD HYDROCOLLOIDS

correspond to a necessary shear stress for disintegration of 144 Pa. At a concentration of 5 %, the yield point of guar gum was found to be up to 9.5 times higher compared to xanthan gum. A possible strategy to minimize the influence of swelling of xanthan gum could be to separate the particles, i.e. by diluting with sugar or salt. Guar gum swells slowly, but develops highly viscous phases and strong gels. In free dissolution, it dissolves fast. In application of guar gum, utmost attention should be placed on avoiding lump formation. Xanthan gum, in contrast, swells extremely fast, generating relatively weak pastes, making lump formation very hard to avoid, but lump breakup an option.

In this study, methods to characterize the rehydration behavior were shown using hydrocolloids as model systems. Nevertheless, these methods are also applicable to other systems showing critical rehydration behavior as e.g. protein powders [109].

**Chapter 4 EXPERIMENTAL INVESTIGATION AND SIMULATION OF REHYDRATION
DYNAMICS OF BIOPOLYMER POWDERS**

By Julia Wangler^{1*}, Heike Teichmann¹, Elena Konstanz¹ and Reinhard Kohlus¹

¹University of Hohenheim, Institute of Food Science and Biotechnology, Department
of Process Engineering and Food Powders, Garbenstr. 25, 70599 Stuttgart, Germany

Published 2019 in Powder Technology, Volume 355, p. 461-473

Accessible under DOI: <https://doi.org/10.1016/j.powtec.2019.07.022>

ABSTRACT

Rehydration of biopolymer powders is influenced by dissolution, viscosity development and swelling. Associated dynamic changes of powder characteristics correlate with their rehydration properties. Especially floating and particle aggregation negatively affect the rehydration process and powder quality. A deeper knowledge about these dynamics is crucial with regard to product development and quality improvement. The dynamics of swelling and viscosity development are of special importance. Controlling these parameters by a targeted modification will improve the rehydration process. Within this study the rehydration behavior of xanthan gum, guar gum and alginate was analyzed. Focus was on investigating their dynamic behavior and providing a detailed description of the rehydration process. Experiments were carried out using a model system, consisting of biopolymer coated glass beads. Rehydration was investigated experimentally and by simulation. The importance of dynamic effects and their mutual interaction was demonstrated. Results explain the mechanisms of the dynamic rehydration process of food powders.

KEYWORDS: Fluid bed coating, Food powders, Rehydration, Capillary liquid rise, Physical characterization, Simulation

4.1 INTRODUCTION

Food biopolymers can be used to create special structures and functionalities. Physical stability and sensory characteristics of food products can be improved due to their rheological properties. Usually, an application of small biopolymer concentrations in the range of 0.05 - 1 % is sufficient [20,26,38]. However, to achieve these desired functionalities a complete rehydration of the biopolymer powder is necessary [22,25]. The rehydration process of powders covers several steps, which are divided in wetting, sinking, dispersing and dissolution [8,44]. With focus on biopolymer reconstitution these steps are strongly interrelated and highly dynamic. The associated changes of both powder and liquid properties result in the formation of floating layers and highly stable particle aggregates. These processes are mainly triggered by swelling, dissolution and viscosity development [49,89,112]. Related increase of process times and costs leads to a less convenient application of powdered foods. To improve the rehydration process, a deeper knowledge about the underlying physical powder properties and their dynamics is mandatory.

Powder rehydration was investigated experimentally by measuring the capillary liquid uptake over time. Capillary liquid transport can be described by the Washburn-Equation (Eq. 4.2), which balances the capillary pressure and the opposed hydrodynamic flow resistance. This approach also applies for water uptake into powder bulks which, simplified, can be regarded as an assembly of capillaries [91]. The velocity and height of the rising liquid is presented as a function of the bulk porosity, the viscosity and density of the wetting liquid and of the wettability, expressed as contact angle between powder and liquid. For validity of the Washburn equation, these parameters are assumed constant over the water uptake process [44,49,90].

Rehydration of food powders and in particular biopolymers, is associated with a constantly changing wetting situation due to the dynamic processes described above. This requires a progressive adaption of the Washburn equation. Based on previous studies [88,109], the current work presents methods to quantify dynamic changes of the biopolymer properties in contact with water. Capillary liquid uptake into the model biopolymer system was simulated using a Volume-of-Fluid approach. The Washburn approach was used as basic equation. Variables were adapted to the changing conditions, using results from physical powder characterization. In particular, change of porosity and variation of particle size as a result of swelling as well as the influence of viscosity development were considered in simulation. A parameter variation study

was used to demonstrate the interrelation between these processes and to explain the mechanisms of the rehydration dynamics.

For that purpose, a biopolymer model system consisting of xanthan gum, guar gum and alginate coated glass beads was developed. As previously demonstrated [88,109], dynamic processes after biopolymer-liquid contact proceed too fast to differentiate between the individual contribution of swelling and viscosity development. The idea behind the model system was to limit the extent of the dynamic changes in order to prevent a collapse of the bulk pore system. Swelling and viscosity development were restricted by applying different coating thicknesses. Variation of the coating material enabled a regulation of the velocity and extent of the dynamic processes. Finally, critical parameters related to powder rehydration were identified and quantified.

4.2 MATERIALS & METHODS

4.2.1 MATERIALS

Xanthan gum (Satiaxane CX 801, 200 mesh, Cargill, Germany), alginate (Algogel™, Cargill, Germany) and guar gum (Lay Gewürze OHG, Grabfeld, Germany) were used as model food powders. Due to their special properties as thickening agents, these biopolymers tend to form floating layers and particle aggregates which cause a difficult rehydration behavior. For the preparation of the model system, these biopolymers were coated on glass beads as core material. Glass beads with a size fraction of 400 – 600 µm were obtained from Kuhmichel Abrasiv GmbH (Ratingen, Germany).

4.2.2 METHODS

4.2.2.1 PREPARATION OF THE BIOPOLYMER MODEL SYSTEM

Biopolymer coated glass beads were prepared as a biopolymer model system. The coating process was carried out in a fluidized bed system (WS-CT-L, Allgaier Process Technology GmbH, Uhingen, Germany) equipped with a two-fluid nozzle (nozzle diameter $d_{\text{nozzle}} = 0.8$ mm, Model 970, Düsen-Schlick GmbH, Untersiemau/Coburg, Germany) in top-spray configuration. Xanthan gum, guar gum and alginate were used as coating agents. Solutions were prepared by dissolving the biopolymers in distilled water to a final concentration of 1 % (w/w), respectively 3 % (w/w) for alginate. Subsequently, solutions were allowed to rest for 24 h at 10 °C. The coating solution was heated up to 55 °C by a heating tube (Model RSL OD6/LA25, DN 4, Winkler

GmbH, Germany) in order to reduce the viscosity and to improve the atomization behavior. For coating, 1 L of the glass beads as core material was filled into the device and fluidized with an air flow rate of 110 m³ h⁻¹. The bed temperature was adjusted to 70 °C. The coating solution was added with a spray rate of 5 g min⁻¹ and atomized using an air pressure of 2.5 bar. Throughout the process, samples (~ 100 g) were taken to obtain glass beads with different coating layer thicknesses in-between 0.5 and 5.0 μm. The theoretical thickness of the coating layer, dependent on the applied coating solution, was calculated in advance as proposed by van Kampen & Kohlus [113] using Eq. 4.1.

$$s_{\text{target}} = \frac{d_{4,3}}{2} \cdot \left[\left(1 + \frac{\rho_{\text{core}} \cdot m_{\text{coating}}}{\rho_{\text{coating}} \cdot m_{\text{core}}} \right)^{\frac{1}{3}} - 1 \right] \quad \text{Eq. 4.1}$$

The target coating layer thickness s_{target} was calculated based on the volume-weighted mean diameter of the core particles $d_{4,3}$, the densities ρ of the core and coating material and the applied mass m of the coating and the core particles. The “mass loss” due to sampling was not considered in the calculation. At the end of the coating process, the particles were dried for 2 min. Agglomerates and spray dried coating material were subsequently removed by sieving using sieve mesh sizes of 300 μm and 600 μm (Retsch GmbH, ISO3310, Germany).

The coating quality was evaluated qualitatively by scanning electron microscopy (JSM-IT100, Jeol, Freising, Germany).

ANALYSIS OF COATING LAYER THICKNESS

To determine the yield and the efficiency of the coating process, the actual amount of coating material applied onto the glass beads was analyzed. In a first step, the obtained samples were divided into representative quantities by a rotating sample splitter (Retsch GmbH, Modell PT 100, Germany). Subsequently, the samples were transferred into a 200 mL beaker and agitated in boiling water for at least 60 min to ensure a complete removal of the coating agent from the core particles. The suspension was filtered using a suction funnel which was connected to a water jet pump. Particles were retained by a filter paper (Macherey-Nagel, MN85/70, diameter: 90 mm, Germany). For complete removal of the coating material, the particles were rinsed a second time using 100 mL of boiling distilled water. Finally, the filter paper with the filtrate was dried in a drying chamber at 33 °C for at least 24 h. The

applied coating mass was calculated from the mass difference between initial coated particles and washed-off dried particles. The determined coating mass was used to calculate the actual coating thickness according to Eq. 4.1.

4.2.2.2 CHARACTERIZATION OF PHYSICAL POWDER PROPERTIES AND DYNAMIC REHYDRATION BEHAVIOR

Biopolymer powders and glass beads were characterized according to their bulk density (ISO 60/DIN 53 466), powder density (DIN EN ISO 1183-1 (2013-04)) and particle size (Mastersizer 2000, Malvern Panalytical GmbH, Herrenberg, Germany). Data are summarized in Table 4.1.

The wetting behavior of xanthan gum, alginate and guar gum was characterized by contact angle and capillary rise experiments. Kinetics of swelling and viscosity development, as a result of biopolymer dissolution, were evaluated by rheological measurements. A detailed description of these experiments is given in [88,109].

NMR-MEASUREMENTS: GEL FORMATION AND WATER BINDING STRENGTH

Gel formation and water binding strength of the biopolymers xanthan gum, guar gum and alginate in contact with distilled water was analyzed by NMR measurements (TD-NMR, Minispec 20 Hz, Bruker BioSpin GmbH, Karlsruhe, Germany) using the biopolymer coated glass beads (Sect. 4.2.2.1). To obtain a homogeneous distribution of the sample and to ensure an optimal contact between liquid and sample surface, the coated glass beads were fixed on a transparency (7.4 mm x 10 mm), which was covered with a double-sided adhesive tape. Excess sample was removed with compressed air. The coated plate was additionally wrapped into a tea filter (Teefilter, Größe 3, dm Profissimo, Germany) to ensure a homogeneous liquid transport to the sample. The coated transparency was placed in a NMR-glass tube (outside diameter $d_{OD} = 1$ mm) and directly before measurement 900 μ L of distilled water (20 °C) were added (Fig. 4.1). Measurements were run for 30 min. Change of relaxation time T2 and percentage of fast and slow relaxing protons were measured every minute and finally analyzed by a bi-exponential fit. Measurements were performed at least in duplicate.

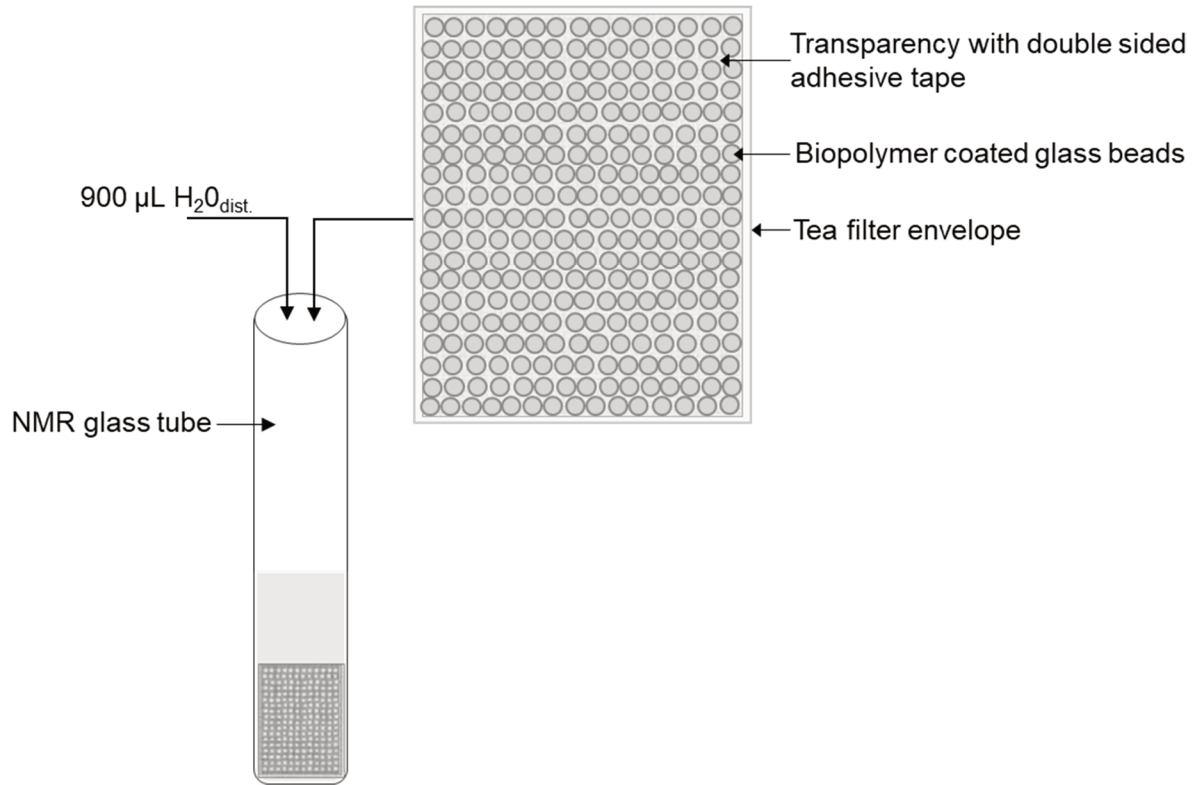


Fig. 4.1: Schematic draw of sample preparation for NMR-measurements.

4.3 SIMULATION OF BIOPOLYMER REHYDRATION

To simulate rehydration of “reactive” powders, methods to characterize dynamically changing powder properties have been developed. These are described in Section 4.2.2 and more detailed in [88,109].

Powder rehydration was described by capillary water uptake into the powder bulk. To simulate this process, the Washburn equation (Eq. 4.2) was used as basic approach.

$$h = \sqrt{\frac{\varepsilon \cdot d_p \cdot \gamma_l \cdot \cos\theta_{\text{eff}} \cdot t}{15 \cdot \eta_l (1 - \varepsilon)}} \quad \text{Eq. 4.2}$$

t : wetting time [s], η_l : dynamic viscosity of the liquid [Pas], ε : porosity of the powder system [-], h : liquid height in the capillary [m], d_p : particle diameter [m], γ_l : surface tension of the liquid [N m⁻¹], θ : contact angle [°]

This work builds on previous studies by Wangler & Kohlus [88,109] which dealt with the characterization of dynamic powder properties and proposed a first approach to simulate the rehydration behavior of dynamically changing powder systems.

4 EXPERIMENTAL INVESTIGATION AND SIMULATION OF REHYDRATION DYNAMICS OF BIOPOLYMER POWDERS

The main focus of the present study is on the simulation and a profound investigation of the dynamic rehydration process.

The dynamic situation of the process mainly results from dissolution, viscosity development and swelling. The associated non-constant parameters, related to changing porosity, particle size and viscosity were resolved, both temporally (t) and locally (x). The change of porosity $\varepsilon(t,x)$ correlates with the volume expansion of the individual particles due to swelling. The time-dependent change of porosity was calculated using Eq. 4.3.

$$\varepsilon(t) = 1 - \frac{N_{\text{Particle}}^* \cdot \pi \cdot d_{3,2}^3(t)}{6 \cdot V_{\text{Powder}}} \quad \text{Eq. 4.3}$$

With the theoretical particle number N_{Particle}^* and the volume of the powder sample V_{Powder} the change of the Sauter mean diameter $d_{3,2}$ due to swelling was calculated as described in [109]. To be consistent with Carman-Kozeny and the dynamic simulation approach, the particle diameter $d_{3,2}$ was used as estimate value for $d_{3,0}$ in Eq. 4.3.

The influence of viscosity on capillary liquid uptake depends on the powder dissolution rate and the viscosity-concentration relationship of the biopolymer. The former was determined as described in [88]. The viscosity development in the rehydration liquid was calculated by balancing the mass of dissolved biopolymer and water uptake into the particles. For the concentration dependent viscosity development, the following correlations were found:

$$\text{Xanthan gum:} \quad \eta = 1368 \text{ Pa s} \cdot e^{4.982 \cdot c} + (0.001 - 1368) \text{ Pa s} \quad R^2 = 0.9864$$

$$\text{Alginate:} \quad \eta = 33.71 \text{ Pa s} \cdot e^{31.54 \cdot c} + (0.001 - 33.71) \text{ Pa s} \quad R^2 = 0.9953$$

$$\text{Guar gum:} \quad \eta = 63.16 \text{ Pa s} \cdot e^{65.83 \cdot c} + (0.001 - 63.16) \text{ Pa s} \quad R^2 = 0.9976$$

η : dynamic viscosity of the liquid [Pa s]; c : biopolymer concentration [kg/kg].

Dissolution rates of the biopolymers are given in Table 4.2. The determination of these rates is not based on a diffusion model and only applies for the specific powder sample. Especially particle size will have a non-trivial effect. Dissolution rates given in Table 4.2 refer to the applied powder mass within the experiment to integrate over the whole process. To consider the surface dependency of dissolution processes, dissolution rates were related to the surface area of the applied powder. Depending on the dissolution rate of the biopolymer powder, the temporal change of the dissolved

powder relative to the initially applied powder mass was calculated according to Eq. 4.4.

$$\frac{d(m_t/m_0)}{dt} = DR * A_{\text{Powder}} * \Delta c \quad \text{with} \quad A_{\text{Powder}} = \frac{6}{d_{3,2}} * \frac{m_{\text{Powder}}}{\rho_{\text{Powder}}} \quad \text{Eq. 4.4}$$

m_t : Powder mass at time t [kg], m_0 : Initial powder mass [kg]

DR: Dissolution rate [$\text{m}^{-2} \text{s}^{-1}$], A_{Powder} : Powder surface [m^2]

Δc : Change of dissolved powder concentration relative to the initially applied powder mass [kg/kg], $d_{3,2}$: Sauter mean diameter [m]

To describe the viscosity development during biopolymer rehydration two different effects were considered. Effect 1 assumes dissolution and thus viscosity increase in the rising liquid (Fig. 4.2A). Effect 2 assumes that viscosity development is limited to the outer boundary layer of the particle (Fig. 4.2B). The occurrence of effect 1 or 2 essentially depends on whether a critical, material dependent concentration is exceeded. Detaching of molecules and thus dissolution is more pronounced below this critical concentration. Above, the hydrated gel layer is stabilized by a strong entanglement network. Thus, swelling processes are prevalent and water absorption is steadily slowed down.

Models describing polymer dissolution assume that rehydration of biopolymers consists of two steps. First, diffusion of the rehydration liquid into the dry polymer and formation of a swollen, viscous layer occurs. In a second step, the solid concentration within the swollen layer is progressively diluted. After a certain induction time and reaching a critical swelling ratio, the polymer molecules start to disentangle and dissolve into the rehydration liquid [99,107,114]. In relation to the explanation proposed in Fig. 4.2 it indicates that biopolymers that behave according to effect 1 have passed both of these steps while biopolymers behaving as proposed by effect 2 have not yet completed the first step or are still in the transition phase.

In the experimental set-up a highly concentrated situation is present, i.e. pure biopolymer powder which is gradually diluted by the rising liquid. According to effect 2 (Fig. 4.2B), dissolution and viscosity increase of the rehydration liquid is assumed to be minimal and liquid rise is mainly delayed by viscous obstruction. Above a certain swelling dimension and layer viscosity, it is further assumed that liquid rise in biopolymer samples can only be accomplished by diffusion.

4 EXPERIMENTAL INVESTIGATION AND SIMULATION OF REHYDRATION DYNAMICS OF BIOPOLYMER POWDERS

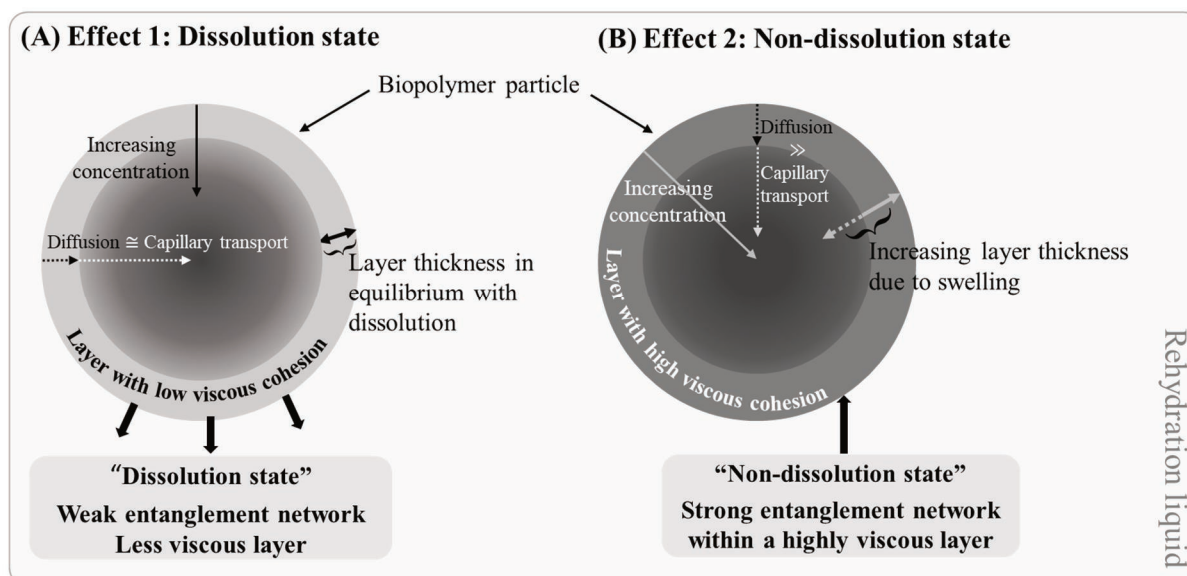


Fig. 4.2: Viscosity development during biopolymer rehydration in concentrated situations. **(A)** Effect 1: Dissolution state, **(B)** Effect 2: Non-dissolution state.

Within the biopolymer coated model system, the processes described in Fig. 4.2 are specifically restricted. This was achieved by controlling the coating layer thickness in order to adjust the dynamic effects in terms of swelling degree, biopolymer concentration in the swollen layer and viscosity increase both in the particle surrounding layer and the rising liquid. Thus the influence of the individual dynamic effects on powder rehydration could be studied.

The simulation approach assumes that the viscosity of the rehydration liquid increases according to the dissolution rate of the biopolymer. However, to translate effect 2 (Fig. 4.2B) into simulation a "non-mobile viscosity" is implemented. Thus, for the liquid transferred to the next layer a viscosity of 1 mPas, according to the viscosity of water, is assumed. A parameter variation study was conducted to gain more insight into whether swelling or viscosity development is the crucial factor.

To simulate the liquid uptake into the powder bulk the following assumptions were made:

- The powder bulk is divided into a certain number of layers with a specific height. Powder and liquid characteristics are assumed to be constant over the defined layer height.
- Capillary pressure and contact angle between powder and liquid are assumed to be constant.

- Swelling is assumed to be spherical. The maximum volume expansion of the particles within a defined layer is restricted to the fill-up of the initially present cavity volume.
- Viscosity development is considered by assuming dissolution of biopolymer molecules out of the swollen layer into the rehydration liquid depending on the experimentally determined dissolution rate.
- The dissolution rate depends on the surface area of the particle. This is considered in simulation by calculating the change of the particle surface area as a result of swelling. Influence of dissolution on particle size was neglected as swelling effects are dominant. With increasing particle volume, the amount of dissolved biopolymer mass per time increases.
- Liquid distribution in the powder bulk is balanced by calculating the liquid mass bound to the particles due to swelling and free liquid available for capillary rise.
- The development of a concentration profile over the bulk height is expected as a consequence of dissolution. It is assumed that the dissolved material is not transported upwards but stays in the respective layer.

4 EXPERIMENTAL INVESTIGATION AND SIMULATION OF REHYDRATION DYNAMICS OF BIOPOLYMER POWDERS

Table 4.1: Powder characteristics: Bulk density, powder density, porosity and particle size.

	Bulk density [kg m ⁻³]	Powder density [kg m ⁻³]	Porosity [-]	d_{10} [μm]	d_{50} [μm]	d_{90} [μm]	$d_{4,3}$ [μm]	$d_{3,2}$ [μm]
Alginate	721 ± 0.2	1654 ± 0.005	0.56	25.9 ± 0.0	110.5 ± 0.2	222.8 ± 0.6	119.3 ± 0.3	50.3 ± 0.3
Alginate <small>sieved <80 μm</small>				14.2 ± 0.6	52.5 ± 1.9	105.9 ± 1.9	56.9 ± 1.7	25.6 ± 1.2
Xanthan gum	542 ± 1.0	1511 ± 0.002	0.64	17.3 ± 0.3	54.1 ± 0.6	115.2 ± 0.9	61.0 ± 0.5	30.6 ± 0.6
Guar gum	594 ± 4.0	1401 ± 0.005	0.58	24.5 ± 0.0	48.5 ± 0.0	87.5 ± 0.0	52.5 ± 0.0	39.8 ± 0.0
Glass beads 400-600 μm	1446 ± 0.006	2496	0.42	402.4 ± 6.2	548.9 ± 9.8	746.4 ± 14.9	560.4 ± 2.4	521.9 ± 5.7

Table 4.2: Physical parameters of powder samples determined from sessile drop method and rheological measurements [88,109].

	Wetting behavior	Wetting dynamics		Dissolution	Capillary rise time [s]	
	Contact angle [°]	Swelling rate [μm s ⁻¹]	Viscosity rate [Pas s ⁻¹]	Dissolution rate <small>Rheometer</small> [m ⁻² s ⁻¹]	Calculated _{0.5 μm}	Experimental _{0.5 μm}
Alginate	52.0 ± 3.2	10.0 ± 0.4	1.7 ± 0.1	89.6 ± 9.9	12.6	16.6
Xanthan gum	58.1 ± 0.9	19.0 ± 0.8	0.2 ± 0.0	9.7 ± 0.5	6.7	9.2
Guar gum	70.0 ± 3.0	8.0 ± 0.3	4.7 ± 0.4	99.8 ± 3.7	15.8	n.d

4.4 RESULTS & DISCUSSION

In the following sections, results from physical powder characterization are summarized. The results are discussed with regard to the rehydration behavior of the biopolymers, taking into account the findings obtained from simulation.

4.4.1 COATING PROCESS

The biopolymer model system was prepared by coating the glass beads with xanthan gum, guar gum and alginate by a fluidized bed process as described in Sect. 4.2.2.1. The coating process was evaluated in terms of coating efficiency. The quality of the coating layer was qualitatively assessed by scanning electron microscopy.

4.4.1.1 EFFICIENCY OF THE COATING PROCESS

The efficiency of the coating process was evaluated by the deviation between the actual and calculated, target coating thickness. Determination of actual and target coating thickness was done as described in Sect. 4.2.2.1. Results are summarized in Table 4.3.

Table 4.3: Target and experimentally determined coating layer thickness of xanthan gum-, guar gum- and alginate coated glass beads (400 - 600 μm).

Coating thickness _{target} :		0.5 μm	1.0 μm	2.0 μm	3.0 μm	4.0 μm	5.0 μm
Coating thickness _{experimental} [μm]:	Xanthan gum	0.68	1.14	1.61	2.42	3.44	4.45
	Guar gum	0.38	0.91	2.38	2.65	4.48	5.92
	Alginate	1.37	1.66	1.43	3.15	3.68	4.64

The experimentally determined values of the coating layer thickness are in an acceptable range compared to the target, theoretical coating layer thickness. With respect to the 5 μm layer, process efficiencies are 89 % for xanthan gum, 118 % for guar gum and 92 % for alginate. The high values of guar gum can probably be explained by an uneven distribution of the guar gum solution on the glass beads due to the high viscosity of the solution and the related difficult atomization behavior.

4.4.1.2 COATING QUALITY

In general, coating quality is usually defined in terms of coating thickness, the degree of surface coverage and homogeneity of the coating layer [113]. Qualitative analysis of the coating layer was done by scanning electron microscopy of the biopolymer coated glass beads (Fig. 4.3).

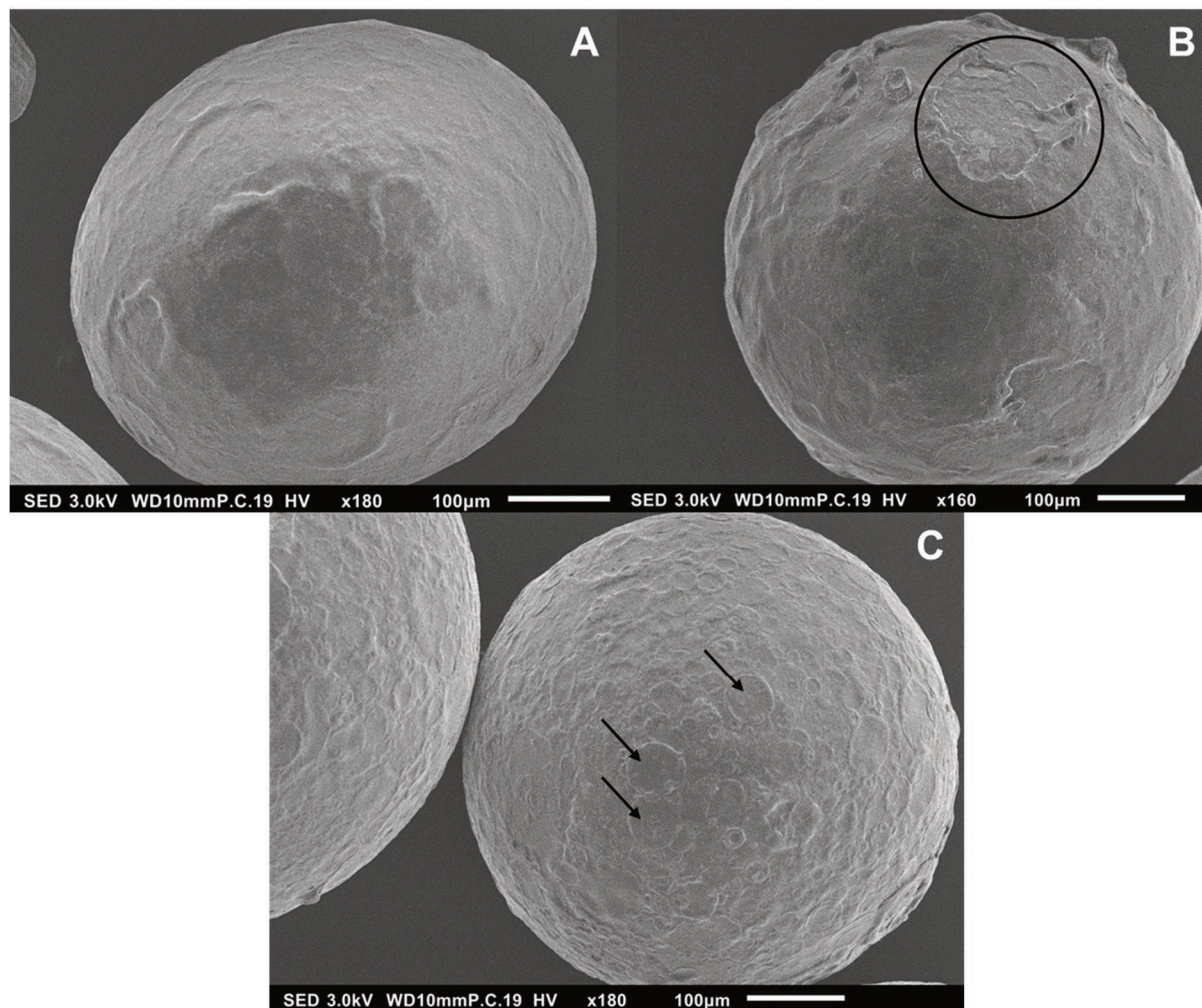


Fig. 4.3: SEM-images of biopolymer coated glass beads (Coating layer thickness: 5 μm). (A) Xanthan gum, (B) Guar gum, (C) Alginate. (Magnification: Xanthan gum, alginate 180x, guar gum 160x).

Xanthan gum coating resulted in homogeneous and smooth surfaces (Fig. 4.3A). For guar gum coated glass beads, the coating structure seemed to be layered and a higher surface roughness was visible. Due to the higher agglomeration tendency coating defects, which may arise from a breakage of agglomerates, could be observed, indicated by the fractured region highlighted in Fig. 4.3B. For alginate coated glass beads, the settled droplets seemed to have difficulties in spreading out, resulting in a rough surface structure with individual droplet spots (Fig. 4.3C).

4.4.2 CONTACT ANGLE

Contact angles between powder and distilled water were analyzed by the sessile drop method as described in [88]. Within this study, the highest wettability with a contact angle of $\sim 52^\circ$ was found for alginate, followed by xanthan gum ($\sim 58^\circ$). Guar gum with a contact angle of $\sim 70^\circ$ showed the lowest wettability.

4.4.3 CAPILLARY RISE

Capillary rise measurements were done to characterize powder wettability. Capillary water uptake is important not only for powder wetting but also for sinking due to oppositely directed drag forces. For inert powder-liquid systems, water height and water uptake velocity can be calculated by the Washburn equation (Eq. 4.2) [43,55,60,64,65]. The validity of the Washburn equation is restricted to constant conditions [44,49,90]. Thus, the original approach is not suited to predict rehydration of systems, which undergo dynamic changes after powder liquid contact. Therefore, capillary rise experiments were performed using a model system made of biopolymer coated glass beads (Sect. 4.2.2.1). The idea behind was to inhibit a collapse of the pore structure of the system due to the inert core of the coated glass beads. By adjusting the coating layer thickness, the extent of swelling and viscosity development were controlled and their influence on powder rehydration could be studied.

4.4.3.1 BLANK-CORRECTION OF EXPERIMENTAL DATA

Capillary rise experiments were performed as described in [88,109]. The powder sample was supported by a metal sieve and a filter paper to inhibit sinking of particles into the liquid. The additional weight increase due to water uptake by the support was considered by blank experiments. For evaluation it was assumed that water is initially absorbed by the support and subsequently by the biopolymer. The blank experiments aimed to determine both the necessary time for complete wetting of the support and the corresponding weight. Obtained data of capillary rise experiments within the model biopolymer system were corrected by subtracting the weight of the fully wetted support from the water uptake curves and by shifting the time- and weight ordinate to 0.

4.4.3.2 EVALUATION OF CAPILLARY RISE EXPERIMENTS

Influence of biopolymer and coating layer thickness: Blank-corrected results from capillary rise experiments are summarized in Fig. 4.4. Results show that water uptake is influenced by the biopolymer and the coating layer thickness. The influence of the biopolymer is shown by the comparison of the water absorption at a layer thickness of 0.5 μm . Here, alginate absorbed the highest amount of water and showed the fastest increase. These results can be explained by the different dynamic behavior in terms of viscosity development and swelling (Table 4.2). The influence of the coating thickness is shown by a reduced water uptake with increasing layer thickness. Dynamic effects, even for a coating layer of 0.5 μm , are strong enough to cause a slowdown of water uptake.

Mechanisms of rehydration dynamics: To draw conclusions concerning the mechanism of dynamic processes and their impact on food powder rehydration, the course of the water uptake curves was evaluated. Two effects are noticeable.

(1) Two different phases of water uptake can be distinguished, as demonstrated in Fig. 4.4D. A first phase, characterized by an almost linear increase of the water uptake, is followed by a second phase, which can be described by a power law dependency. According to the Washburn approach, the linear phase was attributed to the action of capillary forces [44,90,112]. The second phase was related to diffusion [98]. For uncoated glass beads, a 1-phase mechanism, driven by capillary forces, can be seen due to the lack of dynamic processes. The transition point between capillary rise and diffusion mechanism indicates the collapse of the pore network. For determination, the intersection from the linear- and the power law regression was calculated as schematically shown in Fig. 4.4D. Calculated time-frames of capillary rise are summarized in Fig. 4.5. As expected, with increasing coating layer thickness the transition to a diffusional liquid transport occurs faster. Impact of swelling and viscosity development within the swollen layer is more pronounced with increasing coating layer thickness which explains the shorter time-frames.

Comparing xanthan gum and alginate with a coating layer thickness of 1 μm , capillary forces could be maintained ~ 16 s for alginate and ~ 9 s for xanthan gum (Fig. 4.5). These time-frames correlate with the swelling behavior of these biopolymers. The swelling rate of xanthan gum was found to be twice the swelling

4 EXPERIMENTAL INVESTIGATION AND SIMULATION OF REHYDRATION DYNAMICS OF BIOPOLYMER POWDERS

rate of alginate (Table 4.2). Accordingly, capillary liquid uptake of xanthan gum could only be maintained half as long as alginate. This led to the conclusion that capillary liquid uptake of xanthan gum and alginate is dominated by swelling processes.

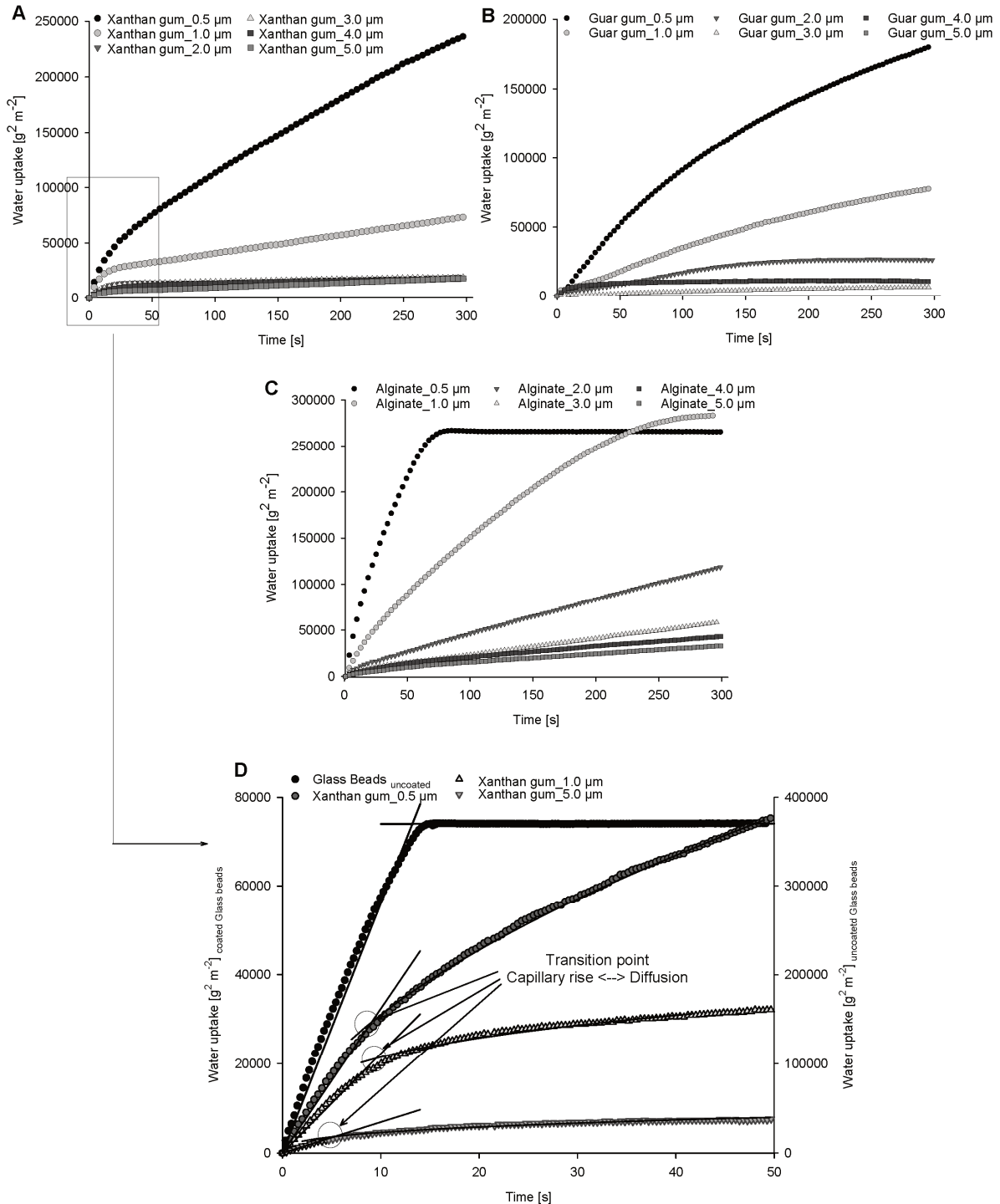


Fig. 4.4: Water uptake of biopolymer coated glass beads (400 - 600 μm) dependent on coating layer thickness (0.5 μm - 5 μm) measured by capillary rise experiments. (A) Xanthan gum, (B) Guar gum, (C) Alginate, (D) Determination of capillary rise time.

4 EXPERIMENTAL INVESTIGATION AND SIMULATION OF REHYDRATION DYNAMICS OF BIOPOLYMER POWDERS

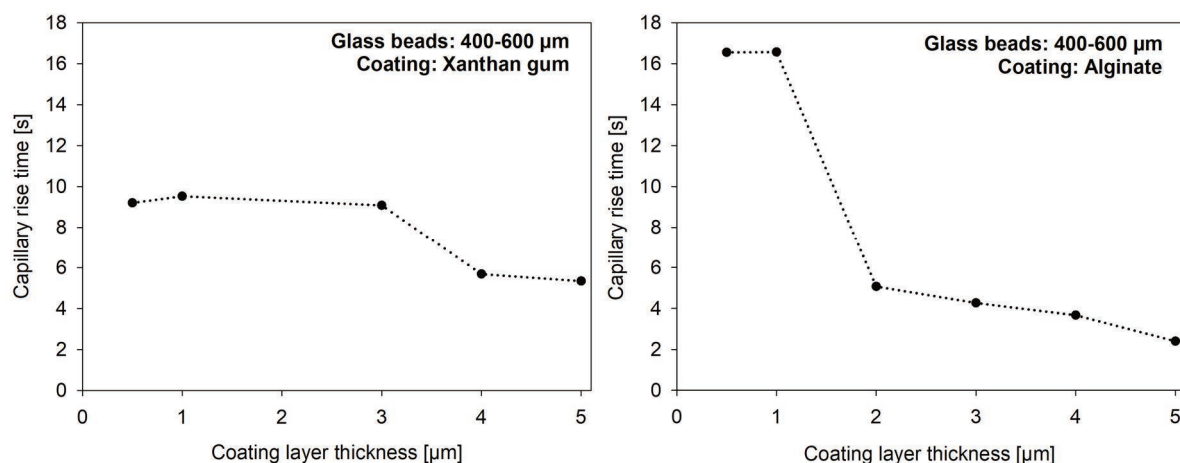


Fig. 4.5: Transition point between capillary and diffusional liquid uptake dependent on the biopolymer and coating layer thickness.

(2) In Fig. 4.4D, it can be seen that the slope of the linear phase decreases with increasing coating layer thickness. This observation was explained by the effect introduced in Fig. 4.2B. It is assumed that the fast hydration of the biopolymers leads to an instantaneous volume increase of the particles and to viscosity development in the swollen layer. These local dynamics are too fast to be recorded by the measurement system. Thus, obtained data from the first phase of powder rehydration are characterized by the formation of constant conditions. With increasing layer thickness the viscosity in the hydrated layer increases. This causes a higher flow resistance, which explains the more pronounced slowdown of capillary liquid rise with increasing layer thickness.

In case of guar gum, results could not be evaluated in terms of such a two-phase mechanism. Physical characterization of guar gum showed that the concentration-dependent viscosity increase of guar gum is higher compared to xanthan gum and alginate. Therefore, the influence of a hydrodynamic flow resistance is more pronounced and transition from capillary to diffusion mechanism is too fast to be assessed by the measuring system.

Dynamic capillary pressure: Further considerations to explain the deviant behavior of guar gum, focus on the existence of a concentration-dependent capillary pressure. If dissolution according to effect 1 (Fig. 4.2A) is assumed, the viscosity of the rising liquid increases. Compared to alginate and xanthan gum, concentration-dependent viscosity and gel stability is higher for guar gum [88,109]. To verify the assumption of a capillary pressure depending on concentration and rheological characteristics of the biopolymer

gels, the following experiment was performed. Glass capillaries with an inner diameter of $d_i = 472.6 \mu\text{m}$ (Hirschmann Laborgeräte GmbH&Co.KG, Eberstadt, Germany) were used to study capillary rise of differently concentrated solutions of xanthan gum, guar gum and alginate. The glass capillaries were immersed into the test solution and liquid height was measured after 24 h. Contact angles between capillary wall and biopolymer solution were determined by image analysis and used to calculate the corresponding capillary pressures. In Fig. 4.6, these are plotted against the biopolymer concentration in the solution. For guar gum, a dependency of the capillary pressure on the biopolymer concentration was found. For solutions above 1 % (w/w), measured contact angles differed strongly from the theoretically calculated values and no further increase of the contact angles was observed. This could be explained by a “separation” of the biopolymer solution due to molecule aggregation above a certain guar gum concentration. The liquid meniscus and thus the shape of the contact angle is then caused by a less concentrated solution. Aggregation of guar gum molecules has been investigated by Gittings *et al.* [115], which could confirm this assumption. However, the results of this study refer only to guar gum solution below a concentration of $< 1.1 \%$.

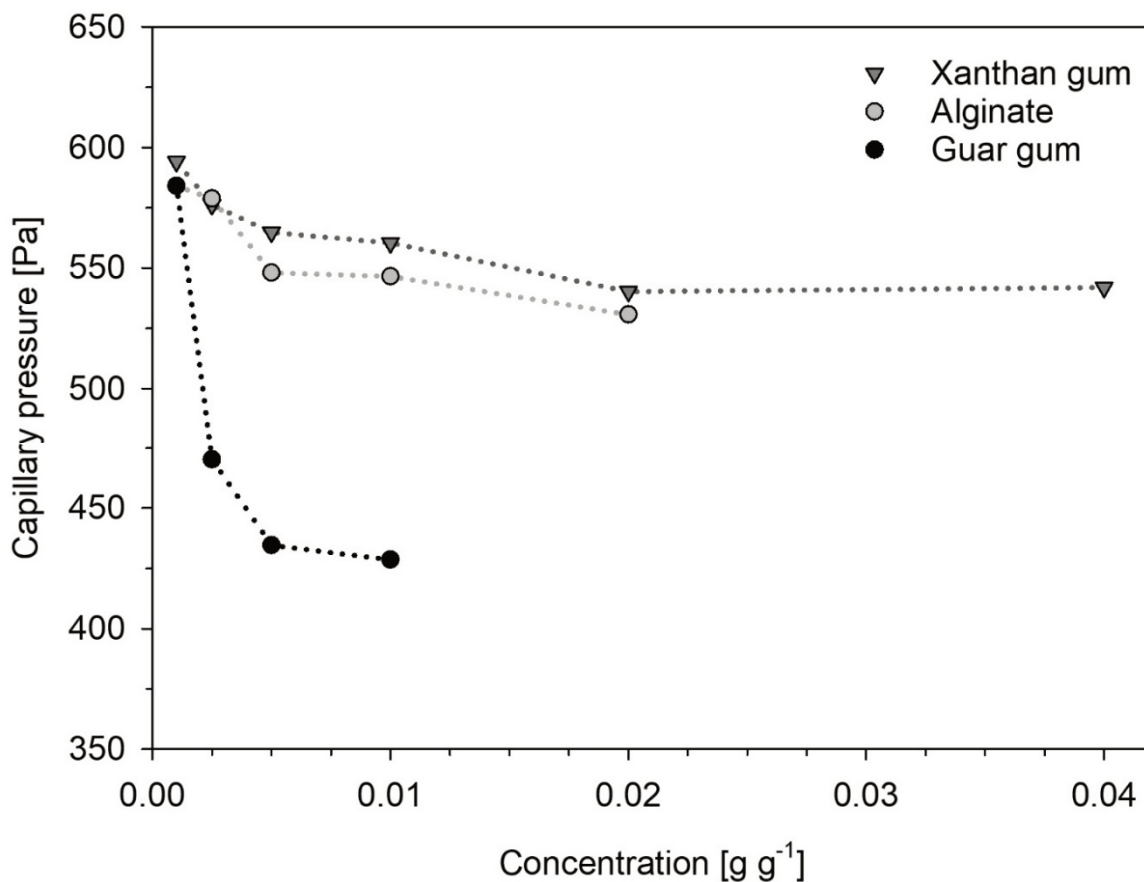


Fig. 4.6: Variation of capillary pressure dependent on biopolymer concentration.

The results presented above affirm that the deviant rehydration behavior of guar gum can be attributed to both differences in the rehydration dynamics in terms of viscosity development and swelling and to differences in the rheological gel properties and their impact on the dynamic capillary pressure.

4.4.4 GEL FORMATION AND WATER BINDING STRENGTH

NMR analysis was used to investigate the gel- and water binding strength of the biopolymer model system. Change of relaxation time was measured over time. Obtained data were fitted by a bi-exponential function (Eq. 4.5) and T2 relaxation times were determined.

$$\text{Intensity [\%]} = A_{\text{fast}} \cdot e^{-t/T2(1)} + A_{\text{slow}} \cdot e^{-t/T2(2)} \quad \text{Eq. 4.5}$$

Mobility of less mobile protons was determined by relaxation time T2(1) and of protons with higher mobility by relaxation time T2(2). The corresponding amplitudes $A_{\text{fast}}/A_{\text{slow}}$ express the relative proportion of free and bound water in the powder-water mixture. Results of NMR-analysis are shown in Fig. 4.7. For all hydrocolloids, an increase of fast relaxing, less mobile protons was observed over time. Furthermore, the percentage of bound water varied dependent on the biopolymer and the applied coating layer thickness. Comparing the results of glass beads with a coating layer thickness of 5 μm , xanthan gum exhibits the highest amount of bound water (45.5 %) followed by alginate (32.2 %) and guar gum (25.7 %). This result is in accordance with the higher water uptake capacity and higher water binding strength of xanthan gum compared to alginate and guar gum [88]. Especially for thicker coating layers of xanthan gum a continuous increase of the relative amount of bound protons could be observed. For guar gum and alginate, the limit of water uptake capacity was reached earlier and especially for alginate coated glass beads with a layer thickness of 0.5 μm and 1.0 μm a decrease of the amount of bound water could be observed. This decrease can be explained by the onset of dissolution of biopolymer molecules into the surrounding liquid. Viscosity increase in the liquid also restricts the mobility of protons, but not as pronounced as the highly viscous swollen layer. A higher proton mobility in viscous solutions compared to gels was also reported in literature [114, 116]. This explains the decreasing percentage of bound protons in the sample.

4 EXPERIMENTAL INVESTIGATION AND SIMULATION OF REHYDRATION DYNAMICS OF BIOPOLYMER POWDERS

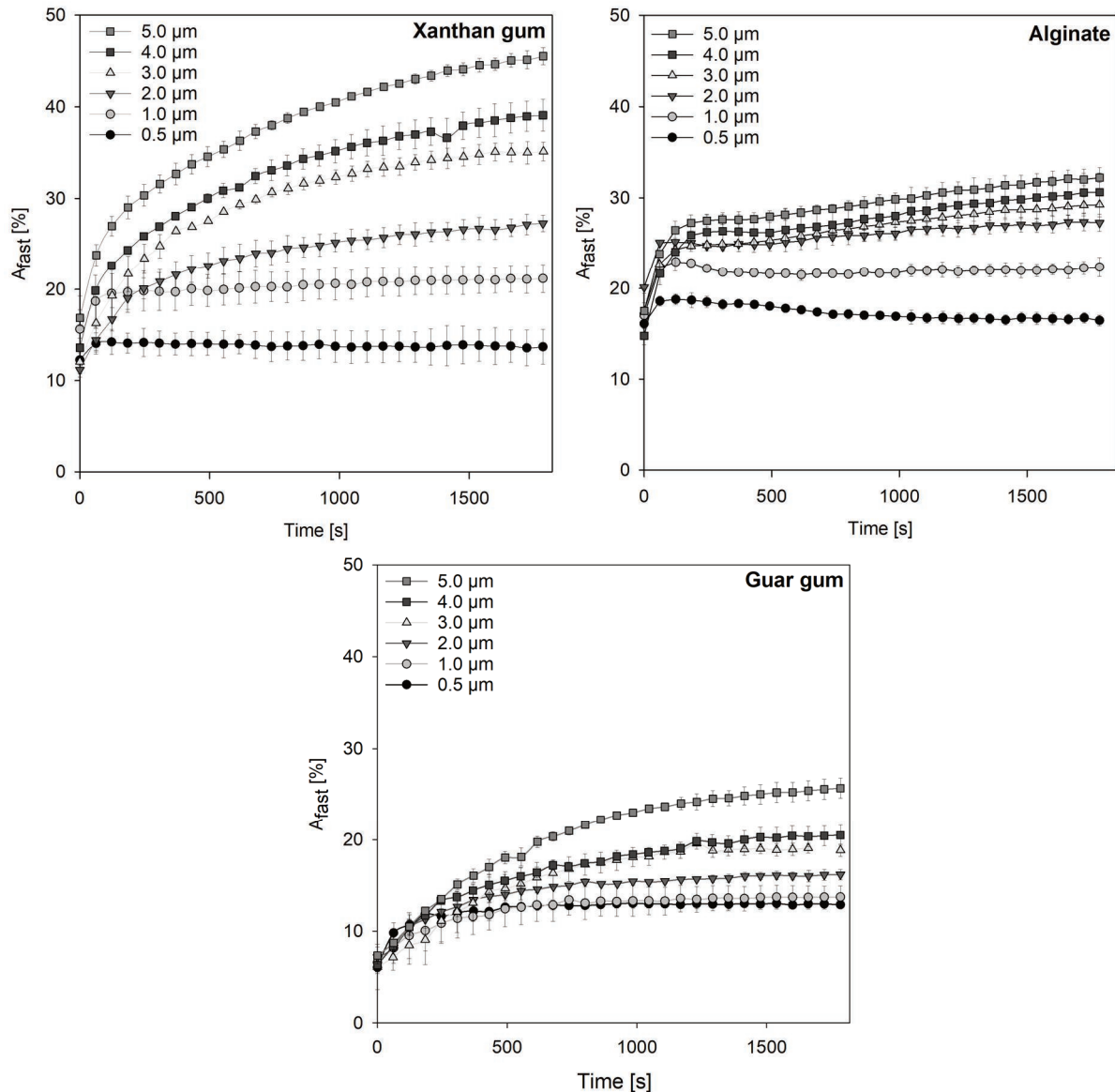


Fig. 4.7: Percentage of fast relaxing protons over time obtained from bi-exponential regression of NMR results.

To draw conclusions on biopolymer rehydration, the applied set-up and sample preparation simulates rehydration of a single biopolymer particle. Models to describe biopolymer rehydration assume a two-step process: (1) Phase transition from solid to dissolved powder and (2) diffusion of dissolved material through the surrounding surface layer into the liquid [64]. The velocity of these steps is mainly influenced by the viscosity of the layer surrounding the particle, the liquid density and particle size, but also by process parameters such as applied shear forces or temperature [43,99,114]. NMR measurements (Fig. 4.7) simulate the process of liquid diffusion into the inner parts of the particle. It is assumed that a steady increase of A_{fast} , as found for xanthan gum, correlates with progressive swelling. The subsequent water uptake into the inner

parts of the particle is retarded, which could explain the slow but continuous progression of water binding for xanthan gum. It can be concluded that the strong tendency of xanthan gum to aggregate in contact with water is a consequence of that dynamic interaction. In contrast, for alginate, the fast initial increase and the approach to an almost constant final value suggests that alginate exhibits a faster rate of molecule disentanglement. This enables a faster penetration of liquid molecules into the layer and, together with the lower viscous cohesion, detachment of alginate molecules out of the layer can proceed more easily. The importance of polymer disentanglement as precondition for water uptake has been described previously. Belton [13] emphasized that a slow polymer disentanglement together with swelling is often rate limiting for rehydration and determines the velocity of water transport. A higher water uptake velocity for alginate compared to xanthan gum at the beginning of powder-liquid contact was confirmed by previous analysis of the water uptake capacity of these biopolymers [88]. This behavior was attributed to a lower viscosity of the surrounding layer, which leads to a lower hydrodynamic flow resistance for liquid rise.

4.4.5 SIMULATION OF BIOPOLYMER REHYDRATION

For simulation, a Volume-of-Fluid approach was established under the assumptions hypothesized in Sect. 4.3. A parameter variation study was conducted to demonstrate the influence of swelling and dissolution on capillary liquid rise in food biopolymers. Parameters were varied in the range of experimentally determined physical characteristics. In Fig. 4.8, 3D-plots of the influence of swelling, dissolution and coating layer thickness on capillary liquid uptake are shown, based on the results obtained from simulation. Corresponding to that, the impact of dissolution and swelling on liquid height is summarized in Fig. 4.9.

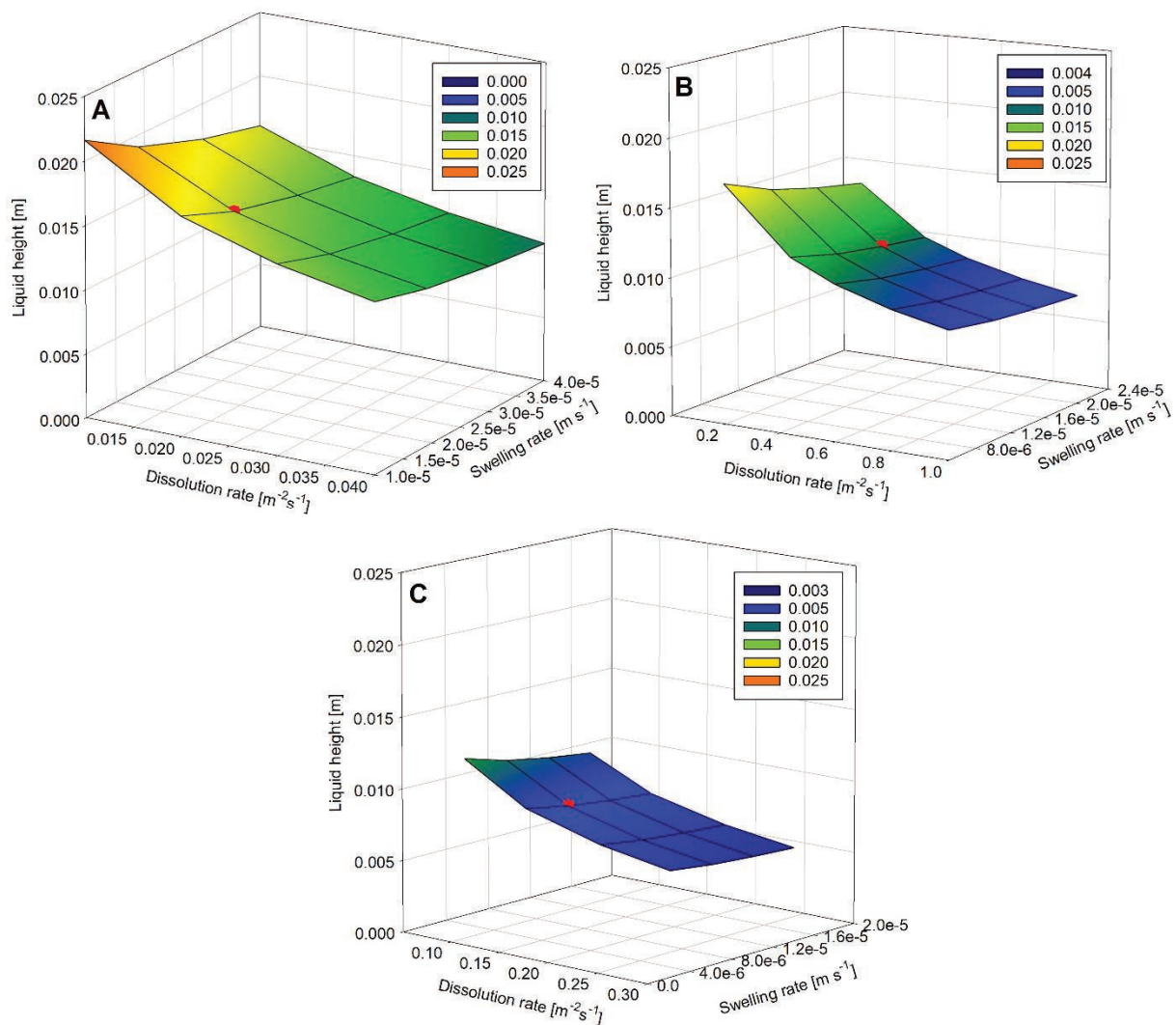


Fig. 4.8: Influence of swelling and dissolution on the capillary liquid uptake of food biopolymers obtained from simulation studies. (A) Xanthan gum, (B) Alginate, (C) Guar gum. Red dots represent simulated liquid heights corresponding to the physical characteristics of the respective biopolymer. Liquid heights represent the maximum heights before liquid velocity is 0.

4 EXPERIMENTAL INVESTIGATION AND SIMULATION OF REHYDRATION DYNAMICS OF BIOPOLYMER POWDERS

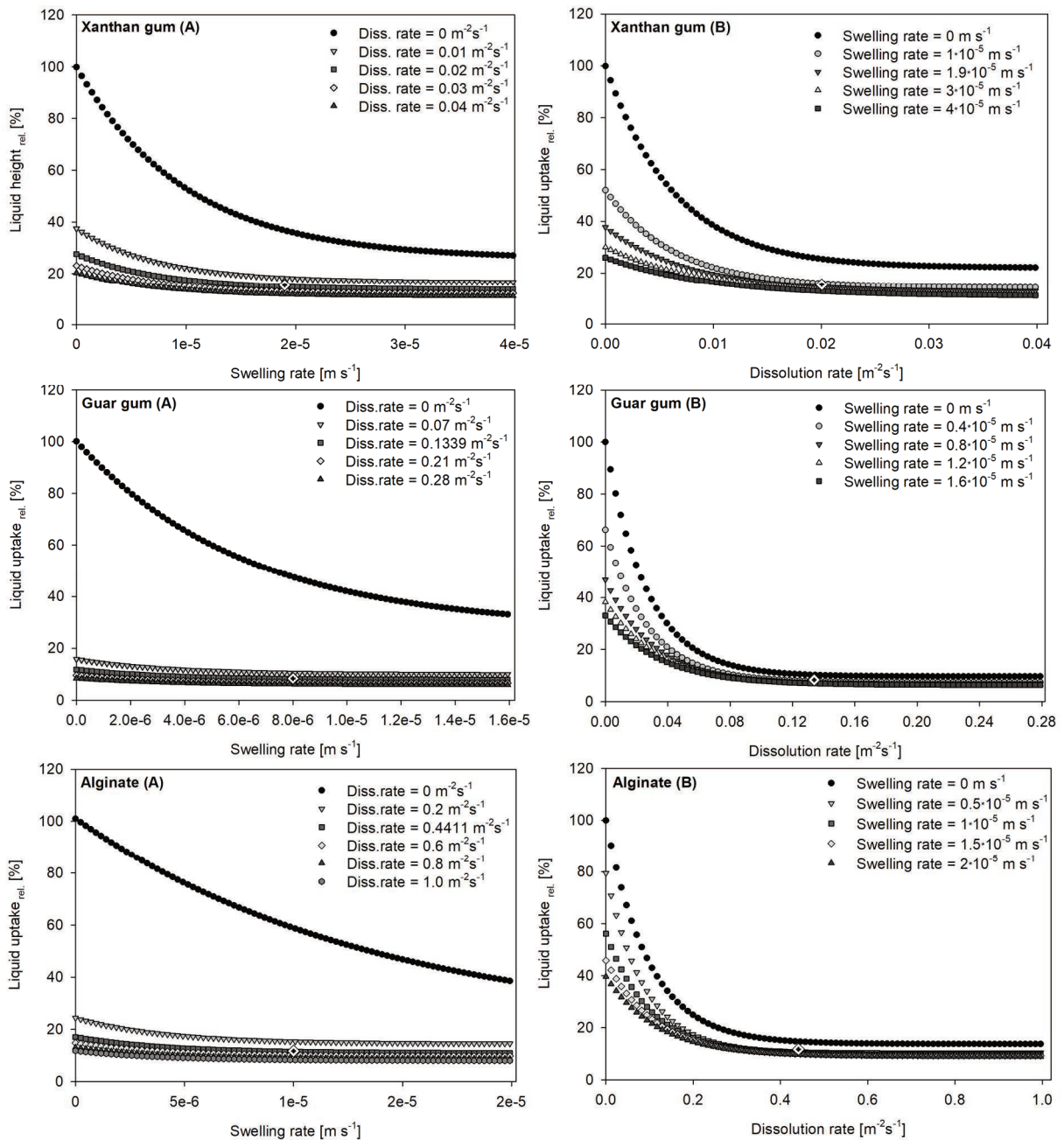


Fig. 4.9: Influence of swelling (A) and dissolution (B) on capillary liquid rise obtained from simulated parameter variation study. Crossed diamonds represent the liquid height corresponding to the respective physical parameters of the biopolymer. Data are given relative to a situation without dissolution or swelling, corresponding to a liquid uptake height of 0.1 m.

Simulated results qualitatively confirmed experimental data under the assumption of non-dissolution conditions (Fig. 4.2B). However, if dissolution according to effect 1 (Fig. 4.2A) is considered, associated viscosity development in the rehydration liquid dominates the process of capillary liquid uptake.

The influence of the coating thickness on capillary liquid uptake was implemented in simulation. Results summarized in Fig. 4.8 showed that all curves lie on top of each

other. Water absorption is therefore independent of the layer thickness. This is in contrast to experimental measurements and related to the low solubility of the swollen layer as discussed below.

Further simplifications focus on translating swelling and viscosity development into a simulation approach. In particular, the influence of the viscosity of the swollen layer is difficult to assess. With regard to swelling, a spherical volume increase of the particles was assumed. In reality, it is more likely that the shape of the particle changes with proceeding volume expansion. This loss of the spherical particle shape and the resulting continuous film of swollen biopolymer particles accelerates the collapse of the pore network and finally stops capillary liquid rise.

Deviations between simulation and experiments could be explained by the two effects proposed in Fig. 4.2. In simulation, viscosity development is considered by assuming dissolution of biopolymer molecules into the rehydration liquid (Fig. 4.2A). However, as experimental measurements [88] supported the assumption of a non-dissolution state as proposed by Fig. 4.2B, a non-mobile viscosity was implemented in simulation as explained in Sect. 4.3. The minor influence of biopolymer dissolution into the rehydration liquid was additionally supported by calculating the necessary dissolution time of the coating layer. According to the results summarized in Fig. 4.10, the high dissolution times and low changes of viscosity suggest that the influence of biopolymer dissolution can be neglected.

Within the period of capillary liquid rise (Fig. 4.4, Fig. 4.5), only for alginate, dissolution times are within a relevant time-frame of ~ 5 min for the $0.5 \mu\text{m}$ layer. Based on these considerations, effect 2 (Fig. 4.2B), is more likely to explain the influence of viscosity in highly concentrated situations. The decline of the viscosity values of the rehydration liquid with increasing coating layer thickness (Fig. 4.10) results from the associated increase of the total particle diameter. In consequence, within a bulk layer the particle number is decreased by ~ 5 %, the biopolymer mass by ~ 10 % and particle surface area by ~ 1.8 % which explains the slight decrease of viscosity (Fig. 4.10). However, this dependency was not considered further.

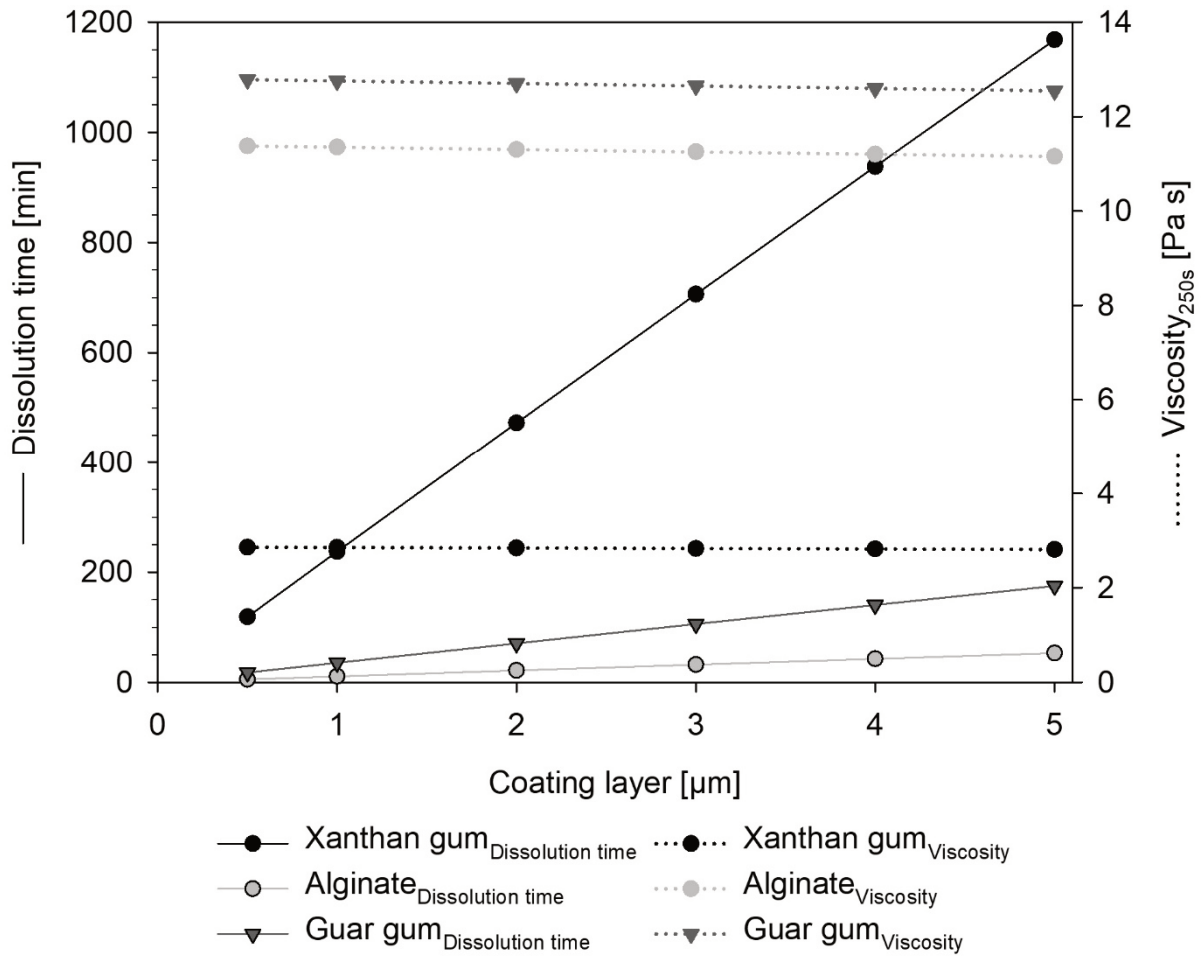


Fig. 4.10: Time for complete dissolution of the biopolymer coating layer and liquid viscosity after 250 s dependent on the coating layer thickness. Calculation is based on the specific dissolution rate, biopolymer concentration and available particle surface.

4.5 REMARKS CONCERNING CAPILLARY LIQUID RISE IN FOOD POWDERS

Dissolution, viscosity development and swelling processes influence the formation of particle aggregates and floating layers. In particular, rehydration of biopolymer powders is strongly affected by these dynamics. Biopolymers are able to bind high amounts of water, to swell and to develop highly viscous phases even with low concentrations. Due to their high affinity for hydrophilic liquids, these processes take place directly after powder-liquid contact which causes an immediate change of their water uptake ability. According to the Washburn equation (Eq. 4.2), swelling and associated decrease of the capillary diameter as well as increase of liquid viscosity as a result of biopolymer dissolution slowdown capillary liquid rise. If a powder is added to a liquid surface, these dynamic changes lead to the formation of a viscous layer

between liquid and powder phase. Within this layer the pore network collapses and further water uptake can only be accomplished by diffusional liquid transport. Difficulties associated with biopolymer rehydration, such as floating and the formation of particle aggregates with dry powder inside, can be explained by these dynamic processes.

Due to the spatial and temporal overlap, viscosity and swelling processes cannot be separated from each other. Hydration of the biopolymer coating layer within the model system leads to an absorption of liquid and to the formation of an entangled biopolymer network. The coating layer expands due to swelling associated with the formation of a viscous gel-like structure. With increasing swelling and “dilution” a concentration profile within the swollen gel layer develops. Detachment of biopolymer molecules only occurs if a critical swelling/dilution state is exceeded. As specified in a previous study [109] these critical swelling states range in-between $1.6 \text{ g}_{\text{water}}/\text{g}_{\text{powder}}$ for alginate, $5.6 \text{ g}_{\text{water}}/\text{g}_{\text{powder}}$ for xanthan gum and $1.1 \text{ g}_{\text{water}}/\text{g}_{\text{powder}}$ for guar gum. These values correspond to swelling times of $\sim 100 \text{ s}$, $\sim 90 \text{ s}$ and $\sim 200 \text{ s}$ and are beyond the relevant time-frame of simulated capillary liquid rise (Fig. 4.5).

In order to support the dominance of swelling versus dissolution processes, theoretical time-frames of capillary rise were estimated by calculation. Calculations were based on the hydraulic pore diameter of the bulk and the swelling rate of the respective biopolymer. Results are summarized in Table 4.2 with the example of a $0.5 \mu\text{m}$ coating layer. In comparison, calculated and experimental data agree within an acceptable range. With regard to pure biopolymer powder bulks, calculated time-frames range in-between 1 and 2 s. This is in accordance with experimental data specified in previous studies [109].

However, even if dissolution of biopolymer molecules plays only a minor role, viscosity increase within the swollen gel layer contributes to a slowdown of liquid rise. In the Washburn approach capillaries are considered cylindrical without inter-connections, which does not represent the situation in real powder bulks [44,91,117]. Swelling processes, together with the barrier-like effect of the viscous boundary layer, further increase the flow resistance for capillary rise. Assuming non-spherical volume increase and associated increase of capillary tortuosity additionally contributes to a slowdown of capillary liquid transport.

The influence of swelling processes on capillary rise was also investigated by Saguy *et al.* [108]. It was found that a change of pore size distribution affects the rate of capillary rise in porous media. Same was stated by Shi & Gardner [118] who investigated the impact of polymer swelling on contact angle determination by capillary rise measurements. According to their study, swelling results in a change of particle geometry, a decrease of the capillary diameter and in a loss of energy due to release of absorption energy. These processes cause a decrease in the rate of capillary rise.

Fig. 4.9 shows the influences of swelling and viscosity development on capillary liquid rise in the biopolymer model system. Results from parameter variation study demonstrate the sensitivity of capillary liquid rise to dynamic processes. Comparing Fig. 4.9A and B, results indicate that the influence of viscosity is more pronounced than swelling. As soon as dissolution is implemented in simulation, liquid rise immediately decreases. Increase of the swelling rate has only a minor impact (Fig. 4.9A).

4.6 CONCLUSION

Within this study, the rehydration behavior of xanthan gum, guar gum and alginate was investigated. It could be shown that this process is highly dynamic and subjected to changing powder characteristics which result from dissolution, viscosity development and swelling of powder particles. Profound knowledge about the relationship between physical characteristics, their dynamics and the rehydration behavior of the powder is essential to optimize powder properties with regard to their rehydration behavior.

Due to their highly hydrophilic character, these dynamic processes start immediately after powder-liquid contact. The speed of these dynamics leads to aggregation and the formation of floating layers. As strategy to improve powder quality in terms of a convenience application, powder characteristics could be adjusted to delay these dynamic changes. Possible strategies should focus on the dominating characteristics of the powder. E.g. for xanthan gum pore blocking takes place almost immediately after powder-liquid contact due to the very fast and strong swelling behavior [88,109]. For that reason, the focus should be on improving the dispersion behavior. Here, the production of dense particles with a small surface-to-volume ratio could be a strategy. In case of powders with a slower or only a minor change of their characteristics, the rehydration behavior could be improved by agglomeration. Beside an easier dispersability, the higher porosity enables a better liquid transport into the inner parts of the particle. However, a proof of principles is still required.

Rehydration was investigated based on a model system consisting of biopolymer coated glass beads to control the extent and strength of dynamic interactions. It was concluded that rehydration of xanthan gum and alginate is mainly influenced by swelling processes whereas guar gum rehydration is dominated by dissolution and viscosity development in the rehydration liquid. Dynamic effects are strong enough to cause a slowdown of capillary liquid rise even with the thinnest coating layer of 0.5 μm . This suggests that the difficulties in rehydrating biopolymers can be attributed to dynamic changes at the particle surface.

The interaction between swelling and viscosity development was explained by two effects, which distinguish between a “dissolution” (effect 1) and a “non-dissolution” (effect 2) mechanism (Fig. 4.2). Due to the highly concentrated situation within the experiment the “non-dissolution” mechanism (Fig. 4.2B) was assumed to be more likely. According to this assumption, viscosity development is restricted to the hydrated, swollen surface layer around the particle. In consequence, viscosity development and swelling processes must be regarded as interrelated processes. Both contribute to an increase of hydrodynamic flow resistance and to an associated slowdown of capillary liquid rise.

The simulation of the rehydration process confirmed the experimental data qualitatively. With the help of a parameter variation study the sensitivity of the rehydration process to dynamic processes was confirmed. The combined evaluation of experimental and simulated data provided deeper knowledge about the interactions between the dynamic powder properties. The presented results are a step forward to describe their mechanisms in connection with food powder rehydration.

4.7 SYMBOLS USED

SYMBOLS

A	$[m^2]$	Surface
c	$[kg/kg]$	Concentration
d	$[m]$	Diameter
$d_{3,2}$	$[m]$	Surface weighted mean diameter
$d_{4,3}$	$[m]$	Volume weighted mean diameter
h	$[m]$	Height
m	$[kg]$	Mass
N_{Particle}^*	$[-]$	Theoretical particle number in powder sample
p_c	$[N\ m^{-2}]$	Capillary pressure
s_{target}	$[m]$	Target coating layer thickness
t	$[s]$	Time
V	$[m^3]$	Volume

GREEK SYMBOLS

γ	$[N\ m^{-1}]$	Surface tension
ε	$[-]$	Porosity
η	$[Pas]$	Dynamic viscosity
θ	$[^\circ]$	Contact angle
ρ	$[kg\ m^{-3}]$	Density

SUB- AND SUPERSCRIPTS

i	Inner
l	Liquid
OD	Outer diameter
p	Particle

ABBREVIATIONS

DR	$[m^{-2}\ s^{-1}]$	Dissolution rate
BD	$[kg\ m^{-3}]$	Bulk density
$A_{\text{fast}}, A_{\text{slow}}$	$[\%]$	Percentage of fast and slow relaxing protons
T2(1)	$[ms]$	Relaxation time of fast relaxing component
T2(2)	$[ms]$	Relaxation time of slowly relaxing component

Chapter 5 DISCUSSION AND CONCLUDING REMARKS

DISCUSSION

Dynamic processes such as dissolution, viscosity development and swelling make food powder reconstitution a complex process. Within this thesis the importance of dynamically changing powder characteristics related to the rehydration behavior of food powders is shown. The biopolymer powders xanthan gum, guar gum and alginate were used as exemplary model systems. Within this thesis, it has been demonstrated that common difficulties in powder rehydration, such as formation of floating layers and highly stable particle aggregates, are associated to these dynamically changing properties.

Methods to characterize powder rehydration have been presented in literature previously. However, in case of dynamically changing powder systems, a physically-based quantification of rehydration kinetics has not been reported so far. As demonstrated by the results presented in Chapter 2 - Chapter 4, the processes taking place after powder-liquid contact are highly dynamic. For that reason, measurement and quantification of these kinetics is challenging. The same applies to the differentiation of the individual dynamic effects. These questions have been addressed within this thesis.

Within the present thesis it was demonstrated that capillary water uptake and thus the characteristics of powders in terms of aggregation tendency and dispersability correlate with the velocity of the proceeding changes. To meet the demand for a convenient application of food powders a better understanding of the rehydration dynamics is mandatory. Therefore, attention was given on the analysis of the dynamics of powder-liquid interaction and the associated changes of powder/liquid properties. Obtained findings were evaluated with respect to their effects on the powder rehydration process. Accordingly, within this thesis, three main topics were investigated:

1. Evaluation and development of methods and definition of standard procedures to characterize steps of biopolymer rehydration (Chapter 2).
2. Physical characterization of biopolymer powders and identifying critical characteristics with regard to the rehydration behavior (Chapter 3)

3. Set-up and development of a model to simulate rehydration of dynamically changing powder systems based on their physical properties (Chapter 4)

In a first step methods to analyze the physical powder properties with focus on their dynamics were established. Results are presented within the first publication “*Dynamics of Capillary Wetting of Biopolymer Powders*” (Chapter 2). Quantitative data regarding the influence of wettability, viscosity development and swelling on the rehydration process of biopolymer powders are presented. Kinetics of swelling and viscosity development were determined by a rheological measurement set-up. The velocity of these processes is however so fast that one has to consider these values as semi-quantitative. Especially initial effects might be underestimated by the presented measurement system. Furthermore, due to their temporal superposition, the impact of swelling on viscosity development could not be assessed separately with this set-up. Results given for viscosity development presumably represent an overlay of these processes. The same applies to results of contact angle analyses. Surface roughness as well as a change of surface characteristics during analyses was minimized by the use of compressed tablets, but could not be excluded (Table 9.2). However, focus of the study presented in Chapter 2 was to categorize and differentiate between different food powders with regard to their rehydration behavior. Here, the presented methods have proven to be sufficiently sensitive.

Despite these restrictions, data given within this study (Chapter 2) are a step forward to approaches published so far. However, a combined consideration of different analyses is recommended to enable a profound description of the rehydration dynamics.

In Chapter 2 it has been shown that the rehydration steps wetting, sinking and dispersing are decisively influenced by the rate of swelling and viscosity increase. The relation between these processes and powder rehydration was demonstrated by dynamic capillary rise measurements. In case of biopolymers, results confirmed the highly dynamic situation. Rate of dynamic changes was shown to proceed so fast that the available time-frame for capillary water uptake was in the range of 1 s. This short time frame is a consequence of swelling-induced pore blocking, viscosity increase and the associated increase of the hydrodynamic flow resistance. Based on these results and with regard to powder processing, it is recommended to complete the step of

powder dispersion within that critical time-frame to avoid the formation of floating layers or aggregates.

Based on the data represented in Chapter 2, differences in the dynamic behavior of the analyzed biopolymers were quantified. It has been shown that, depending on the biopolymer characteristics, either viscosity or swelling mainly influence the formation and disintegration of aggregates. Obtained findings allow individualized recommendations concerning dispersing strategies based on the respective powder characteristics.

To predict the process of powder rehydration, a Volume-of-Fluid (VoF) approach was established within the first publication. Compared to other methods, e.g. simulation by finite and discrete elements which rather focus on the description of processes concerning single particles, the VoF approach was regarded most suited to describe capillary liquid rise. The general view of dynamics related to the whole process is more suitable to simulate capillary liquid rise in food powders. Additionally, the necessary time for computation is reduced with this approach.

For simulation, physical properties and dynamic changes of powder characteristics were translated into a model approach. The advantage of this model over empirical simulation approaches is the physically based description of the rehydration processes. Provided that the physical characteristics of a powder, respectively their dynamic behavior, are known, a universal applicability to other powder systems is possible.

The idea behind the simulation, represented in Chapter 2, is a stepwise adaption of the Washburn approach which was used as basic equation. Experimentally, rehydration was investigated by capillary liquid rise into a powder bulk. The established model enabled a qualitative description of key parameters and an estimation of their relevance for powder rehydration. Simulation showed that swelling leads to a slowdown of the water uptake rate and to a reduced height of capillary liquid rise. Furthermore, the impact of viscosity was affirmed. It has been shown that even a small increase of viscosity delays water uptake and slows down liquid penetration into the powder bulk. These results are in accordance with general principles concerning capillary liquid transport and can be explained by an increase of the hydrodynamic flow resistance. This increase of resisting forces was attributed to (1) a swelling-induced reduction of the capillary diameter, (2) the viscosity of the swollen layer surrounding

the particles and (3) the increase of liquid viscosity, induced by biopolymer dissolution out of the swollen layer. These effects and their interaction demand higher capillary forces to maintain the velocity of liquid rise. Thus, the slowdown of capillary liquid transport is a consequence of these processes.

These results illustrate the relevance of dynamic powder-liquid interactions related to powder rehydration processes. It was shown that even small changes of physical characteristics of the powder-liquid system favor an incomplete powder wetting associated to the formation of particle aggregates and floating layers. Due to the concurrency and mutual interaction of different dynamic effects, their impact on the rehydration performance of food powders is even more pronounced. These findings motivated more intense analyses of physical powder characteristics and their dynamics which was done in the second publication titled "*Development and validation of methods to characterize rehydration behavior of food hydrocolloids*" (Chapter 3). Based on the previous results (Chapter 2), viscosity development and swelling were shown to be most critical. These influencing factors were quantified in more detail by the methods presented Chapter 3. Analyses focused on the determination of the water uptake capability, the water binding strength and the viscous cohesion as a criterion for the aggregate stability.

The combined evaluation of the results given in Chapter 2 and Chapter 3 revealed that difficulties associated with powder rehydration cannot be described only by the dynamics of viscosity development and swelling. Both processes have proven to be key factors to describe the kinetics of layer formation and particle aggregation. It could be affirmed that, due to the high velocity of the proceeding reactions, especially the first instants of powder-liquid contact are crucial for biopolymer rehydration. Assumptions concerning dispersing strategies and disintegration behavior were given based on the characteristics of the biopolymer aggregates. In particular, water uptake capacity, water binding strength and rheological properties of the biopolymer gels were shown to be most relevant. By a rheological set-up the individual steps of rehydration were defined. These were categorized in water uptake and swelling after powder-liquid contact, molecule detachment out of the swollen layer under the action of shear-stress and concentration-driven molecular diffusion into the rehydration liquid. It was demonstrated that powders with a higher water binding strength which form highly viscous gel layers require higher shear forces for aggregate disintegration.

The findings obtained from this study (Chapter 3) revealed the complexity of food powder rehydration. Specific concepts for quality improvement and process adaption with respect to rehydration issues are provided. It could be shown that the critical rehydration behavior of guar gum is attributed to viscosity development, whereas swelling dominates xanthan gum rehydration. Considering the results of aggregate stability, in application of guar gum, focus should be placed on avoiding lump formation. In case of xanthan gum, aggregate formation is difficult to avoid due to the high swellability. However, viscous cohesion within the aggregates is lower which makes aggregate disintegration an option.

Based on the results presented in Chapter 2 and Chapter 3, the study "*Experimental Investigation and Simulation of Rehydration Dynamics of Biopolymer Powders*" (Chapter 4) improved the predictability and quantification of food powder rehydration. The model introduced in Chapter 2 was improved by refining the model assumptions and parameters. This enabled a more precise balancing of liquid flows in terms of liquid bound by swelling or liquid available for capillary rise.

As previously discussed, the spatial and temporal superposition of various dynamic processes makes a separate investigation of the individual effects difficult to assess. This issue has been addressed by the study presented in Chapter 4. This was achieved by the development of a model system consisting of biopolymer coated glass beads. With the help of this model system the rehydration dynamics associated with biopolymer rehydration could be controlled. Dimensions of swelling and viscosity development were adjusted by the variation of the coating layer thickness and the coating material. Thus, swelling induced pore blocking of the bulk as well as critical viscosity development could be delayed and the individual dynamic effects of food powder rehydration could be specified in more detail.

The impact of dynamic effects on powder rehydration was demonstrated by capillary rise experiments. Results revealed that even thin coating layers of 0.5 μm are sufficient to delay and finally stop capillary liquid rise. This provided new insights in the mechanisms of powder rehydration. Contrary to previous assumptions, difficulties in powder rehydration seem to be attributed only to surface related modifications of powder characteristics. In consequence, to improve the rehydration behavior, further strategies besides size enlargement should be considered. These could include the

increase of porosity or the adjustment of wetting characteristics, e.g. by the application of functional coating layers.

As a further result, a two-phase mechanism of liquid uptake could be defined. The first phase of liquid rise is attributed to the action of capillary forces followed by a second phase which is dominated by diffusion processes. For xanthan gum and alginate, a quantitative correlation between the time-frame of capillary rise (first phase) and their swelling potential was demonstrated. This suggests that xanthan gum and alginate rehydration is mainly hindered by swelling processes and corresponding pore blocking conditions. For guar gum the time-frame of capillary liquid rise was too short to be detected. The swelling potential of guar gum however is less pronounced compared to xanthan gum and alginate. Instead, dissolution rate and concentration-dependent viscosity is highest for guar gum. This gives further evidence for the existence of different key factors in context with their rehydration behavior.

The connection between these experimental observations and the dynamic powder characteristics could be explained successfully by simulation. With the help of a parameter variation study, concerning dissolution and swelling, both effects could be distinguished and their influence on powder rehydration could be explained. Against expectations, simulation revealed that the influence of the coating layer thickness can be neglected. Based on the dissolution rates of the biopolymers, calculations showed that a complete dissolution could not be achieved even for the thinnest coating layer within the relevant time-frame of capillary liquid rise. Temporal changes and differences in viscosity were rather attributed to available biopolymer concentration and available surface than to coating layer thickness. This indicates that dissolution processes and increase of liquid viscosity cannot explain the experimental observations and are not relevant for the formation of aggregates.

As affirmed experimentally (Chapter 3), in a water-limited rehydration situation, viscosity development is restricted to the swollen surface layer. Considering this, the deviating behavior of guar gum can be explained by the higher viscosity within the swollen layer. Due to the interaction between the rehydration liquid and the particle surrounding layer, this is associated with higher viscous obstruction opposed to liquid rise.

The influence of swelling on powder rehydration was confirmed by simulation. However, if dissolution is implemented into the simulation approach, viscosity development dominates the powder rehydration process.

Results represented in Chapter 4 demonstrated the influences of dynamic effects on powder rehydration both independently and in combination. It has been demonstrated that the different effects related to powder rehydration cannot be treated separately from each other due to their mutual intensification. Simulation of the rehydration process confirmed the experimental data qualitatively. The combined evaluation of experimental and simulated data provided a deeper understanding about the interactions between the dynamic powder properties. Results are a step forward to describe the mechanisms of dynamic processes and their influence on powder rehydration.

CONCLUDING REMARKS

Within this thesis food powder rehydration was investigated. Methods to characterize associated dynamic changes of powder properties were established. Based on these results a model was established using physical powder characteristics. Although this thesis mainly focused on hydrocolloids as model powders, the presented methods are also applicable to other systems, e.g. protein powders. This also applies to the proposed simulation model. Due to the physically based approach a universal application to various powder systems is possible. The obtained results enable a deeper understanding of food powder rehydration. With regard to product development and process optimization the presented results can be used for purposeful improvement strategies.

In future studies, further food powders should be categorized to obtain a larger database in order to consolidate the relationship between dynamic behavior and rehydration properties. Furthermore, the relationship between aggregate stability and necessary disintegration forces would be of interest for following investigations. Within this thesis, the stability of biopolymer aggregates was investigated using a rheometer set-up. The results of such measurements could be used to assess the disintegration behavior of aggregates in scale-up situations. However, it should be acknowledged that other effects like elongational- and impact stresses will also lead to disintegration. Finally, the suggested simulation approach should be refined by improving the translation of experimentally observed processes into physical based parameters.

Chapter 6 SUMMARY

The rehydration behavior of food powders is of high importance in terms of powder processing and product quality. Rehydration of powders mainly depends on the physical powder characteristics particle size, porosity and wettability, the latter being expressed by the contact angle between solid and rehydrating liquid. With focus on food powders, it could be shown that the rehydration behavior is strongly influenced by dynamic changes of these physical characteristics. This includes the initiation of dissolution and swelling directly after powder-liquid contact. Especially in case of biopolymers, which were investigated in detail by the example of xanthan gum, guar gum and alginate, these processes are important to describe their rehydration behavior. Due to the special characteristics of these biopolymers dissolution and swelling result in an increase of viscosity as well as in a decrease of bulk porosity. The kinetics and interactions of these processes significantly affect the individual steps of rehydration and have to be considered in describing the process of food powder rehydration.

For inert powder-liquid systems capillary liquid uptake into a powder bulk can be described by the Washburn equation which equates the capillary pressure and the hydrodynamic flow resistance. Within this thesis, this approach was used as basic equation to describe capillary liquid uptake of food powders. The validity of the original approach is restricted to the case of constant powder and liquid properties. With regard to food powders, changes within the powder-liquid system were considered by a stepwise adaption of the corresponding variables of the Washburn equation. Thus, the first part of this thesis focused on establishing and defining standard methods to characterize the dynamics of the physical properties particle size, bulk porosity, viscosity as well as contact angle. This enabled a more detailed characterization of the interactions between food powder and liquid over the course of rehydration. Wettability of food powders in contact with distilled water was assessed by contact angle measurements on compressed powder tablets using the sessile drop method. Contact angles of the analyzed biopolymers were 52° for alginate, 58.1° for xanthan gum and 70° for guar gum which confirmed the hydrophilic character of these powders. To describe the change of the bulk porosity a rheological measurement set-up was constructed to quantify the swelling behavior. Swelling rates, referred to a change of the particle diameter $d_{3,2}$ were found to be 18 $\mu\text{m s}^{-1}$ for xanthan gum, 10 $\mu\text{m s}^{-1}$ for

alginate and $8 \mu\text{m s}^{-1}$ for guar gum. Influence of viscosity on rehydration was determined by measuring the concentration dependent viscosity increase and the rate of viscosity increase over time. The change of viscosity as a consequence of dissolution allowed conclusions about the dissolution rate of biopolymers in highly concentrated situations. These results indicated that rehydration of guar gum is mainly influenced by viscosity effects whereas swelling has the highest impact on the rehydration behavior of xanthan gum and alginate. Further methods such as Nuclear Magnetic Resonance analysis (NMR) enabled a more detailed characterization concerning the dynamics of powder-liquid interactions and the strength of water binding within these biopolymer gels. The strength of water binding was found to correlate with the stability of highly concentrated biopolymer aggregates. The aggregate stability was determined by rheological analyses and is of importance, particularly with regard to powder dispersability.

Finally, to predict food powder rehydration, a model was established using a Volume-of-Fluid approach. To simulate capillary liquid rise based on physical characteristics, dynamic changes were resolved both spatial and temporally. To describe particle and liquid properties more precisely, a model system consisting of biopolymer coated glass beads was developed by fluid bed technology. By the variation of the coating layer thickness and the coating material, dynamic changes within the system could be controlled which enabled a more differentiated description.

A parameter variation study was conducted to simulate the influence and interaction of dynamic processes on capillary liquid uptake into such powder systems. Capillary liquid uptake into the coated glass beads was investigated experimentally. It could be shown that even with coating layers of $0.5 \mu\text{m}$ dynamic effects are sufficiently strong to cause a stop of capillary liquid uptake. It has been shown that viscosity development dominates guar gum rehydration whereas swelling is the prevalent mechanism in xanthan gum and alginate rehydration.

Simulation of capillary liquid rise demonstrated that the influence of the coating layer thickness is not significant. This result could be explained by the slow dissolution rates of the biopolymer samples. Calculations indicated that even a coating layer of $0.5 \mu\text{m}$ could only be dissolved partially after a dissolution time of 250 s. This explains the little impact of coating layer thickness on viscosity development and thus on capillary liquid uptake. Further explanations focus on biopolymer swelling. Simulation showed that

6 SUMMARY

coating layers of 0.5 μm are sufficient to cause swelling-induced pore-blocking conditions.

Chapter 7 ZUSAMMENFASSUNG

Das Rehydratationsverhalten von pulverförmigen Lebensmitteln ist von großer Bedeutung in Bezug auf Verarbeitung und Produktqualität. Die Rehydratation von Pulvern wird hauptsächlich von physikalischen Eigenschaften, wie beispielsweise Partikelgröße, Porosität und Benetzbarkeit beeinflusst. Im Fall von Lebensmittelpulvern müssen neben diesen Parametern zusätzliche Faktoren berücksichtigt werden. Im Rahmen dieser Dissertation wurde gezeigt, dass insbesondere dynamische Prozesse, die eine Veränderung der Pulvereigenschaften zur Folge haben, die Rehydratation von Lebensmittelpulvern stark beeinflussen. Hierbei sind insbesondere Löse- und Quellvorgänge von Bedeutung, die häufig direkt nach dem Kontakt zwischen Pulver und Flüssigkeit initiiert werden. Diese Vorgänge spielen insbesondere bei Biopolymer-Pulvern, die im Rahmen dieser Arbeit am Beispiel von Xanthan, Guarkernmehl und Alginat intensiv untersucht wurden, eine wichtige Rolle zur Beschreibung des Rehydratationsverhaltens. Durch die speziellen Eigenschaften dieser Biopolymere resultieren Löse- und Quellvorgänge in einem Anstieg der Viskosität sowie in einer Abnahme der Schüttungsporosität. Die Dynamik und die gegenseitige Beeinflussung dieser Prozesse wirkt sich entscheidend auf den Ablauf der einzelnen Rehydratationsschritte Benetzen, Einsinken, Dispergieren und Lösen aus. Im Fall inerter Pulver-Flüssigkeit-Kombinationen lässt sich die kapillare Flüssigkeitsaufnahme in eine Pulverschüttung mithilfe der Washburn-Gleichung beschreiben. Dieser Ansatz beruht auf der Gleichsetzung des Kapillardrucks mit hydrodynamischen Fließwiderständen. Der durch Washburn etablierte Ansatz wurde im Rahmen dieser Arbeit als Grundlage zur Beschreibung der kapillaren Flüssigkeitsaufnahme in Lebensmittelpulvern verwendet. Die Gültigkeit des ursprünglichen Ansatzes beschränkt sich auf den Fall konstanter Pulver- und Flüssigkeitseigenschaften. Im Fall der untersuchten Lebensmittelpulver wurde daher die dynamische Veränderung des Systems durch schrittweise Anpassung der relevanten Variablen der Washburn-Gleichung berücksichtigt. Dementsprechend wurden im ersten Teil dieser Arbeit Standardmethoden zur Beschreibung der dynamischen Veränderungen der physikalischen Eigenschaften Partikelgröße, Schüttungsporosität und Viskosität sowie zur Bestimmung des Kontaktwinkels etabliert. Dies ermöglichte eine detaillierte Charakterisierung der Wechselwirkungen zwischen Lebensmittelpulvern und Flüssigkeit im Verlauf der Rehydratation. Die

Benetzbarkeit der Pulver mit destilliertem Wasser wurde mithilfe der „Sessile drop“-Methode auf komprimierten Pulvertabletten bestimmt. Die Werte der dabei gemessenen Kontaktwinkel betragen 52° für Alginat, 58.1° für Xanthan und 70° für Guarkernmehl was den hydrophilen Charakter der Pulver bestätigte. Zur Beschreibung der Porositätsänderung der Pulverschüttung wurde eine rheologische Messanordnung zur Quantifizierung des Quellverhaltens der Biopolymer-Pulver aufgebaut. Die so ermittelten Quellraten, bezogen auf eine Änderung des Sauter-Durchmessers $d_{3,2}$, betragen $18 \mu\text{m s}^{-1}$ für Xanthan, $10 \mu\text{m s}^{-1}$ für Alginat und $8 \mu\text{m s}^{-1}$ für Guarkernmehl. Der Einfluss der Viskosität auf die Rehydratation wurde sowohl mithilfe der konzentrationsabhängigen Viskositätsänderung als auch dynamisch über die Zeit ermittelt. Diese dynamische Viskositätsänderung in Folge von Lösevorgängen ermöglicht Rückschlüsse auf die Lösegeschwindigkeit in hochkonzentrierten Systemen. Basierend auf diesen Ergebnissen zeigte sich, dass die Rehydratation von Guarkernmehl hauptsächlich durch Viskositätseffekte beeinflusst wird, wohingegen Quellprozesse die Haupteinflussfaktoren bei der Rehydratation von Xanthan und Alginat darstellen. Durch weitere Methoden, wie beispielsweise Magnetische Kernresonanz-Spektroskopie erfolgte eine weitere Charakterisierung der dynamischen Wechselwirkungen zwischen Pulver und Flüssigkeit sowie der Art der Wasserbindung innerhalb der Biopolymergele. Die Stärke der Wasserbindung korrelierte dabei mit der Stabilität hochkonzentrierter Biopolymeraggregate. Diese wurde mithilfe rheologischer Messungen bestimmt und ist insbesondere für das Dispergierverhalten von Biopolymeren von Bedeutung.

Zur Vorhersage der Rehydratationseigenschaften von Lebensmittelpulvern, wurde ein Modell, basierend auf einem Volume-of-Fluids Ansatz, aufgestellt. Die ermittelten physikalischen Eigenschaften sowie ihre dynamischen Änderungen wurden sowohl zeitlich als auch räumlich (2D) aufgelöst, um die kapillare Flüssigkeitsaufnahme in solchen Pulversystemen zu simulieren. Um sowohl die Partikel- als auch die Flüssigkeitseigenschaften präziser zu beschreiben, wurde mithilfe einer Wirbelschichtanlage ein Modellsystem aus Biopolymer-gecoateten Glaspartikeln aufgebaut. Durch Variation der Coatingschichtdicke und des Coatingmaterials konnten die Eigenschaften und die dynamischen Änderungen innerhalb des Systems kontrolliert und beschreibbar gemacht werden. Der Einfluss und die Wechselwirkung zwischen Viskositäts- und Quelleffekten auf den kapillaren Flüssigkeitsanstieg in Pulverschüttungen, wurde mithilfe einer Parameterstudie simuliert.

Die kapillare Flüssigkeitsaufnahme durch die gecoateten Glaskugeln wurde experimentell untersucht. Es zeigte sich, dass auch bei geringen Coating-Schichten von $0.5\ \mu\text{m}$ die dynamischen Effekte stark genug sind, um den kapillaren Flüssigkeitstransport zu stoppen. Hierbei konnte zudem gezeigt werden, dass viskose Effekte die dynamischen Prozesse bei der Rehydratation von Guarkernmehl dominieren, wohingegen Quellen der vorherrschende Mechanismus bei der Rehydratation von Xanthan und Alginat ist.

Die Simulation der kapillaren Flüssigkeitsaufnahme hat gezeigt, dass die Coating-Schichtdicke keinen signifikanten Einfluss auf das Rehydratationsverhalten ausübt. Dieses Ergebnis kann zum einen durch die niedrige Löserate der Biopolymere erklärt werden. Berechnungen ergaben, dass auch die geringste Schichtdicke von $0.5\ \mu\text{m}$ nach einer Zeit von 250 s nur unvollständig gelöst werden konnte. Dies erklärt den geringen Einfluss der Schichtdicke auf die Viskositätsentwicklung und damit auf den kapillaren Flüssigkeitsanstieg. Zum anderen lässt sich dieses Ergebnis durch das ausgeprägte Quellverhalten der Biopolymere erklären. Auch hier sind Coatingschichten von $0.5\ \mu\text{m}$ ausreichend, um einen quell-induzierten Zusammenbruch des Porensystems zu verursachen.

Chapter 8 REFERENCES

- [1] B. Bhandari, N. Bansal, M. Zhang, P. Schuck, *Handbook of food powders: Processes and properties*, Elsevier, 2013.
- [2] G. V. Barbosa-Cánovas, E. Ortega-Rivas, P. Juliano, H. Yan, *Food powders: Physical Properties, Processing, and Functionality*, Springer US, New York, 2005.
- [3] G. V. Barbosa-Cánovas, H. Vega-Mercado, *Dehydration of Foods*, Chapman & Hall, New York, 1996. <https://trove.nla.gov.au/work/15983790>.
- [4] Z. Berk, Chapter 14 - Crystallization and Dissolution, in: *Food Process Eng. Technol.*, Second Edi, Academic Press, San Diego, 2013: pp. 353–371. doi:<https://doi.org/10.1016/B978-0-12-415923-5.00014-9>.
- [5] B. Cuq, E. Rondet, J. Abecassis, Food powders engineering, between knowhow and science: Constraints, stakes and opportunities, *Powder Technol.* 208 (2011) 244–251. doi:10.1016/j.powtec.2010.08.012.
- [6] P. Belitz, H. D., Grosch, H., Schieberte, *Food Chemistry*, Springer. (2004) 939–969.
- [7] D. Dehnad, S.M. Jafari, M. Afrasiabi, Influence of drying on functional properties of food biopolymers: From traditional to novel dehydration techniques, *Trends Food Sci. Technol.* 57 (2016) 116–131. doi:10.1016/j.tifs.2016.09.002.
- [8] W.R. Mitchell, L. Forny, T.O. Althaus, G. Niederreiter, S. Palzer, M.J. Hounslow, A.D. Salman, Mapping the rate-limiting regimes of food powder reconstitution in a standard mixing vessel, *Powder Technol.* 270 (2015) 520–527. doi:<https://doi.org/10.1016/j.powtec.2014.08.014>.
- [9] Q. Wang, P.R. Ellis, S.B. Ross-Murphy, Dissolution kinetics of guar gum powders-III. Effect of particle size, *Carbohydr. Polym.* 64 (2006) 239–246. doi:10.1016/j.carbpol.2005.11.032.
- [10] T.O. Vu, L. Galet, J. Fages, D. Oulahna, Improving the dispersion kinetics of a cocoa powder by size enlargement, *Powder Technol.* 130 (2003) 400–406. doi:10.1016/S0032-5910(02)00242-5.
- [11] D. Saha, S. Bhattacharya, Hydrocolloids as thickening and gelling agents in food: A critical review, *J. Food Sci. Technol.* 47 (2010) 587–597. doi:10.1007/s13197-010-0162-6.

- [12] P.A. Williams, G.O. Phillips, Introduction to food hydrocolloids, in: *Handb. Hydrocoll.* Second Ed., 2009. doi:10.1533/9781845695873.1.
- [13] P. Belton, *The Chemical Physics of Food*, 2007. doi:10.1002/9780470995792.
- [14] A. Stephen, S. Churms, Introduction, in: *Food Polysaccharides Their Appl.*, 2006. doi:10.1201/9781420015164.ch1.
- [15] D. Seisun, Introduction, *Food Stabilisers, Thick. Gelling Agents.* (2009). doi:10.1002/9781444314724.ch1.
- [16] P. Stevens, Gelatine, in: *Food Stabilisers, Thick. Gelling Agents*, 2009. doi:10.1002/9781444314724.ch7.
- [17] I.J. Haug, K.I. Draget, 6 - Gelatin BT - *Handbook of Hydrocolloids (Second edition)*, in: *Woodhead Publ. Ser. Food Sci. Technol. Nutr.*, 2009. doi:http://dx.doi.org/10.1533/9781845695873.142.
- [18] P. Kuhnert, B. Muermann, U.-J. Salzer, eds., *Handbuch Lebensmittelzusatzstoffe Technologische, geschmacksgebende, nahrungsergänzende Stoffe*, Behrs Verlag, Hamburg, 2009.
- [19] G. Sworn, Xanthan Gum, in: *Food Stabilisers, Thick. Gelling Agents*, 2009: pp. 325–342. doi:10.1002/9781444314724.ch17.
- [20] F. García-Ochoa, V.E. Santos, J.A. Casas, E. Gómez, Xanthan gum: production, recovery, and properties, *Biotechnol. Adv.* 18 (2000) 549–579. doi:http://dx.doi.org/10.1016/S0734-9750(00)00050-1.
- [21] R.A. Speers, M.A. Tung, Concentration and Temperature Dependence of Flow Behavior of Xanthan Gum Dispersions, *J. Food Sci.* (1986). doi:10.1111/j.1365-2621.1986.tb10844.x.
- [22] G. Sworn, 8 – Xanthan gum, in: *Handb. Hydrocoll.*, 2009: pp. 186–203. doi:10.1533/9781845695873.186.
- [23] B. Urlacher, O. Noble, Xanthan gum, in: A.P. Imeson (Ed.), *Thick. Gelling Agents Food*, Springer US, Boston, MA, 1997: pp. 284–311. doi:10.1007/978-1-4615-2197-6_13.
- [24] A.M. Stephen, G.O. Phillips, P.A. Williams, *Food polysaccharides and their applications*, 2006. doi:10.1016/0924-2244(96)81250-7.
- [25] R.J. Chudzikowski, Guar gum and its applications, *J. Soc. Cosmet. Chem.* 22 (1971) 43–60. doi:10.1016/j.ijbiomac.2016.04.001.

- [26] D. Mudgil, S. Barak, B.S. Khatkar, Guar gum: processing, properties and food applications---A Review, *J. Food Sci. Technol.* 51 (2011) 409–418. doi:10.1007/s13197-011-0522-x.
- [27] W.C. Wielinga, 10 - Galactomannans BT - Handbook of Hydrocolloids (Second edition), in: Woodhead Publ. Ser. Food Sci. Technol. Nutr., 2009. doi:http://dx.doi.org/10.1533/9781845695873.228.
- [28] E.R. Morris, Molecular Interactions in Polysaccharide Gelation, *Br. Polym. J.* 18 (1986) 14–21. doi:10.1002/pi.4980180105.
- [29] M.R. Gittings, L. Cipelletti, V. Trappe, D.A. Weitz, M. In, J. Lal, The effect of solvent and ions on the structure and rheological properties of guar solutions, *J. Phys. Chem. A.* 105 (2001) 9310–9315. doi:10.1021/jp0121825.
- [30] J.E. Fox, Seed gums, in: A.P. Imeson (Ed.), *Thick. Gelling Agents Food*, Springer US, Boston, MA, 1997: pp. 262–283. doi:10.1007/978-1-4615-2197-6_12.
- [31] J.A. Casas, A.F. Mohedano, F. García-Ochoa, Viscosity of guar gum and xanthan/guar gum mixture solutions, *J. Sci. Food Agric.* 80 (2000) 1722–1727. doi:10.1002/1097-0010(20000915)80:12<1722::AID-JSFA708>3.0.CO;2-X.
- [32] W. Wielinga, Seed gums, in: A. Imeson (Ed.), *Food Stabilisers, Thick. Gelling Agents*, Wiley-Blackwell, 2009: pp. 275–292.
- [33] A. Marburger, Alginate und Carrageenane: Eigenschaften, Gewinnung und Anwendungen in Schule und Hochschule, Dissertation, Philipps-Universität Marburg, 2003. doi:https://doi.org/10.17192/z2004.0110.
- [34] K.I. Draget, S.T. Moe, G. Skjak-Bræk, O. Smidsrød, 9 Alginates, in: *Food Polysaccharides Their Appl.*, CRC Press, 2016: p. 289.
- [35] P. Gacesa, Alginates, *Carbohydr. Polym.* 8 (1988) 161–182. doi:10.1016/0144-8617(88)90001-X.
- [36] E. Onsøyen, Alginates, in: A.P. Imeson (Ed.), *Thick. Gelling Agents Food*, Springer US, Boston, MA, 1997: pp. 22–44. doi:10.1007/978-1-4615-2197-6_2.
- [37] H. Ertesvåg, S. Valla, Biosynthesis and applications of alginates, *Polym. Degrad. Stab.* 59 (1998) 85–91. doi:10.1016/S0141-3910(97)00179-1.
- [38] T. Helgerud, O. Gserd, T. Fjreide, P.O. Andersen, C.K. Larsen, Alginates, in: A. Imeson (Ed.), *Food Stabilisers, Thick. Gelling Agents*, Wiley-Blackwell, Oxford, UK, 2009: pp. 50–72. doi:10.1002/9781444314724.ch4.

- [39] A. Haug, S. Myklestad, B. Larsen, O. Smidsrød, Correlation between chemical structure and physical properties of alginates, *Acta Chem Scand.* 21 (1967) 768–778. doi:10.3891/acta.chem.scand.21-0768.
- [40] G.T. Grant, E.R. Morris, D.A. Rees, P.J.C. Smith, D. Thom, Biological interactions between polysaccharides and divalent cations: The egg-box model, *FEBS Lett.* 32 (1973) 195–198. doi:10.1016/0014-5793(73)80770-7.
- [41] C.C. Nnaedozie, C. Sanders, E.C. Montes, L. Forny, G. Niederreiter, S. Palzer, A.D. Salman, Investigation of rehydration of food powder mixtures, *Powder Technol.* (2019). doi:10.1016/j.powtec.2019.05.043.
- [42] Y. Fang, C. Selomulya, X.D. Chen, On Measurement of food powder reconstitution properties, *Dry. Technol.* 26 (2008) 3–14. doi:10.1080/07373930701780928.
- [43] L. Forny, A. Marabi, S. Palzer, Wetting, disintegration and dissolution of agglomerated water soluble powders, *Powder Technol.* 206 (2011) 72–78. doi:10.1016/j.powtec.2010.07.022.
- [44] H. Schubert, Instantization of powdered food products, *Int. J. Chem. Eng.* 33 (1993) 28–45.
- [45] A. Alghunaim, S. Kirdponpattara, B.M.Z. Newby, Techniques for determining contact angle and wettability of powders, *Powder Technol.* 287 (2016) 201–215. doi:10.1016/j.powtec.2015.10.002.
- [46] W.A. ZISMAN, Relation of the Equilibrium Contact Angle to Liquid and Solid Constitution, in: *Contact Angle, Wettability, Adhes.*, n.d.: pp. 1–51. doi:10.1021/ba-1964-0043.ch001.
- [47] M. Lazghab, K. Saleh, I. Pezron, P. Guigon, L. Komunjer, Wettability assessment of finely divided solids, *Powder Technol.* 157 (2005) 79–91. doi:10.1016/j.powtec.2005.05.014.
- [48] J.N. Israelachvili, *Intermolecular and Surface Forces: Third Edition*, Academic Press, 2011. doi:10.1016/C2011-0-05119-0.
- [49] S. Hoge Kamp, H. Schubert, Rehydration of food powders, *Food Sci. Technol. Int.* 9 (2003) 223–235. doi:10.1177/1082013203034938.
- [50] B. Freudig, S. Hoge Kamp, H. Schubert, Dispersion of powders in liquids in a stirred vessel, *Chem. Eng. Process. Process Intensif.* 38 (1999) 525–532. doi:10.1016/S0255-2701(99)00049-5.

- [51] D. Vella, H.E. Huppert, The waterlogging of floating objects, *J. Fluid Mech.* (2007). doi:10.1017/S002211200700715X.
- [52] T. Young, An essay on the cohesion of fluids, *Phil. Trans. R. Soc. A.* 95 (1805) 65–87. doi:10.1098/rspl.1800.0095.
- [53] D. Bonn, J. Eggers, J. Indekeu, J. Meunier, Wetting and spreading, *Rev. Mod. Phys.* 81 (2009). doi:10.1103/RevModPhys.81.739.
- [54] Y. Yuan, T.R. Lee, Contact angle and wetting properties, *Springer Ser. Surf. Sci.* (2013). doi:10.1007/978-3-642-34243-1_1.
- [55] K.C. Link, E.-U. Schlünder, A new method for the characterisation of the wettability of powders, *Chem. Eng. Technol.* 19 (1996) 432–437. doi:10.1002/ceat.270190508.
- [56] L.L. Popovich, D.L. Feke, I. Manas-Zloczower, Influence of physical and interfacial characteristics on the wetting and spreading of fluids on powders, *Powder Technol.* (1999). doi:10.1016/S0032-5910(99)00030-3.
- [57] M. Stieß, *Mechanische Verfahrenstechnik 1*, 2nd ed., Springer-Verlag, Berlin; Heidelberg, 1995. doi:10.1007/978-3-662-08600-1.
- [58] H. Schubert, *Kapillarität in porösen Feststoffsystemen*, Springer-Verlag, 1982.
- [59] P.C. Carman, *Flow of gases through porous media.*, Academic Press, New York, 1956.
- [60] J. Carlos Ramírez-Flores, J. Bachmann, Analyzing capillary-rise method settings for contact-angle determination of granular media§, *J. Plant Nutr. Soil Sci.* 176 (2013) 16–19. doi:10.1002/jpln.201100431.
- [61] S. Thümmler, D. Höhne, K. Husemann, Preparation of defined bulk densities for using the capillary rise method in the case of fine powders, *Granul. Matter.* 10 (2008) 309–314. doi:10.1007/s10035-008-0098-y.
- [62] M. O’Loughlin, K. Wilk, C. Priest, J. Ralston, M.N. Popescu, Capillary rise dynamics of aqueous glycerol solutions in glass capillaries: A critical examination of the Washburn equation, *J. Colloid Interface Sci.* 411 (2013) 257–264. doi:10.1016/j.jcis.2013.05.077.
- [63] Y.Y. Law, D.L. Feke, I. Manas-Zloczower, Method for probing the microstructure of particle beds using infiltration behavior, *Powder Technol.* 237 (2013) 427–431. doi:10.1016/j.powtec.2012.12.034.

- [64] D. Hellborg, B. Bergenståhl, C. Trägårdh, The influence of powder properties on the imbibation rate, *Colloids Surfaces B Biointerfaces*. 93 (2012) 108–115. doi:10.1016/j.colsurfb.2011.12.023.
- [65] M.L.M. Oostveen, G.M.H. Meesters, J.R. van Ommen, Quantification of powder wetting by drop penetration time, *Powder Technol.* 274 (2015) 62–66. doi:10.1016/j.powtec.2014.09.021.
- [66] A. Roman-Gutierrez, J. Sabathier, S. Guilbert, L. Galet, B. Cuq, Characterization of the surface hydration properties of wheat flours and flour components by the measurement of contact angle, *Powder Technol.* 129 (2003). doi:10.1016/S0032-5910(02)00154-7.
- [67] A.B.D. Cassie, Contact angles, *Discuss. Faraday Soc.* 3 (1948) 11–16. doi:10.1039/DF9480300011.
- [68] A.B.D. Cassie, S. Baxter, Wettability of porous surfaces, *Trans. Faraday Soc.* 40 (1944) 546–551. doi:10.1039/tf9444000546.
- [69] U. Zorll, *Hafttechnik – Grundlagen und Anwendungen*, Chemie Ing. Tech. 60 (1988). doi:10.1002/cite.330600304.
- [70] R.N. Wenzel, Resistance of solid surfaces to wetting by water, *Ind. Eng. Chem.* 28 (1936) 988–994. doi:https://doi.org/10.1021/ie50320a024.
- [71] T. Karbowski, F. Debeaufort, A. Voilley, Importance of surface tension characterization for food, pharmaceutical and packaging products: A review, *Crit. Rev. Food Sci. Nutr.* 46 (2006). doi:10.1080/10408390591000884.
- [72] A. Siebold, M. Nardin, J. Schultz, A. Walliser, M. Oppliger, Effect of dynamic contact angle on capillary rise phenomena, *Colloids Surfaces A Physicochem. Eng. Asp.* 161 (2000). doi:10.1016/S0927-7757(99)00327-1.
- [73] S. Kirdponpattara, M. Phisalaphong, B.M.Z. Newby, Applicability of Washburn capillary rise for determining contact angles of powders/porous materials, *J. Colloid Interface Sci.* 397 (2013) 169–176. doi:10.1016/j.jcis.2013.01.033.
- [74] E.L. Decker, B. Frank, Y. Suo, S. Garoff, Physics of contact angle measurement, *Colloids Surfaces A Physicochem. Eng. Asp.* 156 (1999). doi:10.1016/S0927-7757(99)00069-2.
- [75] J. Dupas, L. Forny, M. Ramaioli, Powder wettability at a static air–water interface, *J. Colloid Interface Sci.* 448 (2015) 51–56. doi:http://dx.doi.org/10.1016/j.jcis.2015.01.086.

- [76] W.R. Mitchell, L. Forny, T. Althaus, G. Niederreiter, S. Palzer, M.J. Hounslow, A.D. Salman, Surface tension-driven effects in the reconstitution of food powders, *Chem. Eng. Res. Des.* 146 (2019) 464–469. doi:10.1016/j.cherd.2019.04.015.
- [77] C. Schober, J.J. Fitzpatrick, Effect of vortex formation on powder sinkability for reconstituting milk powders in water to high solids content in a stirred-tank, *J. Food Eng.* 71 (2005). doi:10.1016/j.jfoodeng.2004.09.027.
- [78] J.J. Fitzpatrick, K. Weidendorfer, E. Teunou, Reconstitution of dairy powders to high solids content in a stirred-tank: The effect of agitation, *Milchwissenschaft.* 55 (2000) 437–440.
- [79] J.J. Fitzpatrick, R. Cuthbert, Effect of temperature on the reconstitution of milk powder to high solids content in a stirred-tank, *Milchwissenschaft.* 59 (2004).
- [80] R.W. Thring, M.F. Edwards, Experimental investigation into the complete suspension of floating solids in an agitated tank, *Ind. Eng. Chem. Res.* 29 (1990). doi:https://doi.org/10.1021/ie00100a029.
- [81] Z. Berk, *Food Process Engineering and Technology*, 2013. doi:10.1016/B978-0-12-415923-5.00020-4.
- [82] S.P. Rwei, I. Manas-Zloczower, D.L. Feke, Observation of carbon black agglomerate dispersion in simple shear flows, *Polym. Eng. & Sci.* 30 (1990) 701–706. doi:10.1002/pen.760301202.
- [83] S.P. Rwei, I. Manas-Zloczower, D.L. Feke, Characterization of agglomerate dispersion by erosion in simple shear flows, *Polym. Eng. & Sci.* 31 (1991) 558–562. doi:10.1002/pen.760310804.
- [84] A. Scurati, D.L. Feke, I. Manas-Zloczower, Analysis of the kinetics of agglomerate erosion in simple shear flows, *Chem. Eng. Sci.* 60 (2005). doi:10.1016/j.ces.2005.05.059.
- [85] M.A. Salas Cazón, *Untersuchungen zur abrasiven Beanspruchung von Feststoffpartikeln in einem Rührreaktor*, Technische Universität Berlin, 2002. <http://dx.doi.org/10.14279/depositonce-584>.
- [86] L. Bouvier, A. Moreau, A. Line, N. Fatah, G. Delaplace, Damage in Agitated Vessels of Large Visco-Elastic Particles Dispersed in a Highly Viscous Fluid, *J. Food Sci.* 76 (2011). doi:10.1111/j.1750-3841.2011.02183.x.

-
- [87] A.D.S. W. Robert Mitchell, Tim O. Althaus, Laurent Forny, Gerhard Niederreiter, Stefan Palzer, Michael J. Hounslow, Modeling the Disintegration and Dissolving of Water-Soluble Bulk Solids from Online Particle Concentration Measurements, in: 10th Int. Symp. Agglom., 2013.
- [88] J. Wangler, R. Kohlus, Development and validation of methods to characterize rehydration behavior of food hydrocolloids, *Food Hydrocoll.* 82 (2018). doi:10.1016/j.foodhyd.2018.04.018.
- [89] T.P. Kravtchenko, J. Renoir, A. Parker, G. Brigand, A novel method for determining the dissolution kinetics of hydrocolloid powders, *Food Hydrocoll.* 13 (1999) 219–225. doi:10.1016/S0268-005X(99)00002-8.
- [90] E.W. Washburn, The dynamics of capillary flow, *Phys. Rev.* 17 (1921) 273–283. doi:10.1103/PhysRev.17.273.
- [91] S. Palzer, Anreichern und Benetzen von pulverförmigen Lebensmitteln mit Flüssigkeiten in diskontinuierlichen Mischaggregaten, Dissertation, Technische Universität München, 2000.
- [92] J. Cai, B. Yu, A Discussion of the Effect of Tortuosity on the Capillary Imbibition in Porous Media, *Transp. Porous Media.* (2011). doi:10.1007/s11242-011-9767-0.
- [93] D. Benavente, P. Lock, M. Ángeles García Del Cura, S. Ordóñez, Predicting the capillary imbibition of porous rocks from microstructure, *Transp. Porous Media.* (2002). doi:10.1023/A:1016047122877.
- [94] J.J. Fitzpatrick, J. Salmon, J. Ji, S. Miao, Characterisation of the wetting behaviour of poor wetting food powders and the influence of temperature and film formation, *KONA Powder Part. J.* 2017 (2017) 282–289. doi:10.14356/kona.2017019.
- [95] W.R. Mason, Starch Use in Foods, in: *Starch*, 2009: pp. 745–795. doi:10.1016/B978-0-12-746275-2.00020-3.
- [96] J. Oikku, C.K. Rha, Gelatinisation of starch and wheat flour starch-A review, *Food Chem.* 3 (1978) 293–317. doi:10.1016/0308-8146(78)90037-7.
- [97] O.K. Ozturk, P.S. Takhar, Water transport in starchy foods: Experimental and mathematical aspects, *Trends Food Sci. Technol.* 78 (2018) 11–24. doi:10.1016/j.tifs.2018.05.015.

- [98] U. Goerke, A.H.L. Chamberlain, E.A. Crilly, P.J. McDonald, Model for water transport into powdered xanthan combining gel swelling and vapor diffusion, *Phys. Rev. E - Stat. Physics, Plasmas, Fluids, Relat. Interdiscip. Top.* 62 (2000) 5353–5359. doi:10.1103/PhysRevE.62.5353.
- [99] A. Parker, F. Vigouroux, W.F. Reed, Dissolution kinetics of polymer powders, *AIChE J.* 46 (2000) 1290–1299. doi:10.1002/aic.690460703.
- [100] V.F. Frolov, Dissolution of disperse materials, *Theor. Found. Chem. Eng.* 32 (1998) 357–368.
- [101] A. Marabi, G. Mayor, A. Burbidge, R. Wallach, I.S. Saguy, Assessing dissolution kinetics of powders by a single particle approach, *Chem. Eng. J.* 139 (2008) 118–127. doi:10.1016/j.cej.2007.07.081.
- [102] J. Sujja-Areevath, D.L. Munday, P.J. Cox, K.A. Khan, Relationship between swelling, erosion and drug release in hydrophilic natural gum mini-matrix formulations, *Eur. J. Pharm. Sci.* 6 (1998) 207–217. doi:10.1016/S0928-0987(97)00072-9.
- [103] L. Masaro, X.X. Zhu, Physical models of diffusion for polymer solutions, gels and solids, *Prog. Polym. Sci.* 24 (1999) 731–775. doi:10.1016/S0079-6700(99)00016-7.
- [104] J. Crank, E.P.J. Crank, *The Mathematics of Diffusion*, Clarendon Press, 1979.
- [105] J. Van Brakel, Pore space models for transport phenomena in porous media review and evaluation with special emphasis on capillary liquid transport, *Powder Technol.* 11 (1975) 205–236. doi:10.1016/0032-5910(75)80049-0.
- [106] J. Dupas, V. Girard, L. Forny, Reconstitution properties of sucrose and maltodextrins, *Langmuir.* 33 (2017) 988–995. doi:10.1021/acs.langmuir.6b04380.
- [107] B.A. Miller-Chou, J.L. Koenig, A review of polymer dissolution, *Prog. Polym. Sci.* 28 (2003). doi:10.1016/S0079-6700(03)00045-5.
- [108] I.S. Saguy, A. Marabi, R. Wallach, Liquid imbibition during rehydration of dry porous foods, *Innov. Food Sci. Emerg. Technol.* 6 (2005) 37–43. doi:10.1016/j.ifset.2004.11.002.
- [109] J. Wangler, R. Kohlus, Dynamics of Capillary Wetting of Biopolymer Powders, *Chem. Eng. Technol.* 40 (2017). doi:10.1002/ceat.201600607.

- [110] Q. Wang, P.R. Ellis, S.B. Ross-Murphy, Dissolution kinetics of guar gum powders. I. Methods for commercial polydisperse samples, *Carbohydr. Polym.* 49 (2002) 131–137. doi:10.1016/S0144-8617(01)00327-7.
- [111] Q. Wang, P.R. Ellis, S.B. Ross-Murphy, Dissolution kinetics of guar gum powders - II. Effects of concentration and molecular weight, *Carbohydr. Polym.* 53 (2003) 75–83. doi:10.1016/S0144-8617(03)00009-2.
- [112] M. Wollny, Über das Gestalten der Eigenschaften von Instantprodukten mit dem Verfahren der Strahlagglomeration, Dissertation, Karlsruher Institut für Technologie, 2002.
- [113] A. van Kampen, R. Kohlus, Systematic process optimisation of fluid bed coating, *Powder Technol.* 305 (2017) 426–432. doi:10.1016/j.powtec.2016.10.007.
- [114] I. Devotta, V. Premnath, M. V. Badiger, P.R. Rajamohanam, S. Ganapathy, R.A. Mashelkar, On the Dynamics of Mobilization in Swelling–Dissolving Polymeric Systems, *Macromolecules.* (1994). doi:10.1021/ma00080a030.
- [115] M.R. Gittings, L. Cipelletti, V. Trappe, D.A. Weitz, M. In, C. Marques, Structure of Guar in Solutions of H₂O and D₂O: An Ultra-Small-Angle Light-Scattering Study, *J. Phys. Chem. B.* (2002). doi:10.1021/jp9943833.
- [116] R. Hinrichs, J. Götz, H. Weisser, Water-holding capacity and structure of hydrocolloid-gels, WPC-gels and yogurts characterised by means of NMR, in: *Food Chem.*, 2003. doi:10.1016/S0308-8146(02)00539-3.
- [117] I.S. Saguy, A. Marabi, R. Wallach, New approach to model rehydration of dry food particulates utilizing principles of liquid transport in porous media, *Trends Food Sci. Technol.* 16 (2005) 495–506. doi:10.1016/j.tifs.2005.07.006.
- [118] S.Q. Shi, D.J. Gardner, New model to determine contact angles on swelling polymer particles by the column wicking method, *J. Adhes. Sci. Technol.* (2000). doi:10.1163/156856100742564.
- [119] K.P. Hapgood, J.D. Litster, S.R. Biggs, T. Howes, Drop penetration into porous powder beds, *J. Colloid Interface Sci.* 253 (2002) 353–366. doi:10.1006/jcis.2002.8527.
- [120] H.J. Busscher, A.W.J. van Pelt, P. de Boer, H.P. de Jong, J. Arends, The effect of surface roughening of polymers on measured contact angles of liquids, *Colloids and Surfaces.* 9 (1984) 319–331. doi:10.1016/0166-6622(84)80175-4.

- [121] J. Ji, J. Fitzpatrick, K. Cronin, A. Crean, S. Miao, Assessment of measurement characteristics for rehydration of milk protein based powders, *Food Hydrocoll.* 54 (2016) 151–161. doi:10.1016/j.foodhyd.2015.09.027.
- [122] J.J. Fitzpatrick, A. van Lauwe, M. Coursol, A. O'Brien, K.L. Fitzpatrick, J. Ji, S. Miao, Investigation of the rehydration behaviour of food powders by comparing the behaviour of twelve powders with different properties, *Powder Technol.* (2016). doi:10.1016/j.powtec.2016.04.036.
- [123] L. Galet, T.O. Vu, D. Oulahna, J. Fages, The wetting behaviour and dispersion rate of cocoa powder in water, *Food Bioprod. Process.* 82 (2004) 298–303. doi:10.1205/fbio.82.4.298.56399.
- [124] Y. Fang, C. Selomulya, S. Ainsworth, M. Palmer, X.D. Chen, On quantifying the dissolution behaviour of milk protein concentrate, *Food Hydrocoll.* 25 (2011) 503–510. doi:10.1016/j.foodhyd.2010.07.030.
- [125] C. Gaiani, S. Banon, J. Scher, P. Schuck, J. Hardy, Use of a turbidity sensor to characterize micellar casein powder rehydration: Influence of some technological effects, *J. Dairy Sci.* 88 (2005) 2700–2706. doi:10.3168/jds.S0022-0302(05)72948-9.
- [126] C.K. Larsen, O. Gåserød, O. Smidsrød, A novel method for measuring hydration and dissolution kinetics of alginate powders, *Carbohydr. Polym.* 51 (2003) 125–134. doi:10.1016/S0144-8617(02)00139-X.
- [127] L. Wang, B. Xie, J. Shi, S. Xue, Q. Deng, Y. Wei, B. Tian, Physicochemical properties and structure of starches from Chinese rice cultivars, *Food Hydrocoll.* (2010). doi:10.1016/j.foodhyd.2009.09.007.
- [128] J.A. Robertson, F.D. De Monredon, P. Dysseler, F. Guillon, R. Amadò, J.F. Thibault, Hydration properties of dietary fibre and resistant starch: A European collaborative study, *LWT - Food Sci. Technol.* (2000). doi:10.1006/fstl.1999.0595.

Chapter 9 APPENDIX

9.1 Characterization of food powder rehydration: Methods and general aspects

Within this thesis the biopolymer powders xanthan gum, guar gum and alginate were investigated with regard to their rehydration behavior. Due to their characteristic to rehydrate completely in cold water in combination with the ability to develop highly viscous structures, they are excellent model systems to study the rehydration behavior of dynamically changing food powder systems.

To fulfil the demand for convenient application of food powders a better understanding of the rehydration dynamics is mandatory for a purposeful optimization of the relevant powder characteristics. In this context, analysis of the relationship between powder properties and rehydration behavior have been conducted in the past. Within these studies the influence of e.g. particle size on dispersability was studied by the example of cocoa [10] and the relationship between bulk porosity and capillary liquid rise could be shown successfully [61,73]. Furthermore, particle aggregation and tendency to form floating layers was studied dependent on process conditions [8,89,106]. However, most of these studies were carried out with inert powder systems or food material which only exhibit low levels of swelling and viscosity development.

Due to the importance of powder rehydration in various industrial sectors as well as in daily life, a large number of methods can be found in literature to characterize the wetting, sinking, dispersion and dissolution behavior of powders. Within the first steps of this thesis several of these methods were chosen and adapted to assess the rehydration behavior of food powder systems, especially of the biopolymer powders xanthan gum, guar gum and alginate. Advantages and disadvantages of some of these methods with respect to biopolymer characterization are discussed below.

To investigate wetting of a powder bulk, Wollny [112] introduced an experimental set-up consisting of a conical powder bulk which is brought in contact with a liquid surface. Rise of liquid can be observed directly by image analysis and wetted height over time and critical bulk height can be calculated according to the geometric data of the sample holder (Fig. 9.1) using Eq. 9.1.

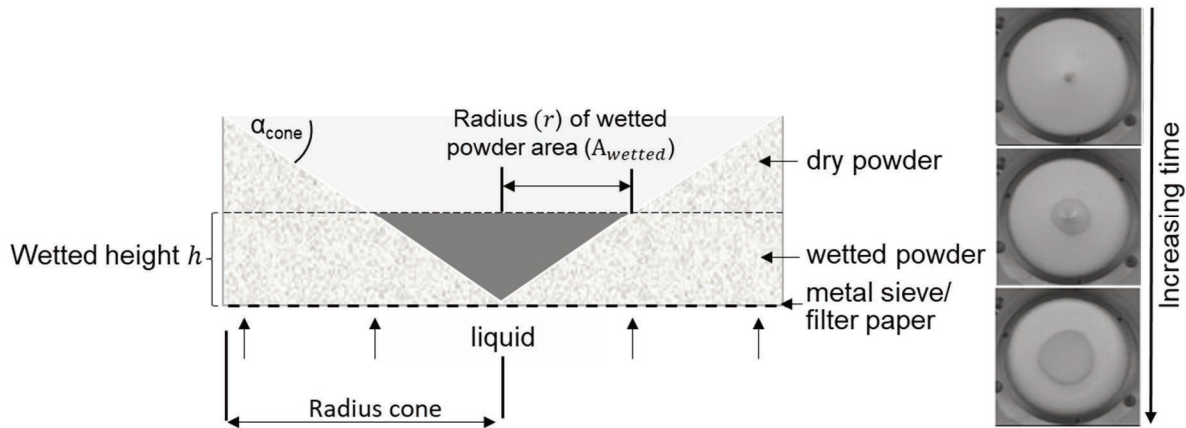


Fig. 9.1: Schematic draw of the cone method to analyze wettability of powders.

$$r(t) = \sqrt{\frac{A_{wetted}}{\pi}} \quad h(t) = r(t) \cdot \tan \alpha_{cone} \quad \text{Eq. 9.1}$$

$$h_{crit.} = h(t \rightarrow \infty) = r(t \rightarrow \infty) \cdot \tan \alpha_{cone}$$

This method could be applied successfully for instant powder products. With regard to biopolymers as well as various other common food powders this method was not suited as no or only little increase of liquid could be observed. In Fig. 9.2 results from cone method analysis are shown for several food powders after a wetting time of 30 min.

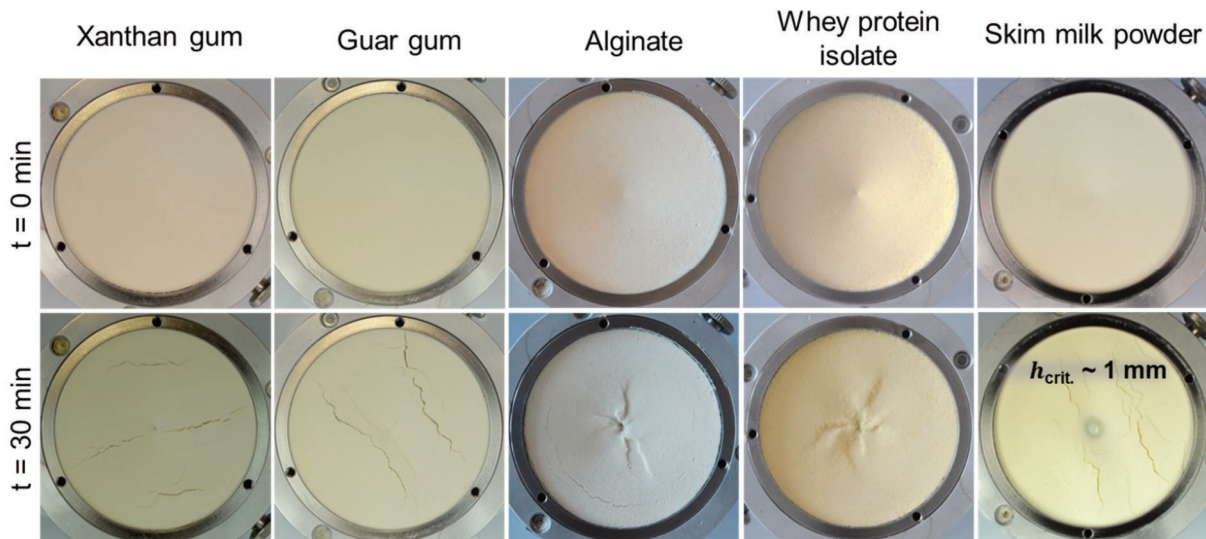


Fig. 9.2: Cone method to analyze wettability of food powders.

Only for skim milk powder a slight increase of the water within the powder bulk could be observed and a critical bulk height of 1 mm was determined. This result was unexpected as rehydration of skim milk powder was assumed to be less critical. With respect to the other powders, it was assumed that after contact between bottom

powder layer and liquid, the powder particles start to swell and expand which could explain the formation of cracks in the powder bulk and the prevention of further water rise.

Characterization of wettability in terms of drop penetration time was proposed by Hapgood *et al.* [119]. Similar to the Washburn equation, ingress of the liquid into the powder bulk is calculated according to Eq. 9.2 dependent on bulk porosity ε , the radius of the capillaries r_{Pore} , surface tension of the liquid γ_{lv} , contact angle between liquid and solid $\cos \theta$ as well as liquid viscosity μ . As further factor the volume of the liquid droplet is considered for calculation. Depending on the way of droplet penetration two situation can be distinguished: (1) droplet penetration with a constant drawing area (CDA) and (2) droplet penetration with a decreasing drawing area (DDA). For fast wetting the first case is advantageous as the contact angle continuously decreases over time.

$$\tau_{\text{CDA}} = 1.35 \frac{V_0^{2/3}}{\varepsilon^2 \cdot r_{\text{Pore}}} \cdot \frac{\mu}{\gamma_{lv} \cos \theta} \quad \text{Eq. 9.2}$$

$$\tau_{\text{DDA}} = 9 \cdot \tau_{\text{CDA}}$$

Applying this method to biopolymer powders, difficulties occurred due to the highly dynamic interaction between powder and liquid. For analysis, loosely packed powder beds were prepared and water droplets were added to the surface (Fig. 9.3)

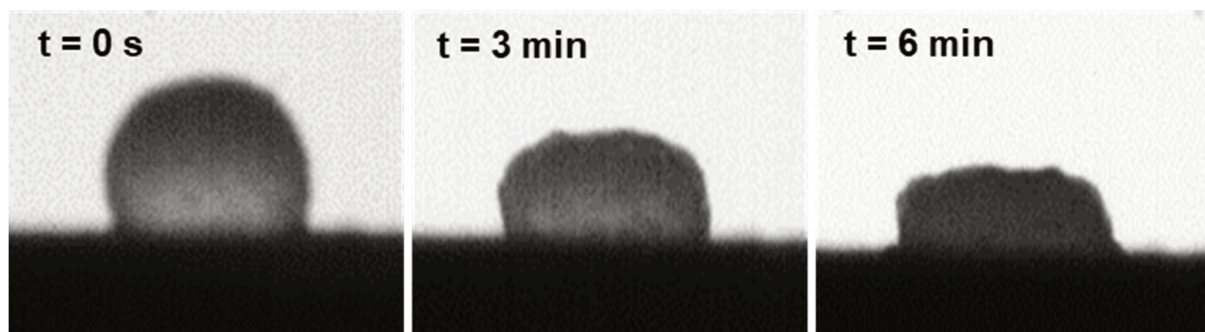


Fig. 9.3: Experiment to determine drop penetration time of water into loosely packed powder bed of xanthan gum

As shown in Fig. 9.3 by the example of xanthan gum, instead of droplet penetration into the powder bed it appears that the powder is “absorbed” by the droplet which leads to viscosity increase within the droplet and finally to a deformation of the droplet shape. Even after an observation time of several hours no further sinking could be detected.

Thus, this method is not suited for a quantitative determination of the wettability of the analyzed biopolymers.

Similar observations could be made during contact angle measurements between biopolymer powders and water. Due to the common application and the possibility of a direct visualization, the sessile drop method was chosen for contact angle analysis. Here, the comparison of different sample preparation methods revealed the influence of this factor. Analyses were performed on loosely packed powder beds as well as on thin powder layers which were fixed on glass slides by adhesive tapes. Furthermore, contact angles were measured on dried layers of previously dissolved biopolymer solution and on compressed powder tablets. Depending on the sample preparation a wide variance of contact angles was measured as summarized in Table 9.1.

Table 9.1: Contact angle between distilled water and biopolymer sample dependent on sample preparation method

Sample preparation method	Contact angle [°]		
	Xanthan gum	Guar gum	Alginate
Loosely packed powder bed	123.5 ± 3.1	112.9 ± 3.38	122.3 ± 3.5
Powder layer	107.2 ± 5.1	114.9 ± 1.8	70.0 ± 2.6
Compressed tablet	58.1 ± 0.9	70.0 ± 3.0	52.0 ± 3.2
Dried layer	76.8 ± 8.0	56.3 ± 5.3	49.3 ± 2.7

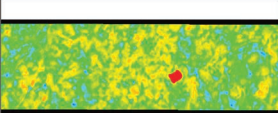
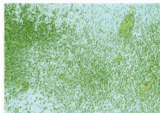
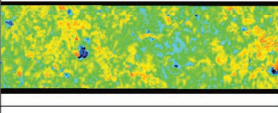
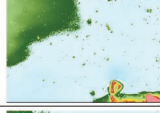
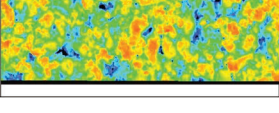
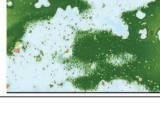
The intention of this analysis was to determine the contact angle that is formed directly after powder-liquid contact as indicator for the initial phase of wetting. Therefore, interaction between powder and liquid should be excluded, if possible. As the liquid droplet was added to the powder surface manually, a settling period of the droplet of around 0.1 s could not be prevented. For that reason, it cannot be excluded that the contact angles, despite this short period, are influenced to a certain part by dynamic powder-liquid interactions. In particular, results obtained from loosely packed powder beds are susceptible, as the loose structure and the comparably high porosity of the powder bulk enables a relative unconstrained penetration of the droplet into the powder bed. Additionally, the phenomena described above for drop penetration are the same within this measurement. For that reason, the sample preparation methods summarized in Table 9.1 aimed to reduce these interactions which seems to be

reflected by the tendency of a decreasing contact angle from loosely packed beds to dried powder layers.

A further important factor of contact angle measurements, which is also influenced by the sample preparation method is the roughness of the sample surface. To assess the influence of this parameter, the surface roughness of both dried powder layers and compressed tablets was determined by confocal laser scanning microscopy (VK X1000, Keyence Deutschland GmbH, Neu-Isenburg). Results of surface roughness analysis (R_A) and 3D images of tablets and dried layer surfaces are summarized in Table 9.2.

Busscher *et al.* [120] investigated the influence of surface roughness on contact angle formation and distinguished three different ranges: for contact angles $> 86^\circ$ on smooth surfaces, increase of roughness tends to increase the measured contact angle. For smooth surfaces with contact angles $< 60^\circ$ surface roughening results in a decreasing contact angle. Contact angle measurements on smooth surfaces in the range between 60° and 86° were not influenced by surface roughness. Furthermore, they found that contact angle analysis is not influenced by surface roughness for R_A values below $0.1 \mu\text{m}$. With regard to the results from surface roughness determination (Table 9.2) it cannot be excluded that contact angles are influenced from surface roughness.

Table 9.2: Surface roughness of compressed biopolymers (compaction pressure 550 bar) and dried powder layers.

Sample	3D surface tablet	$R_{A, \text{tablet}} [\mu\text{m}]$	3D surface dried layer	$R_{A, \text{dried layer}} [\mu\text{m}]$
Xanthan gum		2.065		0.063
Guar gum		2.487		0.025
Alginate		3.413		0.029

Based on these results, measurements on dried layers and compressed tablets were assumed to be best suited for contact angle determination on highly dynamic biopolymer powders. Compression enables both a delay of powder-liquid interaction and a reduction of the surface roughness. By the preparation of dried powder layers, the surface roughness could be further minimized. However, due to the modification of

the powder surface characteristics as a result of dissolution and the subsequent drying step this method possibly does not reflect the true wetting behavior. Surface alteration was also reported as a function of the compaction pressure. Considering assets and drawbacks of the presented methods, measurement on compressed tablets is recommended as standard method for contact angle determination on biopolymer powders. Due to the influence of dynamic powder-liquid interaction on contact angle analysis, other methods described in literature, e.g. Wilhelmy plate method, determination of advancing and receding contact angle on inclined planes etc. were excluded as measurement times should be kept as short as possible.

Methods to analyze sinking, as second step of powder rehydration, were proposed by Hoge Kamp & Schubert [49]. The experimental set-up for analysis consisted of a sample container with a slider on the bottom. The measuring cell is brought in contact with a liquid surface and the slider is pulled away. With the help of a distance sensor fixed above the powder surface, sinking is continuously observed by an increasing distance. A further method, which imitates dynamic sinking conditions comparable to powder rehydration in a stirred vessel, consisted of an annular flow channel configuration. The powder is continuously added to a flowing liquid stream and the distance the particles need to sink is observed [49]. In other studies [121,122], sinking is determined by spreading the powder on a liquid surface and measuring the time for complete sinking visually. A common aspect of all these methods is the importance of reproducible sample preparation and addition to the liquid surface as well as the determination of the point of complete sinking. Within this thesis the slider method and the method of sprinkling of powder on a slowly stirred liquid surface in a vessel were tested to characterize sinkability. With regard to biopolymers the slider method failed as no sinking could be observed. By applying the latter method, sinking was quantified by determining the decrease of powder-covered liquid surface using image analysis Fig. 9.4.

Although with this method a decrease of particles at the liquid surface could be observed, for alginate and xanthan gum these results were rather attributed to a progressive dissolution of the powder layer into the rehydration liquid than to a real sinking procedure. This observation again is triggered by swelling and viscosity development of the biopolymers in contact with water. Swelling and the associated reduction of the density gradient between powder and liquid leads to the formation of layers which float on the liquid surface and prevent particles from sinking.

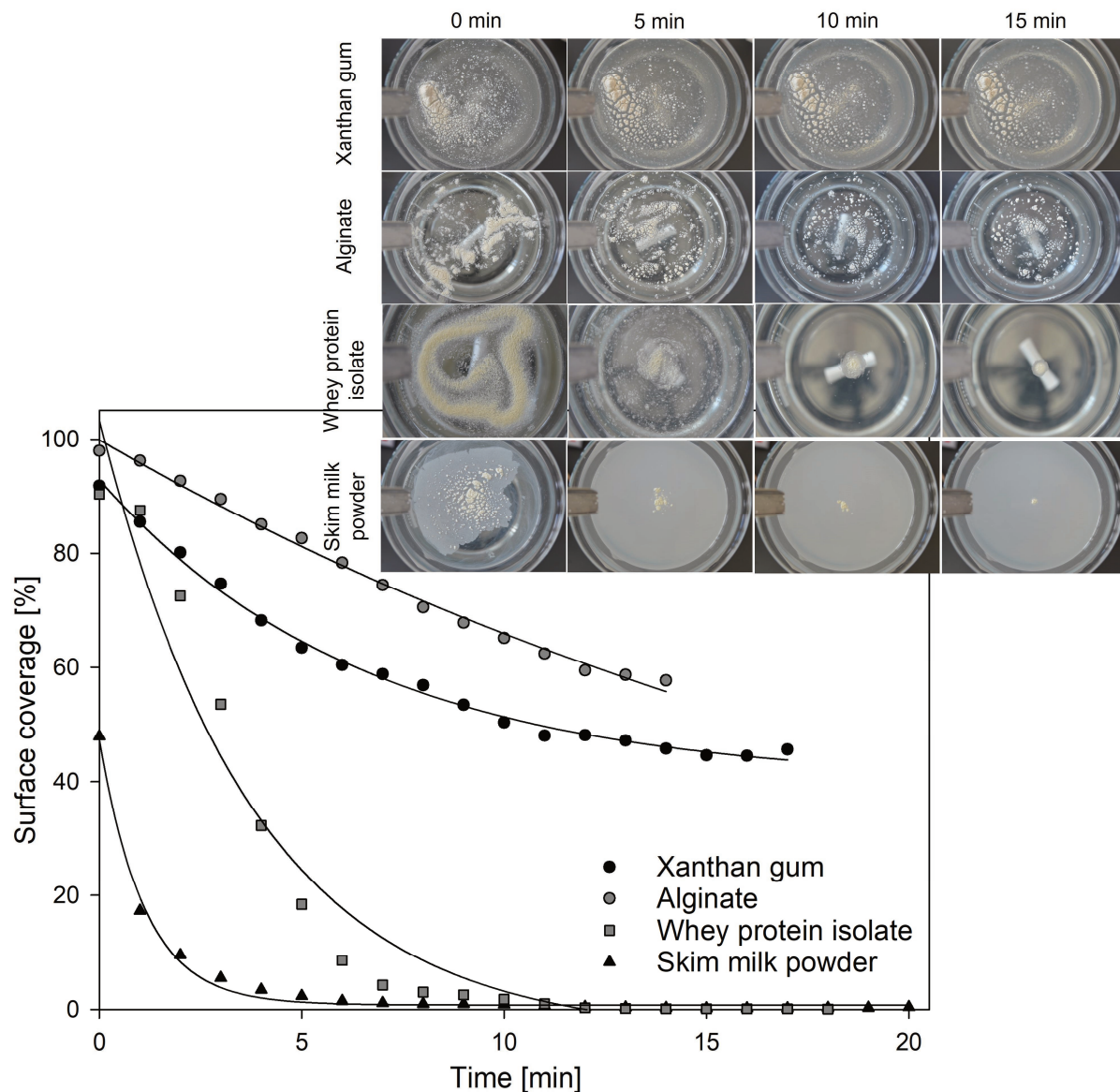


Fig. 9.4: Sinking behavior of powder particles determined by image analysis

The final steps of rehydration involve dispersing and dissolution. The biopolymer powders investigated within this thesis are known for their critical dispersion behavior which is expressed by the formation of large particles aggregates directly after powder-liquid contact. Disintegration of these aggregates can only be achieved by applying high shear forces. Dissolution of biopolymer molecules of these aggregates is very time consuming due to the viscosity of the aggregate-surrounding swollen layer. In literature several methods are described to characterize dispersion and dissolution of food powders both continuously and discontinuously. The dispersion behavior of cocoa powder was analyzed by an optical fiber sensor which measures the backscattered light of the dispersed particles [10,123]. Calibration of the relationship between voltage and concentration of dispersed particle allows the determination of the dispersion state

of the cocoa sample. Dispersion and dissolution of milk protein concentrate was studied by Fang *et al.* [124]. In their study a focused beam reflectance probe (FBRM) was used to measure change of particle size and number in the course of rehydration. Rehydration of native phospho-caseinate and whey protein isolate powder was studied by Gaiani *et al.* [125] using a turbidity sensor. To investigate the rehydration behavior of biopolymer powders, methods mainly focus on the change of rheological characteristics of the rehydration liquid upon dissolution, either inline [89,99,126] or after sampling in certain time intervals [110].

All these methods are well suited to describe dispersion and dissolution of the respective powder samples. Also, dissolution kinetics of particle aggregates were described by Kravtchenko *et al.* [89]. Within this thesis, several of these methods were applied in previous experiments, including inline particle size measurement by a FBRM probe (ECA 313, Sequip Sensor & Equipment, Düsseldorf, Germany), by a fiber-optical spatial filter method (IPP 70S, Parsum GmbH, Chemnitz, Germany) and by static light scattering (MasterSizer 2000, Malvern Panalytical GmbH, Herrenberg, Germany). Dissolution was determined using an inline photometer (AvaSpec-ULS2048, Avantes BV, The Netherlands), by inline turbidity measurements (Mettler Toledo, Germany) as well as by measuring change of torque (ViscoPakt Rheo110, HiTecZang, Herzogenrath, Germany) and viscosity (Kinexus ultra, Malvern Instruments GmbH, Herrenberg, Germany). As mentioned above, rehydration of the model biopolymer powders is strongly influenced by the formation of particle aggregates. For that reason, analysis of the relationship between physical powder characteristics and process condition characteristics is necessary to improve biopolymer rehydration. Based on this target, inline methods to observe change of particle size distribution during the rehydration process continuously were assumed to be best suited. However, it was found that the available methods were not able to detect particle aggregates in the relevant size fraction due to their limited measuring range. For example, the upper size limit that could be detected by the IPP 70S probe does not cover the critical size range of aggregates (>1 μm). Furthermore, due to swelling and viscosity development the edge of the particles could not be distinguished clearly from the surrounding due to the formation of a diffuse layer and air bubbles which are drawn into the liquid under the action of the stirrer also falsify the results from particle size measurements. Based on these findings an experimental set-up was developed to directly observe aggregate formation and disintegration. This was

realized successfully by taking images of the particle aggregates which were formed during rehydration. Change of particle number as well as particle size were determined by image analysis using Matlab (Mathworks R2017a). Fig. 9.5 shows the change of aggregate size over time during a dispersion experiment with model biopolymer aggregates of an initial diameter of 20 μm . Pictures show that even after a process time of 50 min, no complete dissolution could be achieved. This reveals the difficult disintegration behavior of such aggregates.

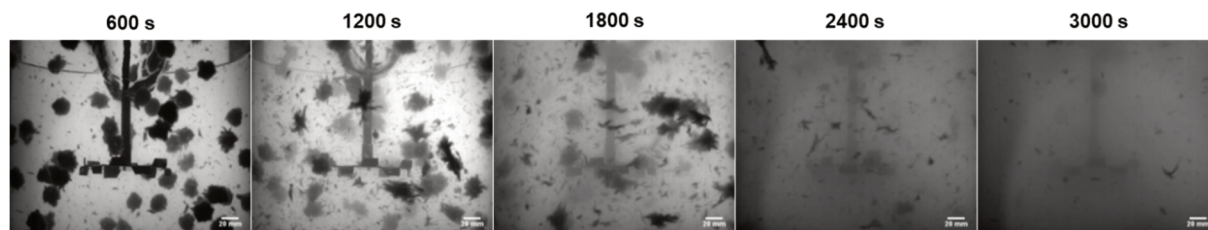


Fig. 9.5: Change of size of xanthan gum aggregate over time (dissolver stirrer, $d/D = 0.345$, $P/V = 0.64 \text{ W/m}^3$)

In conclusion, this experimental set-up is proposed to characterize the dispersion behavior of biopolymer powders. Compared to other common methods, the observation of the whole reaction vessel enables a better control of particle size variation. Nevertheless, picture processing and data analysis is very time consuming and should be improved for further application of this method.

Dissolution of biopolymer particles could be characterized both by methods based on change of torque and viscosity and by turbidity and photometric analysis. Due to the shear-thinning behavior of xanthan gum, guar gum and alginate, results from viscosity based measurements have to be corrected dependent on the applied shear stress. Furthermore, to determine the dissolved biopolymer amount a calibration procedure is necessary.

Methods to quantify dynamic changes of physical properties of biopolymer powders are scarce in literature. As mentioned above, change of viscosity was used to determine dissolution but no claims regarding the effects on powder rehydration were given. This also applies for the characterization of swelling kinetics of biopolymers. In literature [127,128], swelling of powdered food material was determined by mixing a powder sample with liquid in a certain ratio followed by an incubation time to allow swelling. Afterward, samples were centrifuged and dissolved material in the supernatant as well as mass of the sediment were determined. Mass increase of the sediment as a result of water uptake was regarded as swelling. However, swelling

processes during biopolymer rehydration proceed instantly after powder-liquid contact and critical swelling associated with pore blocking conditions is reached in the range of seconds. This method is basically suited to analyze swelling of food powders but too slow to assess the dynamics especially in the first instants after powder liquid contact. Alternatively, swelling was characterized by direct microscopic observation of particle increase in contact with liquid. Disadvantageous hereby is the limited sample number and a time consuming image analysis to process the data. For that reason, within this thesis, a rheological measurement set-up was developed which allows a study of the swelling dynamics as well as easy evaluation of the obtained results.

In conclusive evaluation, the methods proposed in literature are suited to assess powder rehydration properties. However, results are not based on physical principals and depend strongly on the conditions applied in the respective experiment. Furthermore, due to the overlap of different rehydration steps together with their dynamics, these “traditional” methods are not able to decouple the different aspects of rehydration to investigate the different steps separately from each other. To be able to predict the powder rehydration behavior, it is necessary to investigate the correlation between dynamic processes and rehydration behavior of the powders based on their physical characteristics. The physically motivated approach should be favored over traditional “mimicking” techniques as it enables a prediction of the rehydration process independently of the used powder.